1972

Temperature Effects on Integral Abutment Bridges During Final Construction Stages

David Earl Holman

TEMPERATURE EFFECTS ON INTEGRAL ABUTMENT BRIDGES DURING FINAL CONSTRUCTION STAGES

BY

DAVID EARL HOLMAN

A thesis submitted
in partial fulfillment of the requirements for the
degree Master of Science, Major in
Civil Engineering, South Dakota
State University

1972

TEMPERATURE EFFECTS ON INTEGRAL ABUTMENT BRIDGES

DURING FINAL CONSTRUCTION STAGES

This thesis is approved as a creditable and independent investigation by a candidate for the degree, Master of Science, and is acceptable as meeting the thesis requirements for this degree. Acceptance of this thesis does not imply that the conclusions reached by the candidate are necessarily the conclusions of the major department.

Thesis Adviser Date

Head, Civil Engineering Dept. Date

ACKNOWLEDGEMENTS

This work was conducted for the South Dakota Highway Department in cooperation with the U. S. Department of Transportation, Federal Highway Administration. It is a part of HPR Research Study 5; a cooperative study conducted by the South Dakota State University and the South Dakota Highway Department. The opinions, findings, and conclusions expressed in this thesis are those of the author and not necessarily those of the Federal Highway Administration.

The author wishes to express his sincere appreciation to Lorys J. Larson, Associate Professor, Department of Civil Engineering, and Mumtaz B. Sarsam, Assistant, Department of Civil Engineering, for their invaluable suggestions and guidance throughout the course of this study. Their continued interest, help, and encouragement are greatly appreciated.

Special thanks are extended to Mr. Thomas Biggar, Civil Engineering Technical Assistant, for his aid in the construction and modifications of the equipment used in this study.

DEH

TABLE OF CONTENTS

LIST OF FIGURES

LIST OF FIGURES (continued)

LIST OF FIGURES (continued)

LIST OF TABLES

CHAPTER I

INTRODUCTION

A. General

Bridges of one form or another have been used since man's creation. They have progressed from little more than logs positioned across streams to the gigantic structures man is familiar with today. The typical bridge seen today could take many different forms and could be constructed of a variety of materials. Probably the most common materials used today are steel and concrete.

Usually, the design of steel bridges relies on the end span of the structure being simply supported. Such designs are accomplished by the use of expansion bearings between the girders and abutments. Except for a small horizontal force because of friction, the only forces transmitted by the girders to the abutment are the vertical forces which include both dead and live loads. To complete the design, an expansion joint is incorporated between the abutment wall and bridge deck. Its function is to eliminate the longitudinal load or reaction transferred to the abutment by expansion and contraction resulting from temperature changes. See Figure 1.

The use of the expansion bearings and joints is not always desirable. In addition to their initial high cost of fabrication and substantial cost of installation, they create difficulties in inspection and maintenance. This is especially true in regions which are subjected to the extremes of both temperature and weather. To overcome the

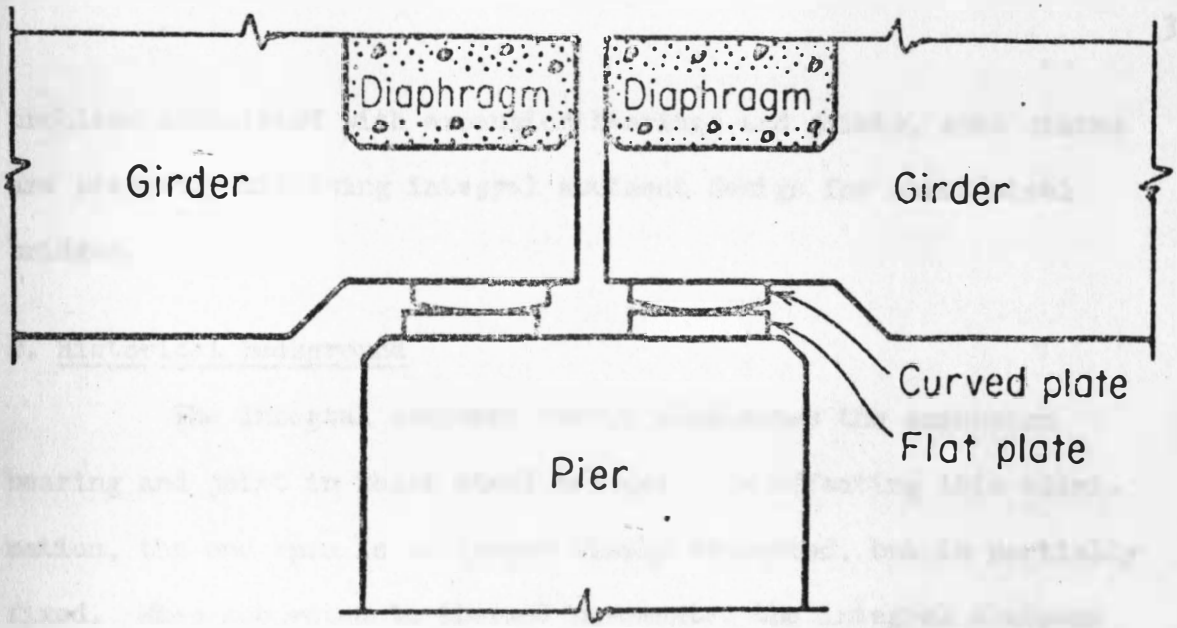

Expansion Bearings

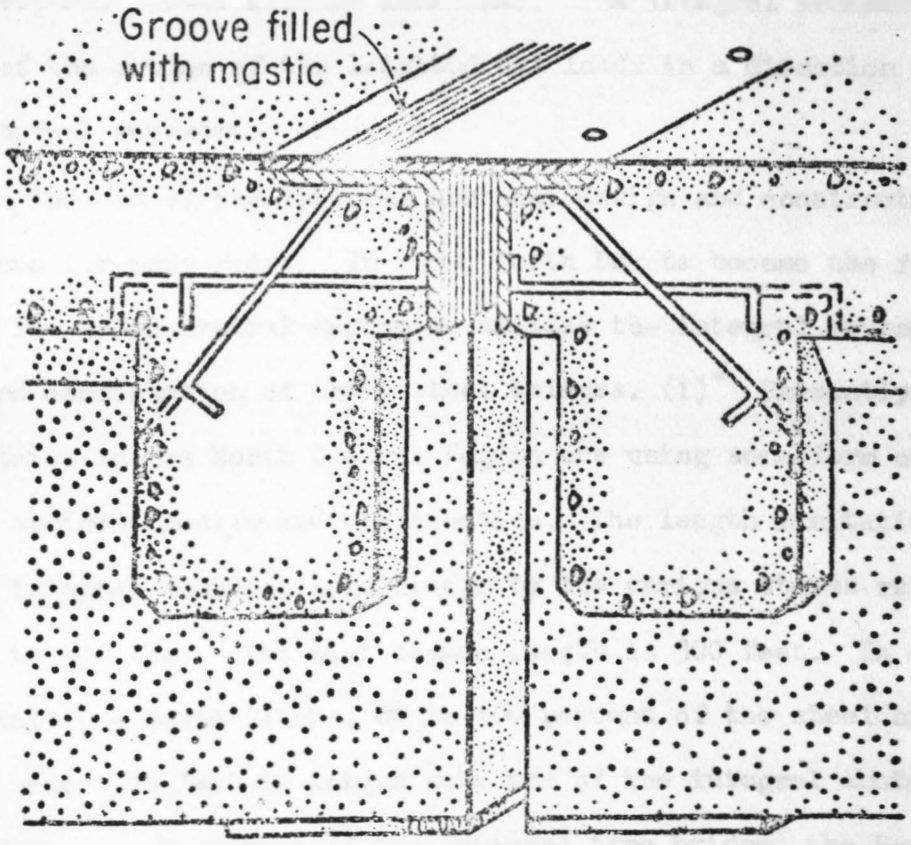

Expansion Joint

FIGURE 1. Typical Expansion Bearing and Expansion Joint Details.

problems associated with expansion bearings and joints, some states are presently utilizing integral abutment design for short steel bridges.

B. Historical Background

The integral abutment design eliminates the expansion bearing and joint in short steel bridges. In effecting this elimination, the end span is no longer simply supported, but is partially fixed. When subjected to thermal movements, the integral abutment receives longitudinal loads resulting from these movements in addition to the vertical forces already mentioned. The integral abutment rotates because of the action of the longitudinal loads in a direction depending on the thermal movement.

The use of the integral abutment design and construction has been common for many years. In 1964, North Dakota became the first state in the North Central Region to utilize the integral abutment in design and construction of short steel bridges. (1)* Presently, most of the states in the North Central Region are using some form of the integral abutment design and construction. The length limitation placed upon the integral abutment type bridge by the various states ranges from 265 to 400 feet. The most common length is 300 feet. In several states including South Dakota, 80 to 100 percent of the steel bridges designed under 300 feet in length make use of the integral abutment. Besides using large numbers of the integral type bridge, the South

* Numbers in parentheses refer to entries in the Bibliography.

Dakota Department of Highways utilizes a design for this type bridge that is different from any other state in the North Central Region.

This study of the integral abutment type bridge was based exclusively on the design used by the South Dakota Department of Highways. The design utilizes an HP10 x 42 steel bearing pile (2) field welded to each bridge girder. To secure proper interaction between the concrete abutment and the steel girder, shear studs or a small stiffener are shop-welded to the girder web on a line coinciding with the eventual center line of the integral abutment which is two feet wide. Reinforced holes are also located in the girder web near the interior face of the integral abutment to accommodate shear bars orientated at 45 degrees with the plane of the web. Their function is similar to that of the previously mentioned shear studs or small stiffener. The end one and one half feet of the girder and the upper two feet of the piling are encased in concrete completing the integral abutment. Figures 2, 3, and 4 illustrate the details of the integral abutment.

C. Object and Scope of Investigation

The main objective of this experimental project was to investigate and evaluate the effects of thermal movements on an integral abutment type bridge during the final stages of construction. This study is a continuation of the research carried out by Mumtaz B. Sarsam. (1) Particular attention was given to the evaluation of the resultant state of stress in the end portion of the girder near and contained within the integral abutment, the upper portion of the steel

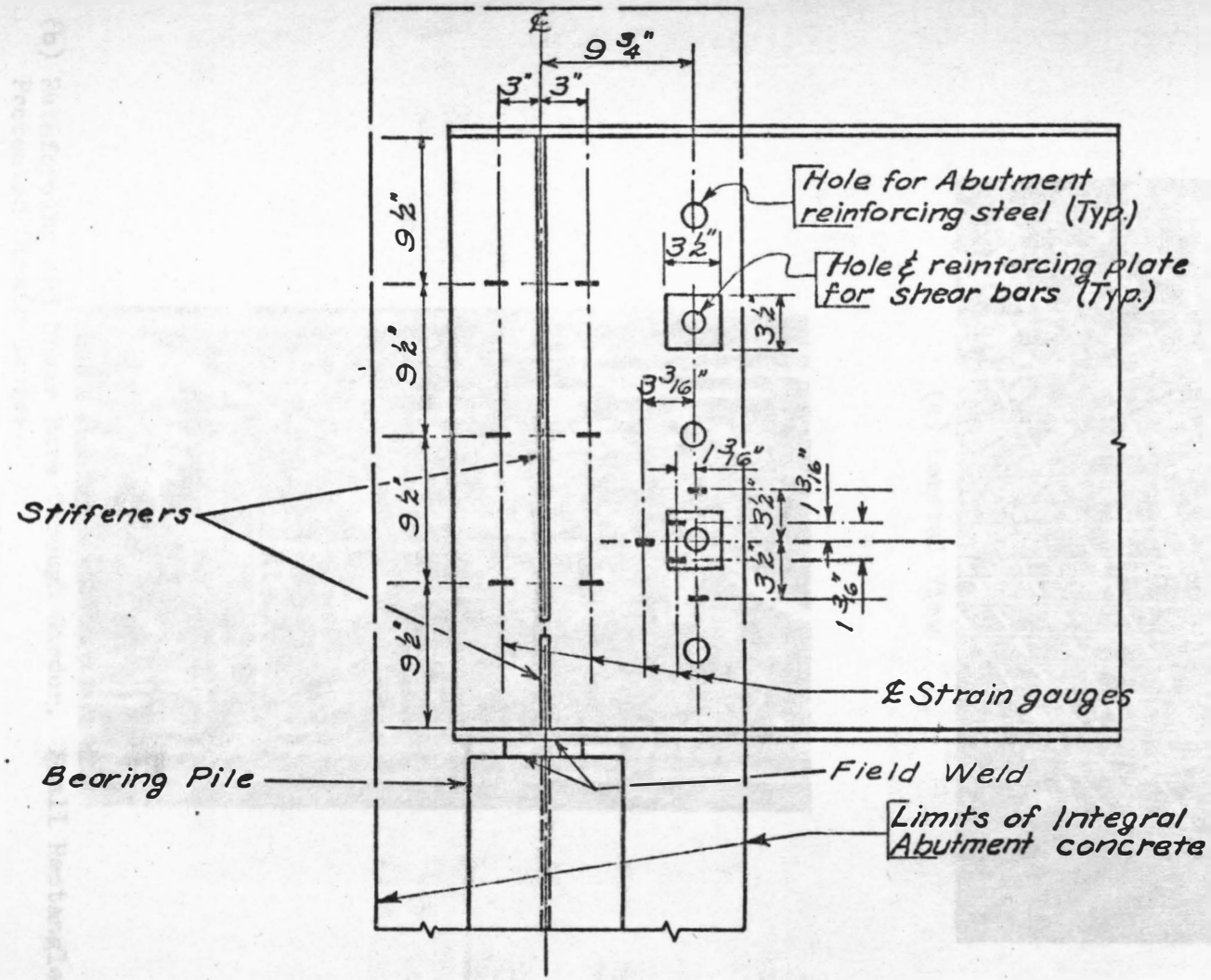

FIGURE 2. Girder and Piling Details at Integral Abutment End.

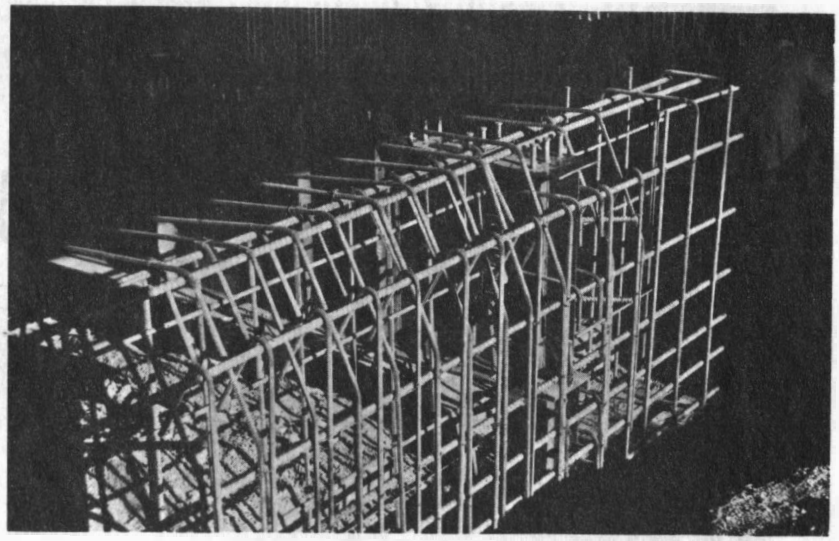

(a) General View

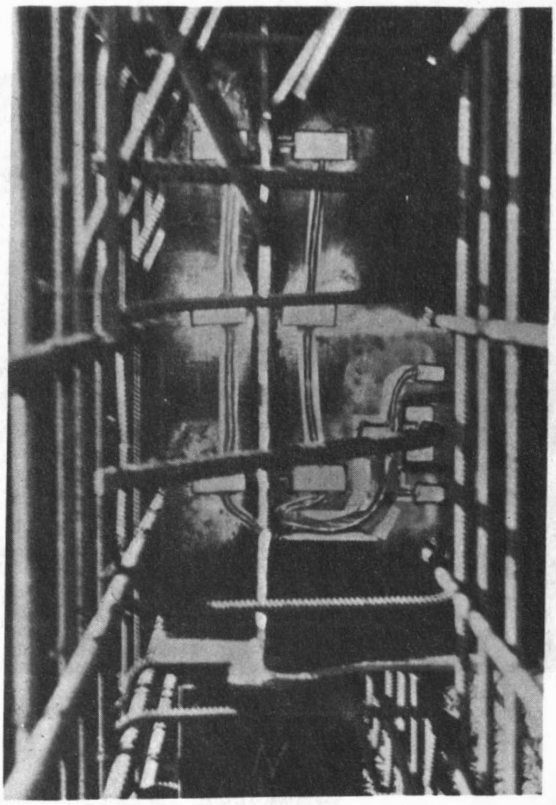

(b) Reinforcing and Shear Bars Through Girder. Small Rectangles are Protected Strain Gauges.

FIGURE 3. Integral Abutment Reinforcing Steel.

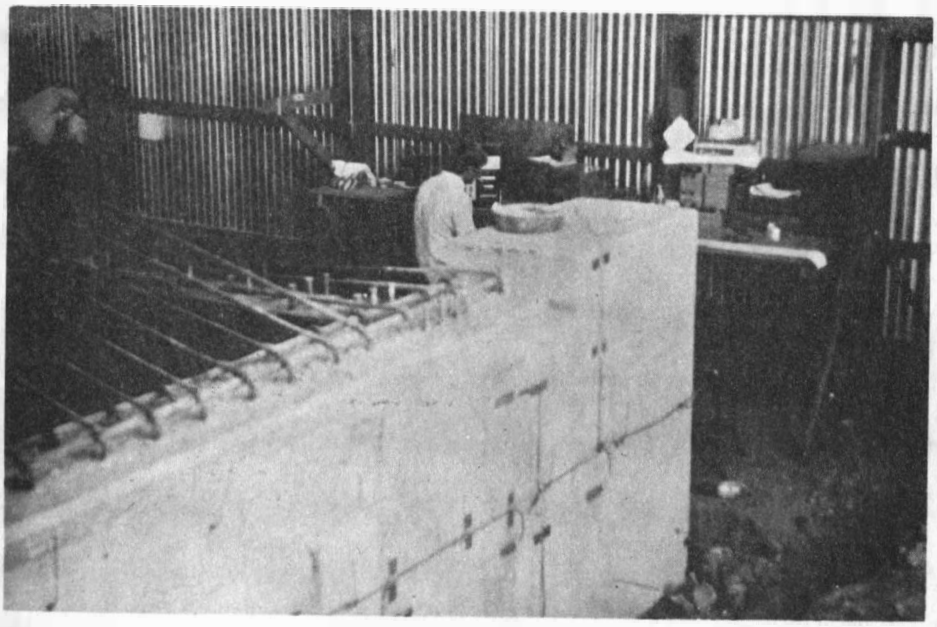

(a) Partial Front View

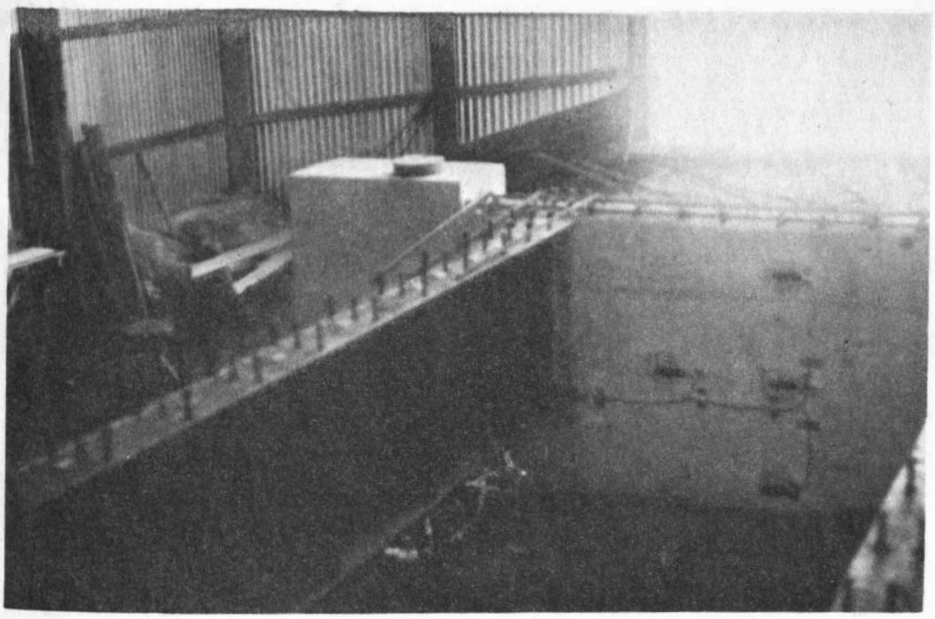

(b) Partial Back View

FIGURE 4. Completed Integral Abutment.

bearing piles, and in selected locations on the concrete abutment. The vertical forces created within the span because of the rotation of the integral abutment were noted. Emphasis was also placed upon the action of the backfill and the resistance that it offered to the simulated thermal movements of the integral abutment type bridge.

A full scale model representing the end portion of a typical highway bridge was constructed and tested in stages. Stages I and II were conducted by Sarsam. (1) The stages of testing reported in this study included Stages III and IV. Stage III included testing of the test model after the concrete deck slab was poured and cured, but before the backfill was placed. See Figure 5. Stage IV included testing of the test model after the backfill was placed and compacted as shown in Figure 6.

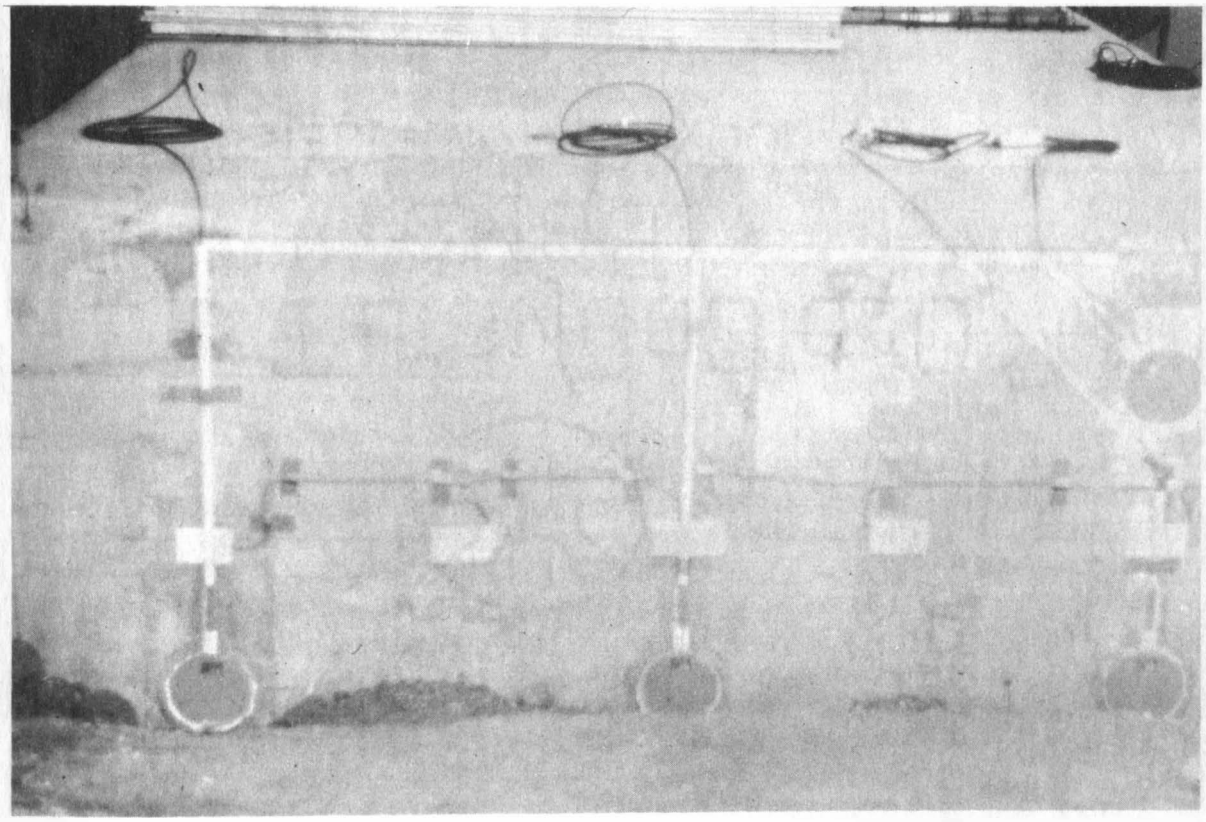

FIGURE 5. Completed Slab.

FIGURE 6. Placed Backfill.

CHAPTER II

TESTING PROGRAM

A. Materials and Test Specimen

The early construction (Stages I and II) consisted of driving the bearing piles, placement of the girders and integral abutment reinforcing steel, and the pouring of the concrete integral abutment. This construction was accomplished by driving two HP10 x 42 steel bearing piles to a depth of 32 feet. The two bearing piles were placed at 8'-6" center to center and were orientated so that their weak axes were normal to the anticipated direction of bending. See Figure 7. Two plate girders, 26'-6" long and having a 12" x 1/2" top flange, a 38" x 5/16" web plate, and a 12" x 3/4" bottom flange, were field welded to the bearing piles. See Figures 7 and 8. The other end of each girder was simply supported on a 5" diameter steel roller. Also at this end, a smaller roller was provided to eliminate the uplift caused by the integral abutment's rotation. Figures 7 and 9 illustrate the rollers and their locations. Transverse intermediate stiffeners were placed mainly against the inside face of the girder web plate in accordance with the American Association of State Highway Officials (AASHO) requirements for HS20-44 loading. (3) See Figure 8. A permanent diaphragm, constructed of two 4" x 4" x 5/16" angles, in the form of an "x" was placed and welded near the simply supported end to provide for lateral stability. The integral abutment reinforcing steel was designed and placed as shown in Figures 3 and 10. The abutment was

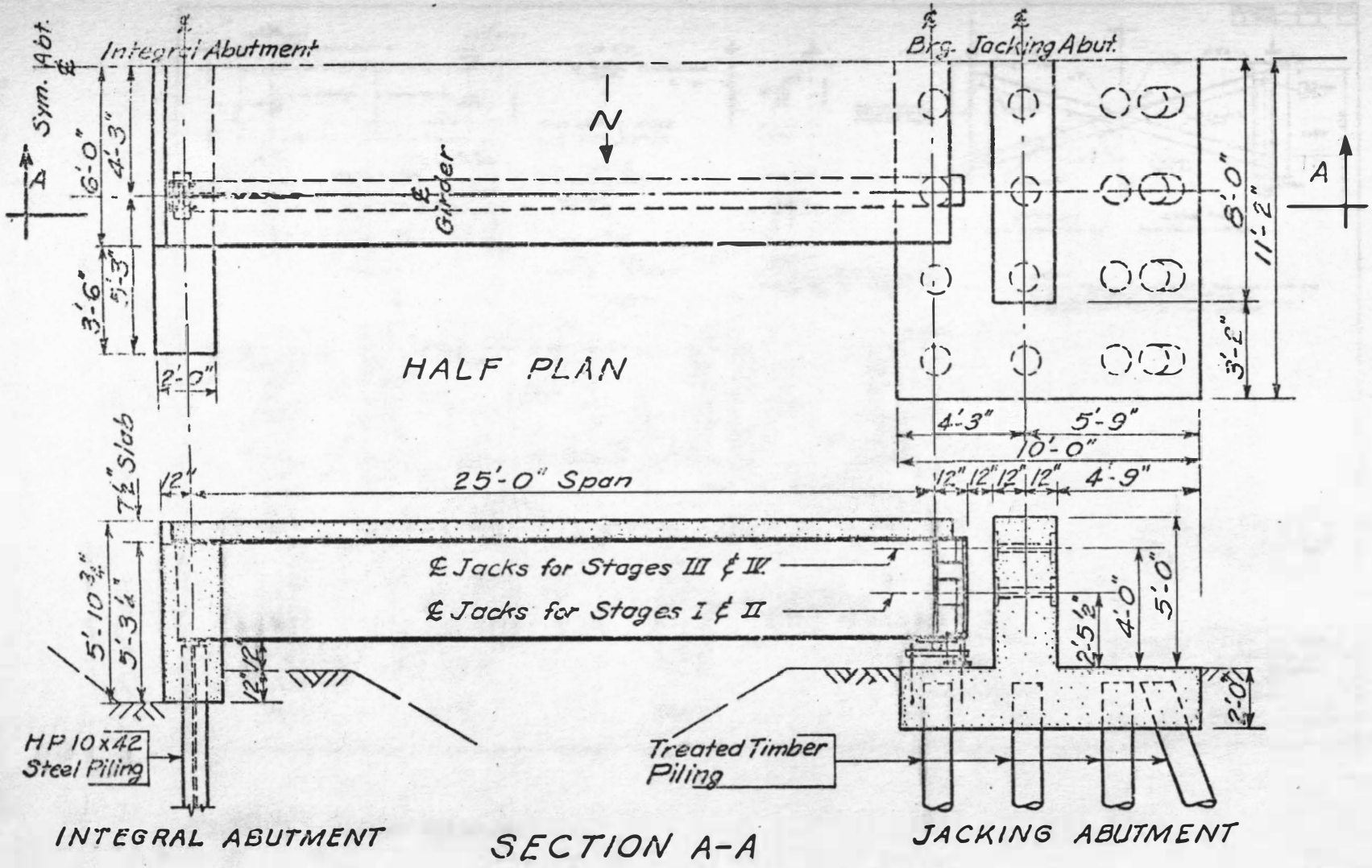

FIGURE 7. General Drawing of Test Model.

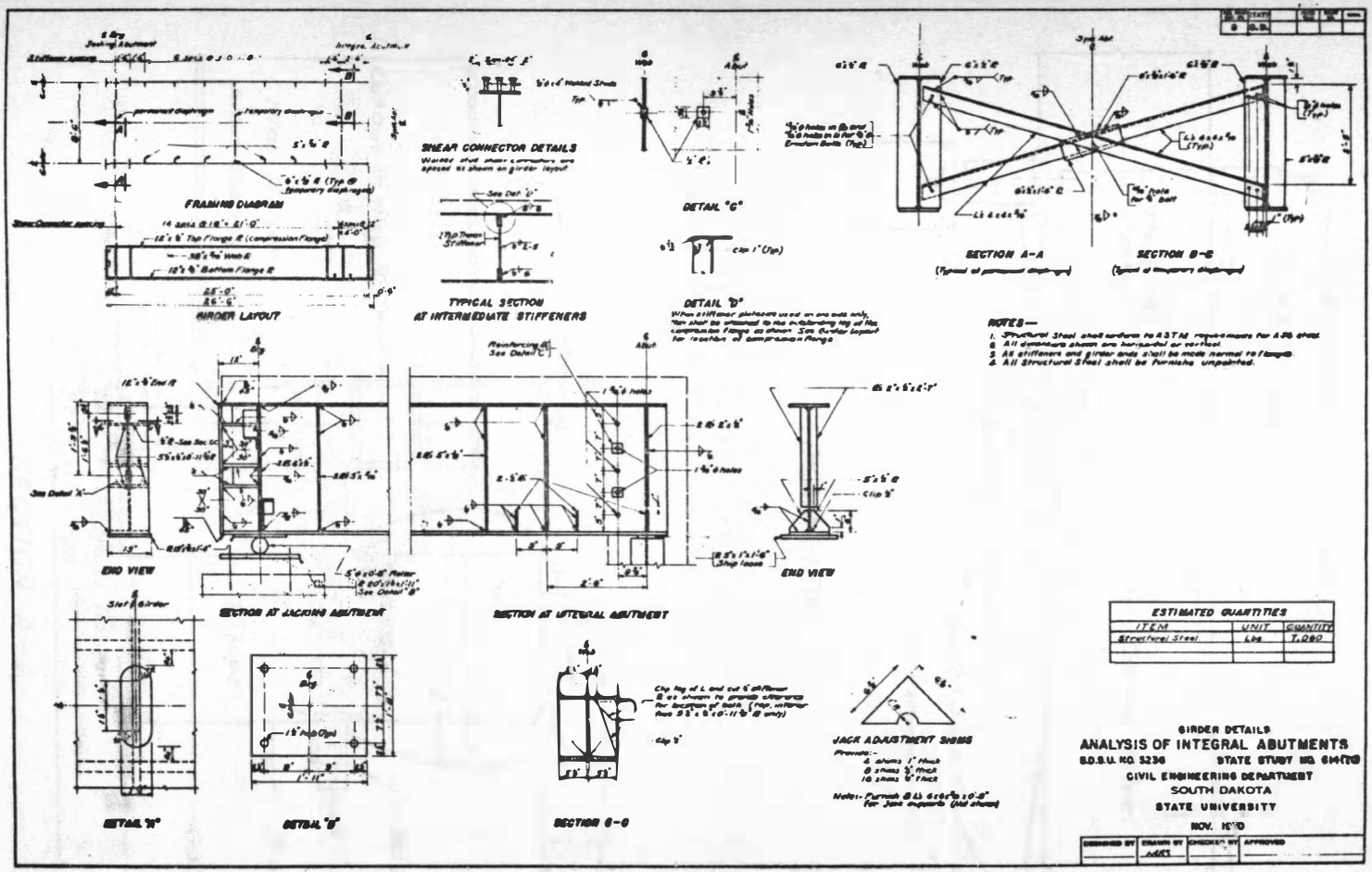

FIGURE 8. Girder Details.

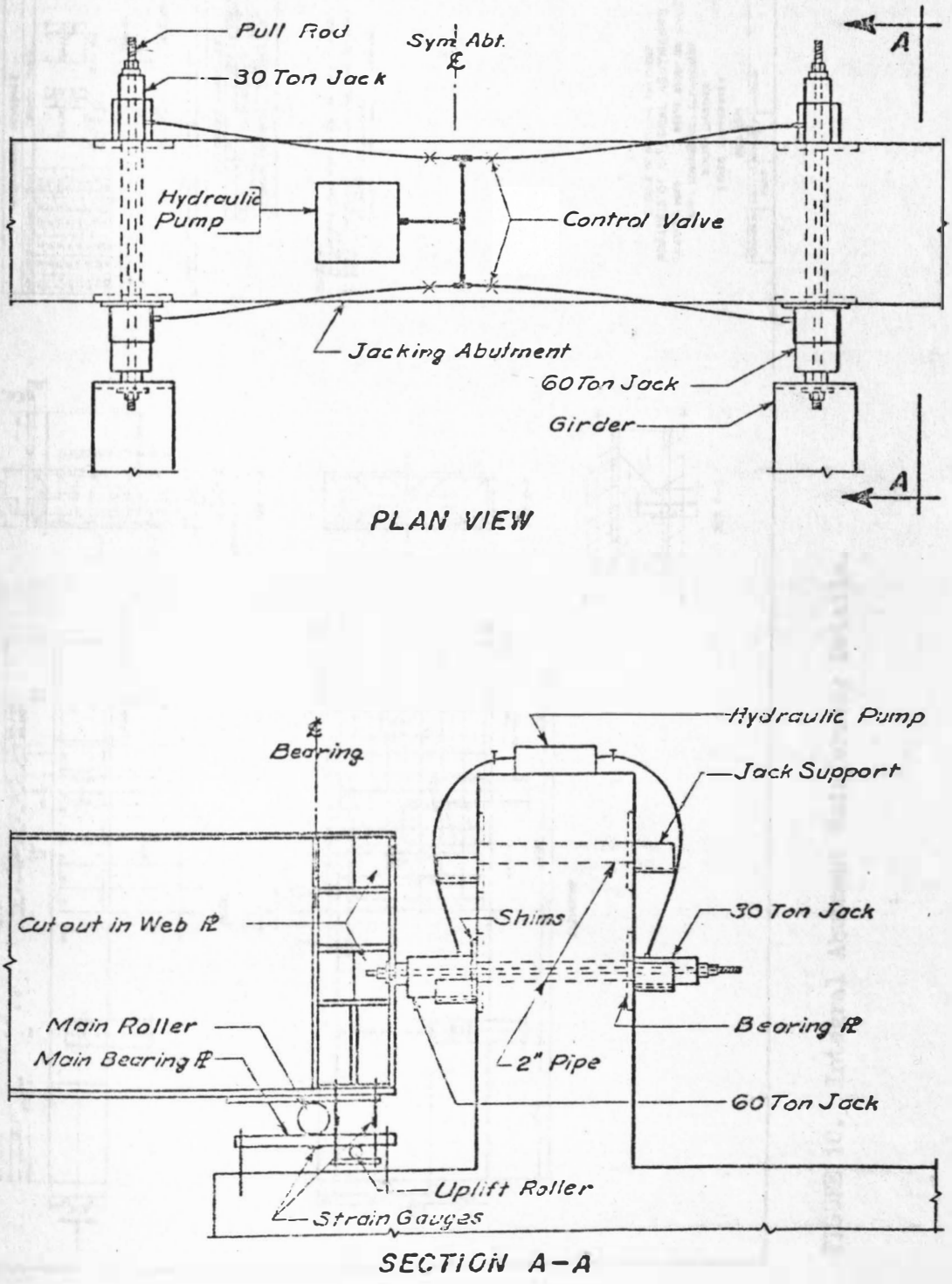

FIGURE 9. Jacking and Bearing Details.

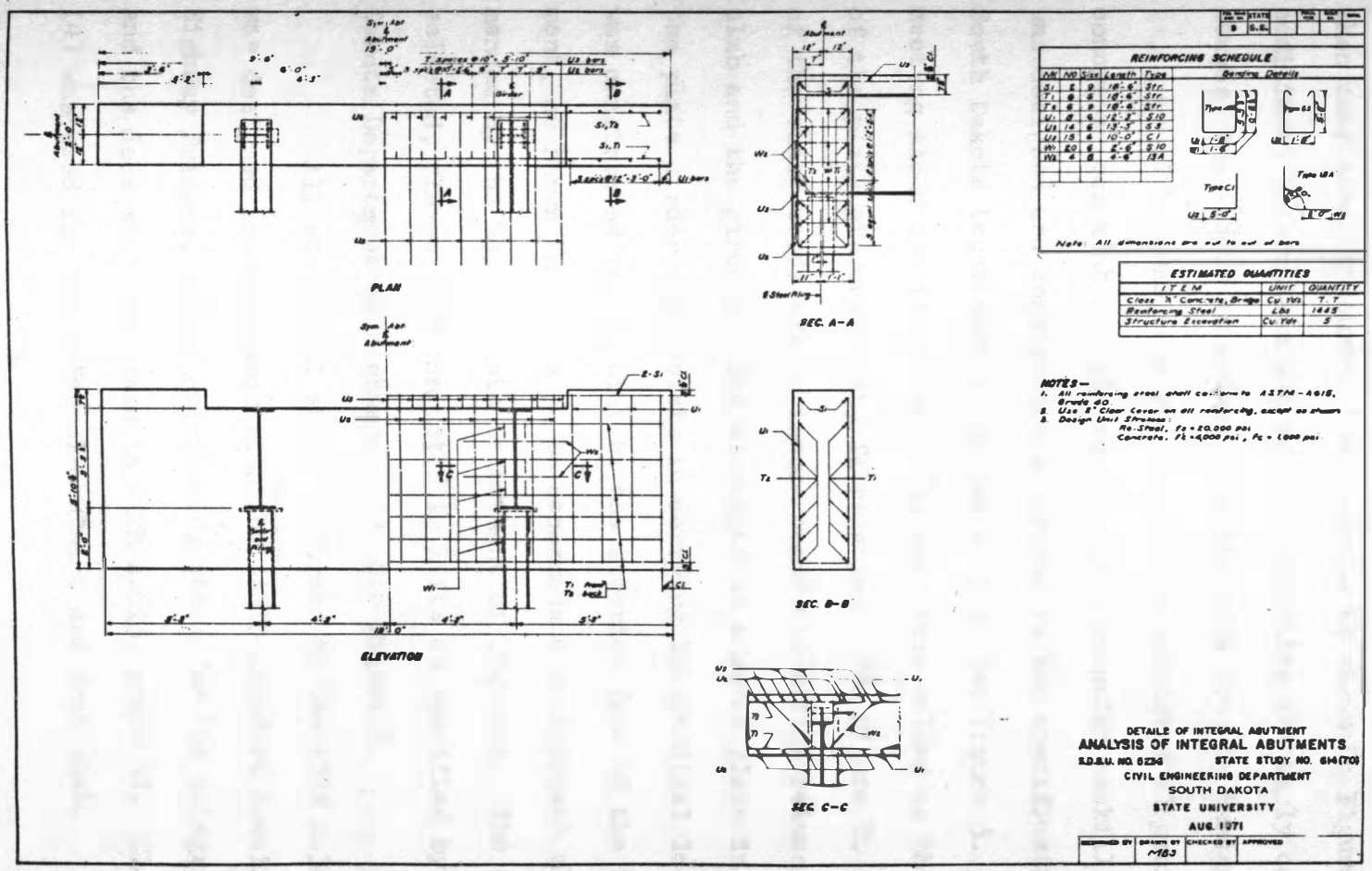

FIGURE 10. Integral Abutment Reinforcing Details.

then completed by pouring the concrete as shown in Figure 4. For additional information and detail concerning the early construction stages, the reader is referred to the work done by Sarsam. (1)

The final construction stages consisted of pouring the concrete deck slab and placement of the granular backfill. The slab was designed and constructed according to the specifications of the South Dakota Department of Highways. (4) See Figure 5. Shear studs, meeting AASHO specifications, (3) were shop-welded to the top flanges of the plate girders during fabrication. See Figure 8. The function of the shear studs was to insure composite action between the concrete slab and the girders. The slab acts as a cover plate in relation to the plate girder and assists in carrying longitudinal loads. A notch was constructed in the slab at the exterior face of the integral abutment, as shown in Figure 5, to accommodate an approach slab as recommended by the South Dakota Department of Highways. The backfill was selected, placed, and compacted in lifts as specified by the South Dakota Department of Highways. (4) See Figure 6.

All structural steel conformed to the ASTM A-36 steel and was designed in accordance with the AASHO Standard Specifications for Highway Bridges, 1969. Reinforcing steel for the integral abutment and the deck slab conformed to ASTM A-615, grade 40. Class "A" concrete (4) was used for the integral abutment and deck slab.

B. Test Apparatus

A jacking abutment (1) was constructed near the simply supported end to provide support in inducing the simulated thermal

movements. Included in the design and construction of this abutment were two sets of bearing plates which were set even with the concrete abutment wall. Circular holes in each set of bearing plates were connected by a hollow steel pipe, providing a hole through the jacking abutment as shown in Figures 7 and 9. The center line of this hole coincided with the neutral axis of the composite section.

In order to accommodate the forces anticipated in inducing the simulated movements, the girders were reinforced at their end sections by stiffened end plates. These plates were fabricated with a slot corresponding to the neutral axis of the composite girder and in line with the hole provided in the jacking abutment. On a line with the slots in the end plates, portions of the girder webs were removed. These special cutouts are used in providing the simulated thermal movements. The end plates and web cutouts are illustrated in Figures 8 and 9.

The longitudinal thermal movements, both expansion and contraction, were simulated by an applied force by means of hydraulic jacks. The jacks were positioned on the bearing plates and supported by brackets field welded thereto. The brackets are shown in Figure 9.

The simulated contraction movements were provided by means of two 30-ton hollow-core jacks positioned on the exterior face of the jacking abutment. The force supplied by the jacks was transferred to each girder by high-strength, continuous-screw rods. These rods were placed through the hollow core hydraulic jacks. the holes through the jacking abutment, the slotted end plates, and into the web cutouts. On

each end of the rods a high-strength nut and washer were placed to complete the arrangement. As the jacks extended, the girders were pulled thereby simulating contraction resulting from a temperature drop. This arrangement is shown in Figure 9.

The simulated expansion movements were provided by two arrangements, namely, one for Stage III and the other for Stage IV. For Stage III expansion, two 60-ton hollow-core jacks were positioned between the jacking abutment and the end plates as shown in Figure 9. For Stage IV expansion, both 30-ton hydraulic jacks were used in addition to the two 60-ton hydraulic jacks as used in Stage III. The additional force was required because of the increased longitudinal restraint offered by the compacted backfill. This arrangement is shown in Figure 11.

A separate control valve was used for each individual hydraulic jack in order to insure equal movement of each girder. The jacks were operated by means of an electrically driven hydraulic pump. Shims were also provided for placement behind the jacks to insure enough travel for inducing the simulated movements. These details are illustrated in Figures 9 and 11.

The simulated movements were monitored with a series of dial indicators for each girder. Each series consisted of four dial indicators placed at various locations along the girder. A dial indicator was placed between the jacking abutment and the end plate of the steel girder. Its function was to monitor the movement of the composite section relative to the jacking abutment. Another dial indicator was

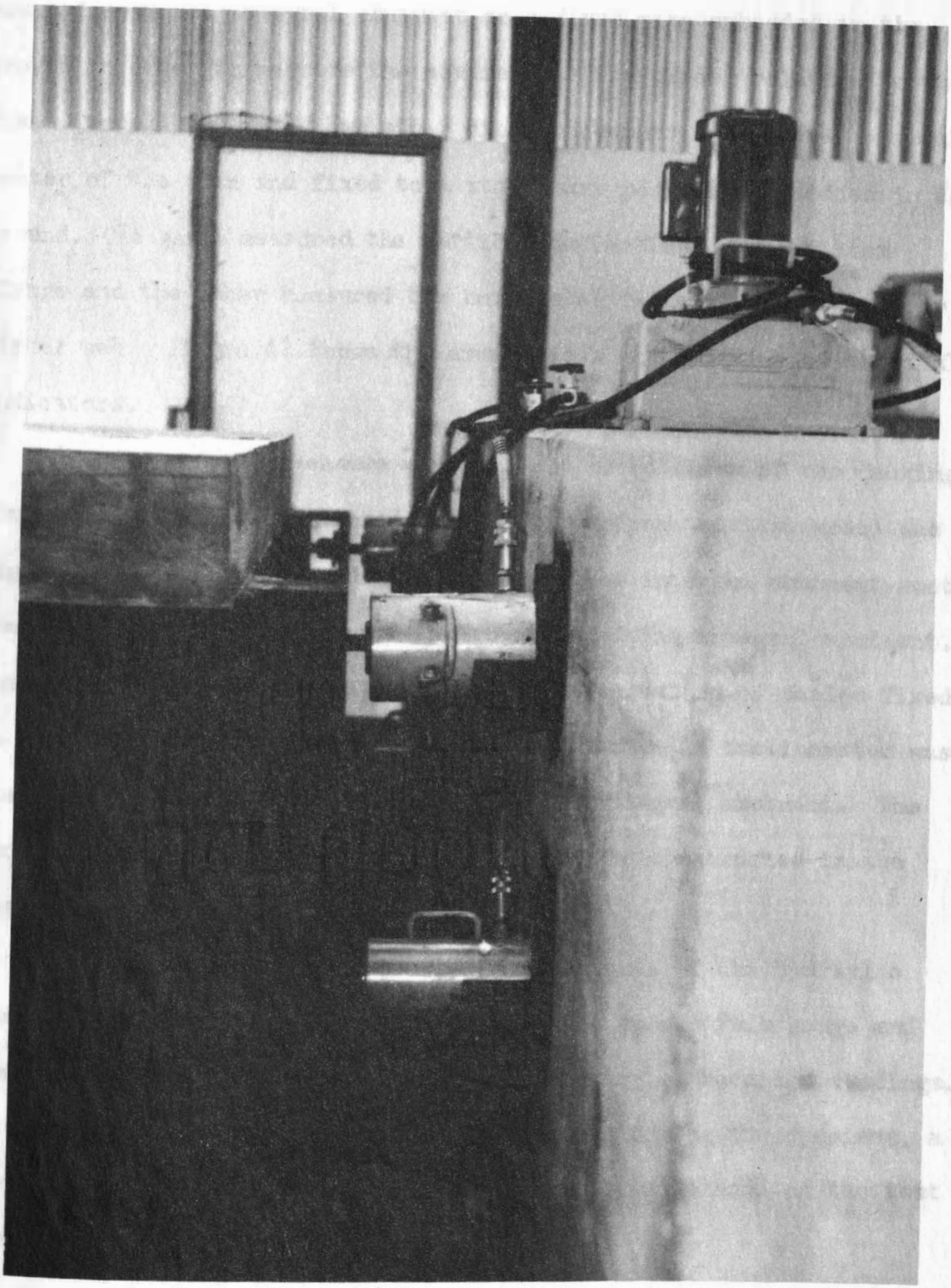

FIGURE 11. Arrangement of Hydraulic Jacks for Stage IV, Spring and Summer Cycles.

mounted near the integral abutment on a fixed pipe embedded in the ground in order to measure the movement of the girder relative to the fixed ground position. Two other dial indicators were placed near the center of the span and fixed to a stationary post also embedded in the ground. One gauge measured the vertical deflection of the bottom flange and the other measured the horizontal deflection of the lower girder web. Figure 12 shows the arrangement and location of the dial indicators.

In order to measure movement and/or rotation of the jacking abutment, a transit positioned some distance from the test model was sighted on the abutment and monitored. At the integral abutment another transit was used. It measured the rotation of the integral abutment. The rotation was determined by continuous observation of scales fixed to both top and bottom of the integral abutment. An inclinometer was also used in monitoring the rotation of the integral abutment. The inclinometer was not a commercial type, but was constructed in the engineering shop.

The force supplied to the jacks because of the hydraulic pump was monitored by a pressure gauge at the pump. This gauge and the jacks were calibrated to insure the accuracy of recorded readings. In addition to the other equipment used in monitoring the specimen, a thermometer, calibrated in degrees Fahrenheit, was placed on the test specimen and observed.

In experimentally determining the stresses created by the simulated thermal movements, SR-4 electrical strain gauges, single and

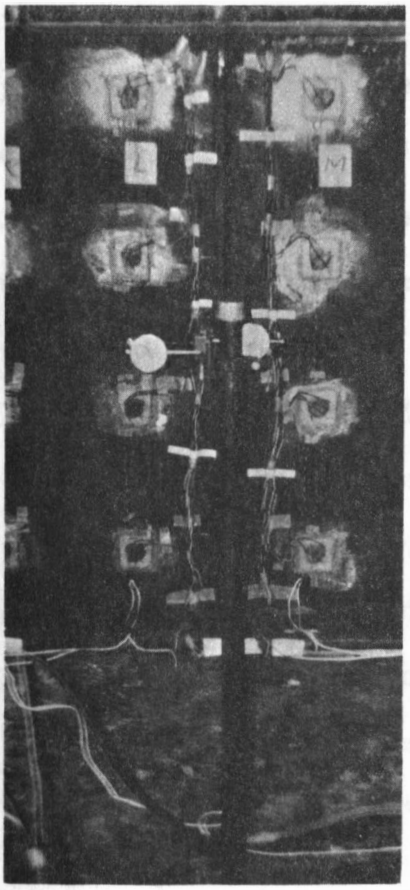

(a) Near Integral Abutment

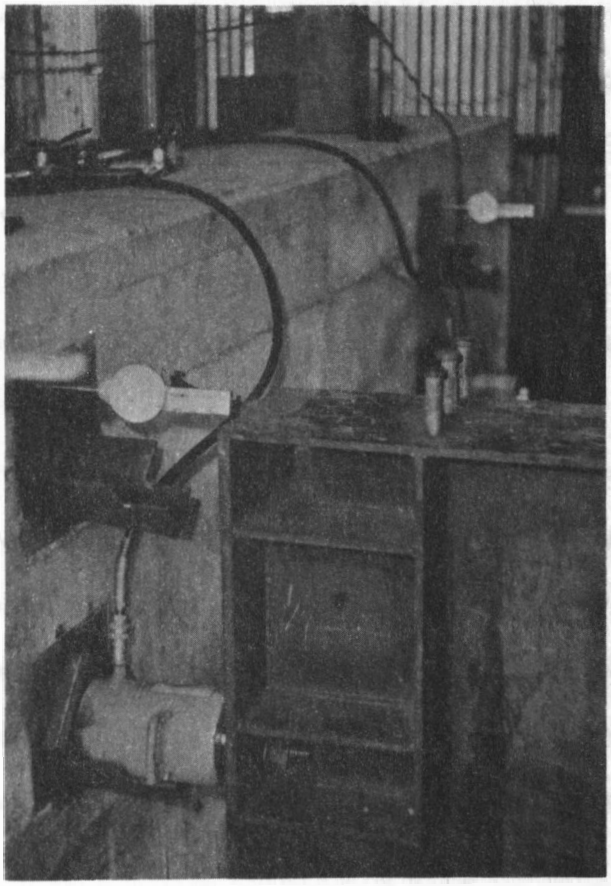

(b) At Jacking Abutment

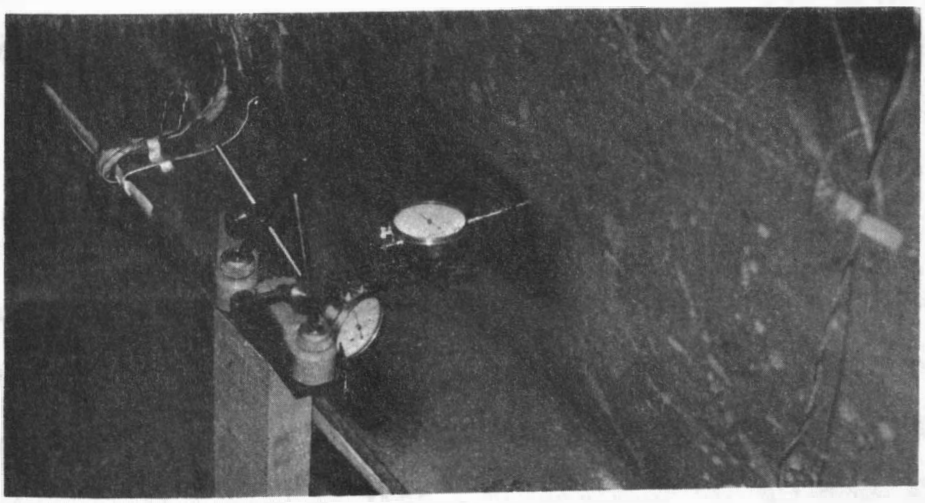

(c) At Mid-Span

FIGURE 12. Series of Dial Indicators.

rectangular rosettes (5) were employed. They were located on the upper portion of the north steel bearing pile, the north girder, and on the concrete surface of the integral abutment as shown in Figures 2, 13, 14, and 15. Strain gauges were also used in monitoring the upward and downward vertical forces created in the north girder at its simply supported end because of the rotation of the integral abutment. Their locations are shown in Figure 9.

All normal precautions (5 and 6) were employed in placing and protecting each gauge to insure its reliability. Other factors were also considered in providing reliable strain data, namely, temperature variations and stray electromotive forces. The effects of these variables were reduced or eliminated by various methods including temperature compensated circuits, heated test area, dummy gauges, and shielding of connecting cables. (1)

Total pressure cells (7) were mounted at the backfill-integral abutment interface in Stage IV as illustrated in Figures 16 and 17. Their function was to measure earth pressures against the integral abutment and to aid in determining general stress patterns.

A rapid method of obtaining the induced strain was required because of the constantly changing earth pressure during the testing cycles. This requirement was filled by using a switching unit, a self-balancing digital strain indicator, and a matching printer as shown in Figure 18. The use of this equipment provided a record of all strain data in a short period of time. In obtaining the pressure from the

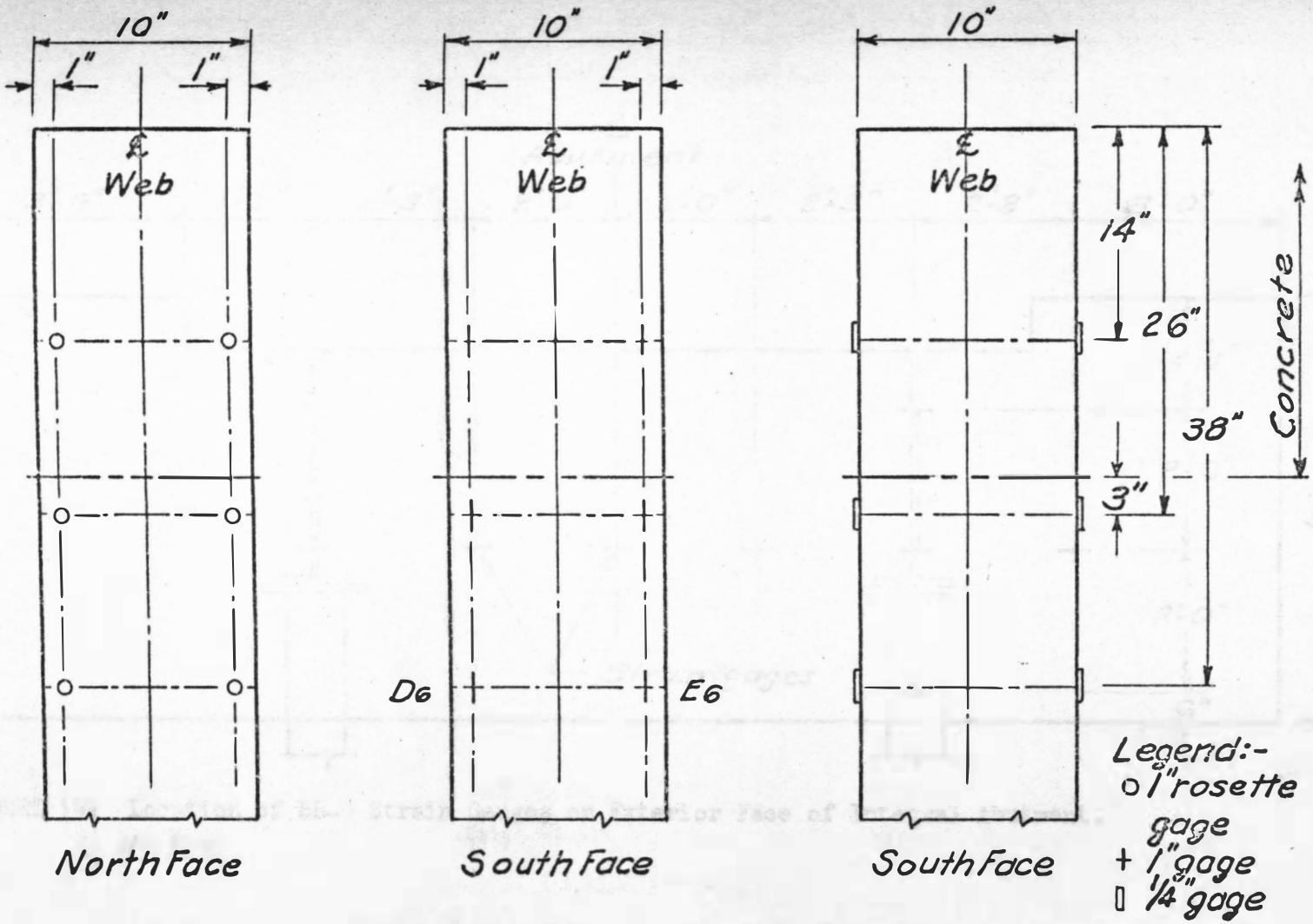

FIGURE 13. Location of SR-4 Strain Gauges on Upper Portion of North Pile.

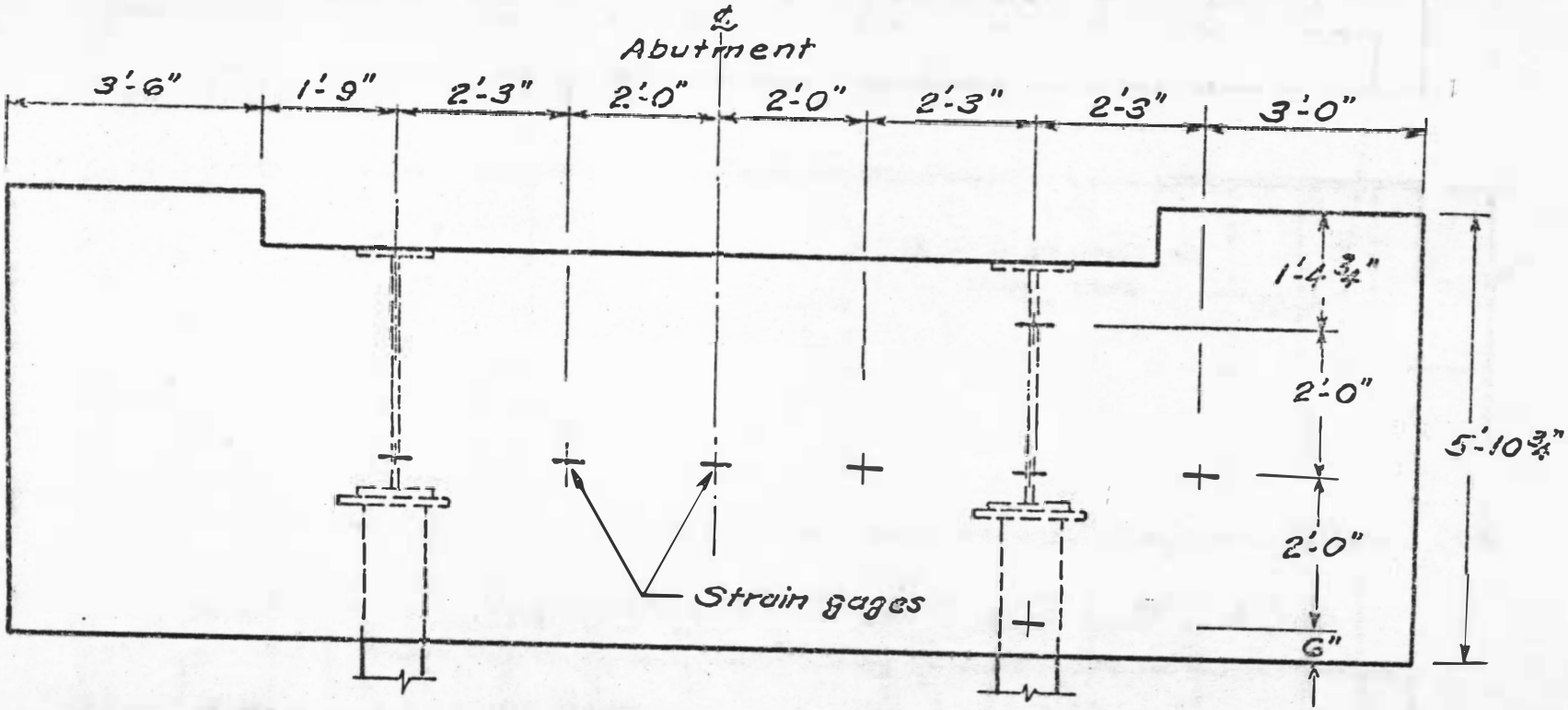

FIGURE 14. Location of SR-4 Strain Gauges on Exterior Face of Integral Abutment.

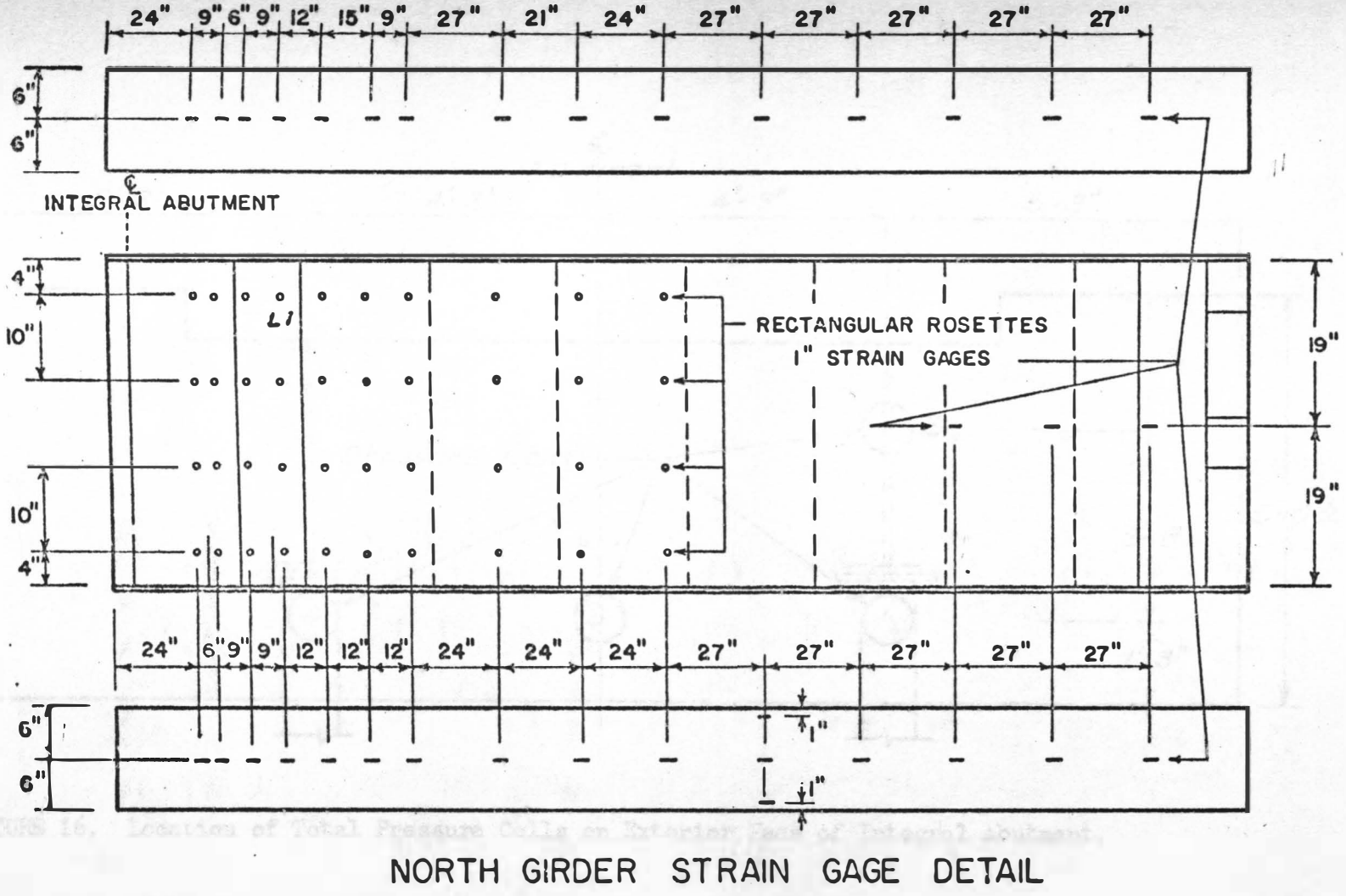

FIGURE 15. Location of SR-4 Strain Gauges on Girder.

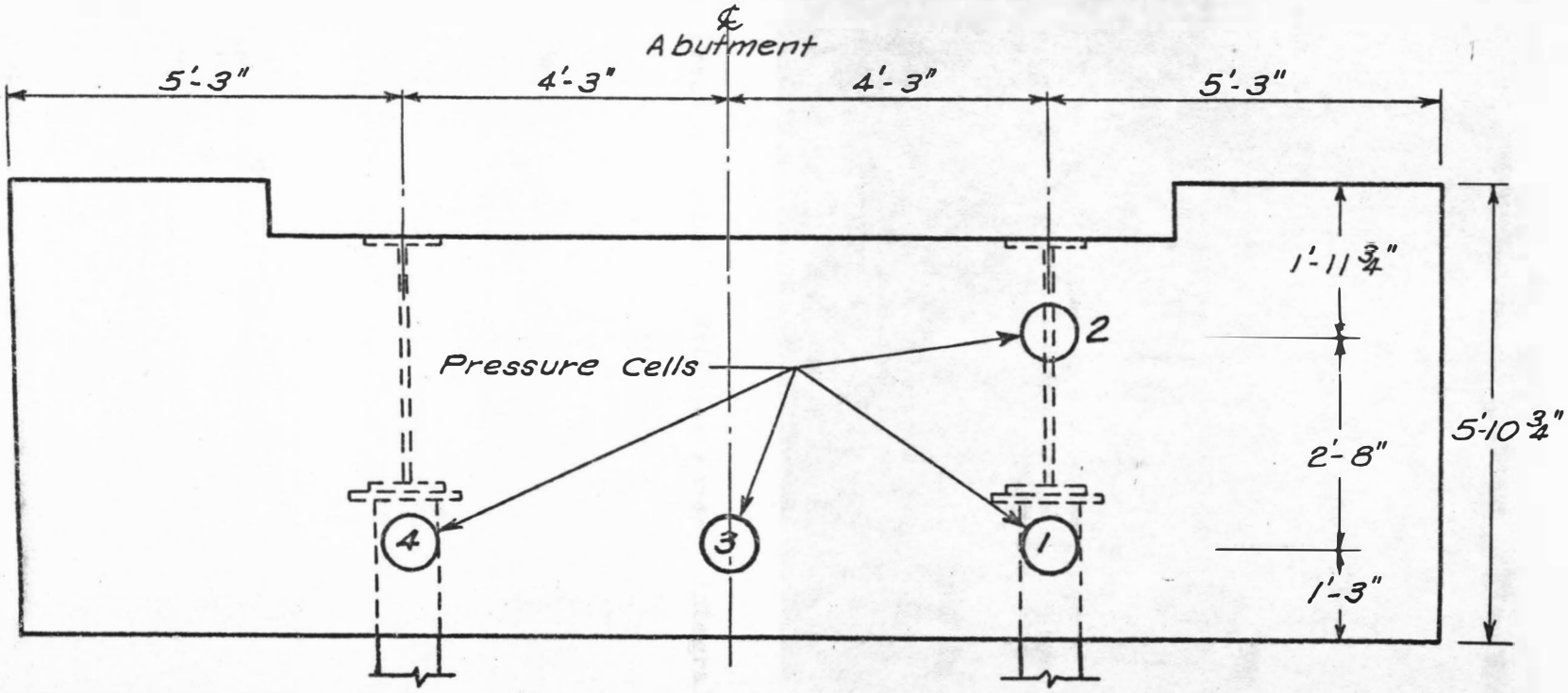

FIGURE 16. Location of Total Pressure Cells on Exterior Face of Integral Abutment.

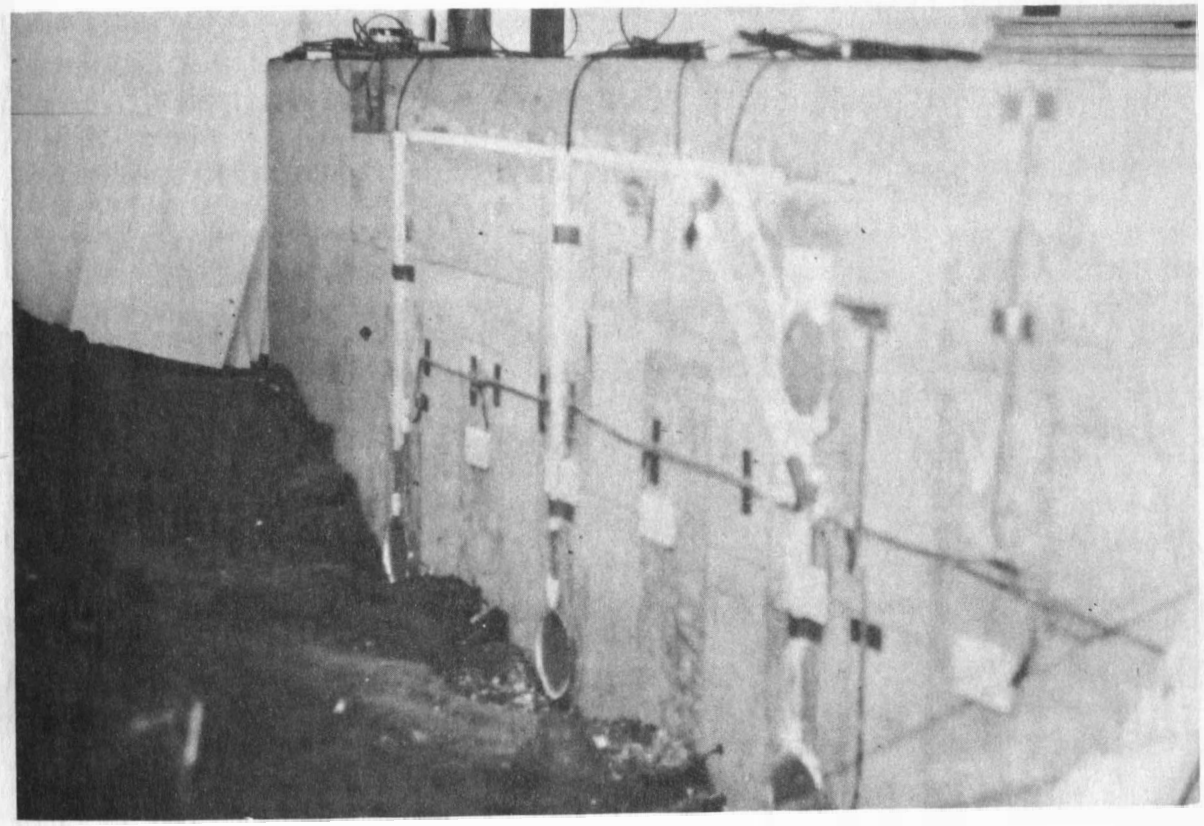

FIGURE 17. Pressure Cells on Exterior Face of Integral Abutment.

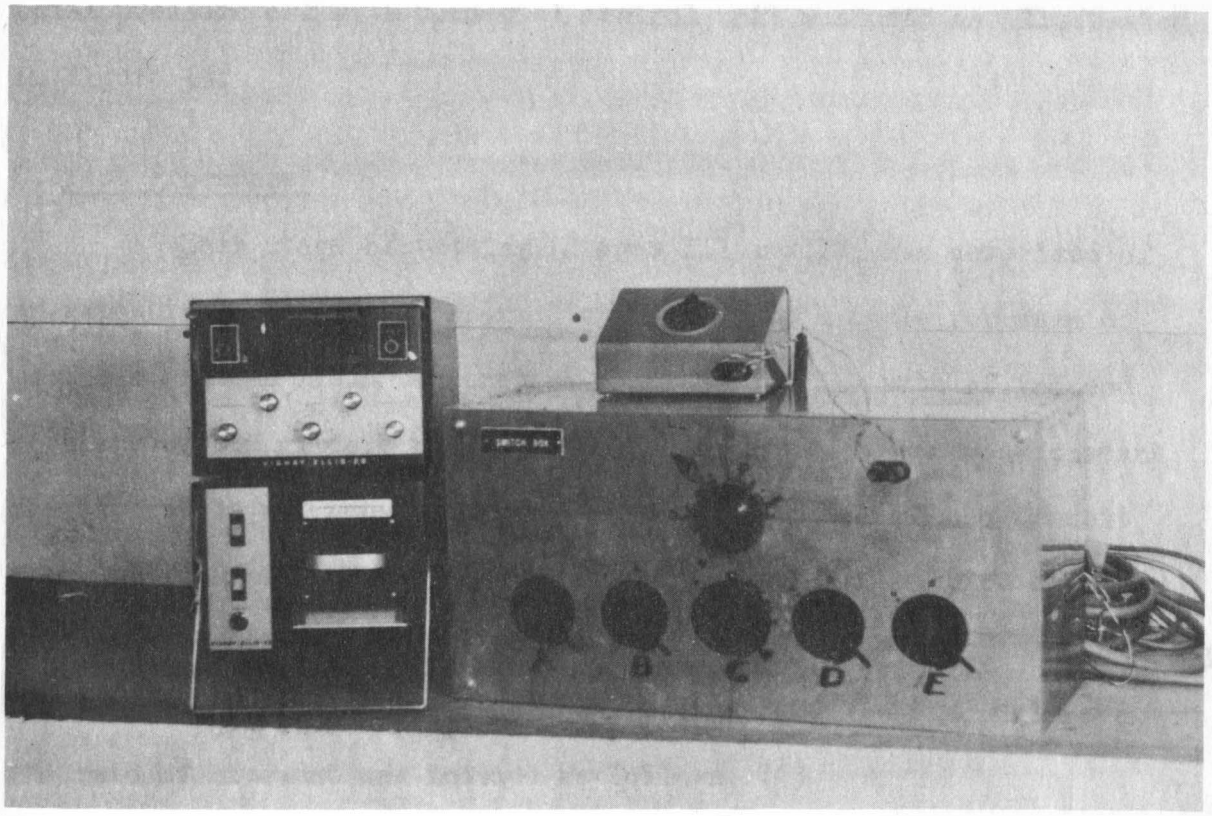

FIGURE 18. Digital Strain Indicator, Printer, and Switching Unit.

total pressure cells, a commerial control unit was used as illustrated in Figure 19.

C. Test Procedure

Each stage of testing, Stages III and IV, was comprised of an expansion cycle and a contraction cycle. Each cycle represented possible extreme field temperature conditions. The rate of induced movement of the girders relative to the jacking abutment was constant for each cycle and amounted to 0.250 inch per hour. If the transit near the jacking abutment indicated any appreciable rotation or movement of the abutment, it was compensated for by increasing or decreasing the relative movement to obtain the predetermined longitudinal movement. The rate of movement was induced as follows: (1)

0 to	5 minutes:	0.050 inch
5 to	10 minutes:	rest
10 to	15 minutes:	0.050 inch
15 to	20 minutes:	rest
20 to	25 minutes:	0.050 inch
25 to	30 minutes:	rest
30 to	35 minutes:	0.050 inch
35 to	40 minutes:	rest
40 to	45 minutes:	0.050 inch
45 to	60 minutes:	take readings
60 to	120 minutes:	repeat above cycle

The expansion cycle was begun at 0.000 inch of movement and proceeded to a +1.000 inch movement (the plus sign indicates expansion) and held for one hour. The movement was then released back to 0.000 inch and beyond to a -0.500 inch movement (the minus sign indicates contraction) and held.

The contraction cycle was begun at -0.500 inch of movement, after being held for a minimum of 12 hours. Movement was continued

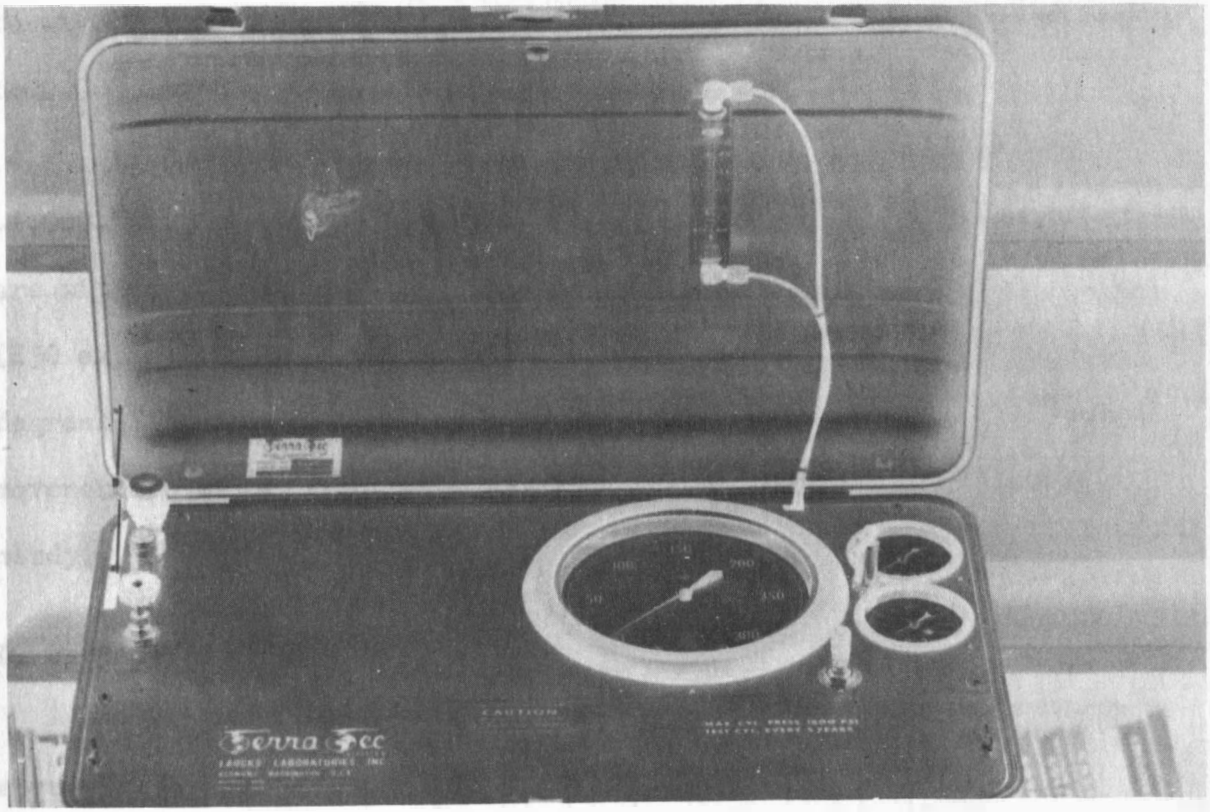

FIGURE 19. Pressure Cell Control Unit.

to -1.000 inch and held for one hour. The movement was released back to 0.000 inch and beyond to +0.500 inch movement.

The maximum induced movements (both the +1.000-inch and -1.000-inch movements) appear extreme at first glance; however, they are within the realm of possibility. For instance, a 500-foot bridge (250 expansion span) subjected to a total temperature change of 75 degrees Fahrenheit, 70 F → 120 F → 45 F, would experience thermal movements similar to those created in the expansion cycle of this study.

D. Reduction of Data

Various span lengths were related to the simulated thermal movements by using the equation: (8)

$$U = (K)\, L\, (\Delta t) \qquad \text{Eq. 1}$$

where

U = horizontal translation, in inches

K = coefficient of thermal expansion, in inches per inch per degree Fahrenheit

L = span length, in inches

Δt = temperature change, in degrees Fahrenheit

The coefficient of thermal expansion was used as 0.0000066 in./in./F.(8)

The strain data collected during Stages III and IV from the single SR-4 strain gauges was converted to stresses by the following relationship: (8)

$$f = E \times e \qquad \text{Eq. 2}$$

where

f = normal stress, in psi

E = Young's Modulus, in psi

e = measured strain, in inches per inch

Young's Modulus was taken as 29×10^6 psi for steel (8) and 3.9×10^6 psi for concrete. (8) The value used for Young's Modulus depended upon the material to which the gauge was bonded.

The strain data obtained from the rectangular rosettes was converted to principal stresses by the following equation: (6)

$$P_1, P_2 = E \left(\frac{e_1 + e_3}{2\,(1-v)} \pm \frac{1}{2\,(1+v)} \sqrt{(e_1-e_2)^2 + (2e_2-e_1-e_3)^2} \right) \qquad \text{Eq. 3}$$

where

P_1, P_2 = principal stresses, in psi

e_1, e_2

and e_3 = strains measured by the horizontal, diagonal, and vertical components of the rectangular rosette, respectively in inches per inch

v = Poisson's Ratio

E = Young's Modulus, in psi

Young's Modulus was used as 29×10^6 psi because all the rectangular rosettes were bonded to steel. Poisson's Ratio for steel was taken as 0.3. (9) To simplify the conversion of the data, a desk computer and program for equation 3 were utilized.

The vertical force downward at the jacking abutment was calculated from the flexural stress at the extreme fibers of the bearing plate

supporting the roller 5 inches in diameter. See Figure 9. The bearing plate, with a strain gauge at its center, was assumed to be simply supported. The force was obtained by use of the following equation: (8)

$$f = \frac{M\,(c)}{I} \qquad \text{Eq. 4}$$

where

f = flexural stress, in psi

M = bending moment, in inch-pounds

c = distance from neutral axis to the extreme fibers of the section, in inches

I = moment of inertia of the section, in inches^4 for a simply supported beam

$$M = \frac{P\,(L)}{4} \qquad \text{Eq. 5}$$

where

P = load, in pounds

L = span length, in inches

The magnitude of the force is obtained by substituting the value of M from equation 5 into equation 4 and solving for P:

$$P = \frac{4\,(f)\,(I)}{L\,(c)} \qquad \text{Eq. 6}$$

Substituting 3.24 in.^{4}, 18 in., and 0.62 in. for I, L, and c respectively, equation 6 reduces to:

$$P = 1.16 \text{ in.}^2\,(f) \qquad \text{Eq. 7}$$

The values used for I, L, and c are characteristic of the bearing plate under consideration.

Averaging the tensile strain observed in the four bolts of the anti-uplift roller permitted the calculation of the upward vertical force at the jacking abutment. See Figure 9. The magnitude of the force was found using the equation: (8)

$$P = f(A) \qquad \text{Eq. 8}$$

where

P = load, in pounds

f = flexural stress, in psi

A = area, in $(\text{inches})^2$

The total area of the four bolts was 1.6 square inches.

CHAPTER III

TEST RESULTS

The results of testing are presented in two parts:

A. Stage III

B. Stage IV

1. Winter Cycle
2. Spring Cycle
3. Summer Cycle
4. Calculation of stresses

The results of Stage III and Stage IV are presented in a manner similar to that used in presenting the results of Stages I and II. (1) The results of Stage III were similar to those obtained in Stage II; therefore, they are presented briefly for comparison with the results of Stage II. For Stage IV, the resultant piling stresses and maximum principal girder stresses are presented graphically for each cycle. The stress distribution on the piling are shown relative to the location of the corresponding strain gauges. The girder stresses are shown as stress contours within the limits outlined by the integral abutment and the position of the rectangular rosettes. The variations of the piling stress corresponding to changes in induced movements are also shown graphically. Stress levels within and on the integral abutment are also presented. For each cycle the applied loads, deflections, time, and temperature are presented in a tabular form. The vertical forces at the

simply supported end and the soil pressure acting on the integral abutment, both resulting from rotation and/or translation of the integral abutment, are also shown in tabular form.

The majority of stresses presented in the body of this study are those corresponding to +1.000 or -1.000 inch induced movement. However, the girder web stresses for the +1/2-inch release of the winter cycle and the stresses corresponding to the spring cycle are also presented. The reason for presenting the stresses in this manner is that the stresses followed a uniform rate of change and usually reached their highest magnitude at the maximum relative deflection of +1000 or -1.000 inch. A complete set of results for piling and girder stresses, plotted for each 1/2 inch interval of induced movement, for Stage IV (winter and summer) is included in Appendix A.

In relation to Stage IV, an attempt was made to verify the stresses recorded for the +1.000 and -1.000 induced movement at points on the bearing pile and girder web. The necessary calculations were performed by the use of the tabular values for various loads.

A. Stage III

The results of Stage III, expansion and contraction, were quite similar to those of Stage II. (1) The only physical difference between the two stages was the additional construction of the concrete deck slab and subsequent action of the composite section.

The stresses in the bearing piles showed the greatest amount of similarity. This similarity is illustrated in Figures 20, 21, 22, and 23 which present piling stress vs induced movement for expansion

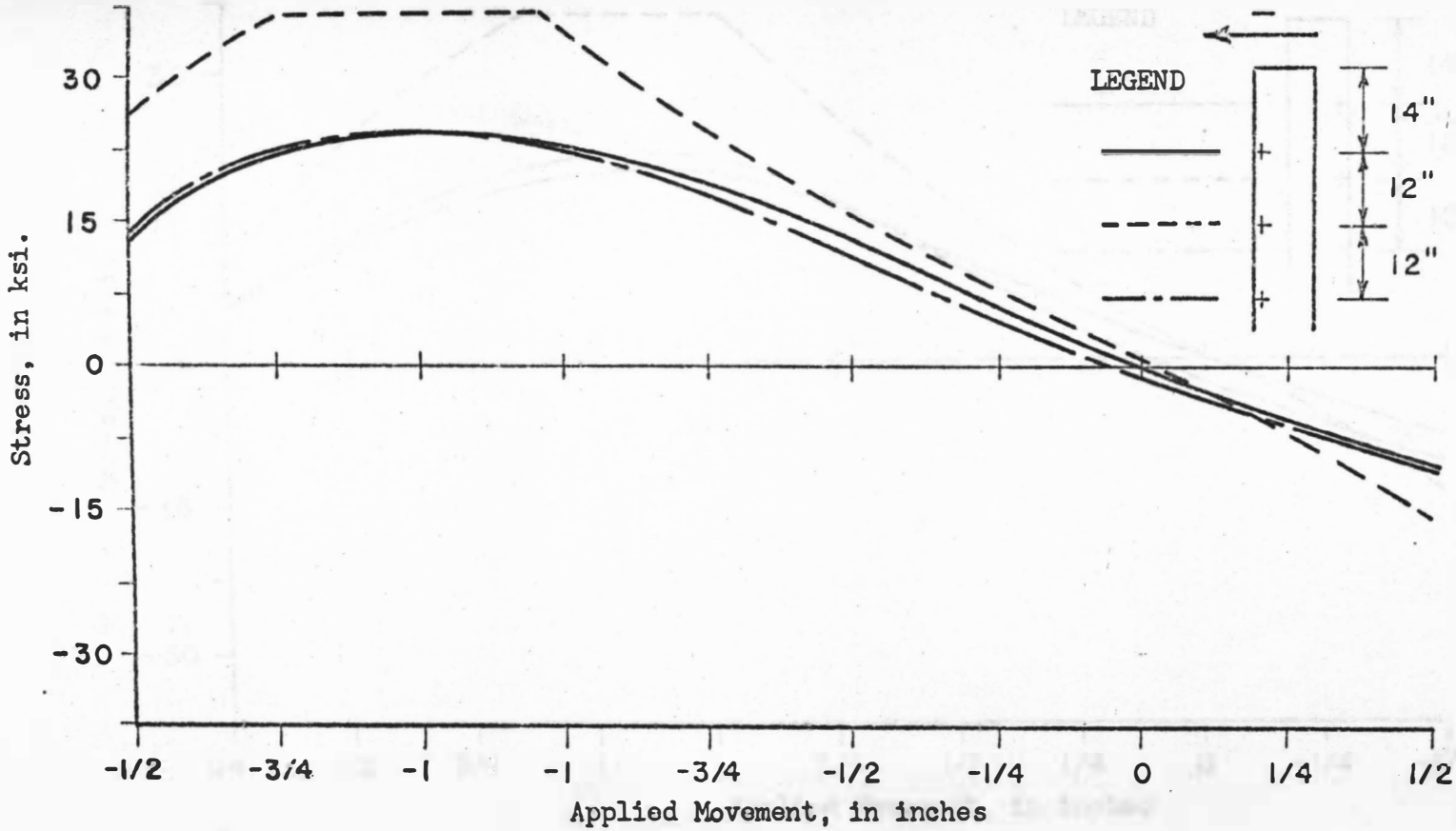

FIGURE 20. Piling Stresses vs Induced Movements. Stage II, Contraction Cycle.

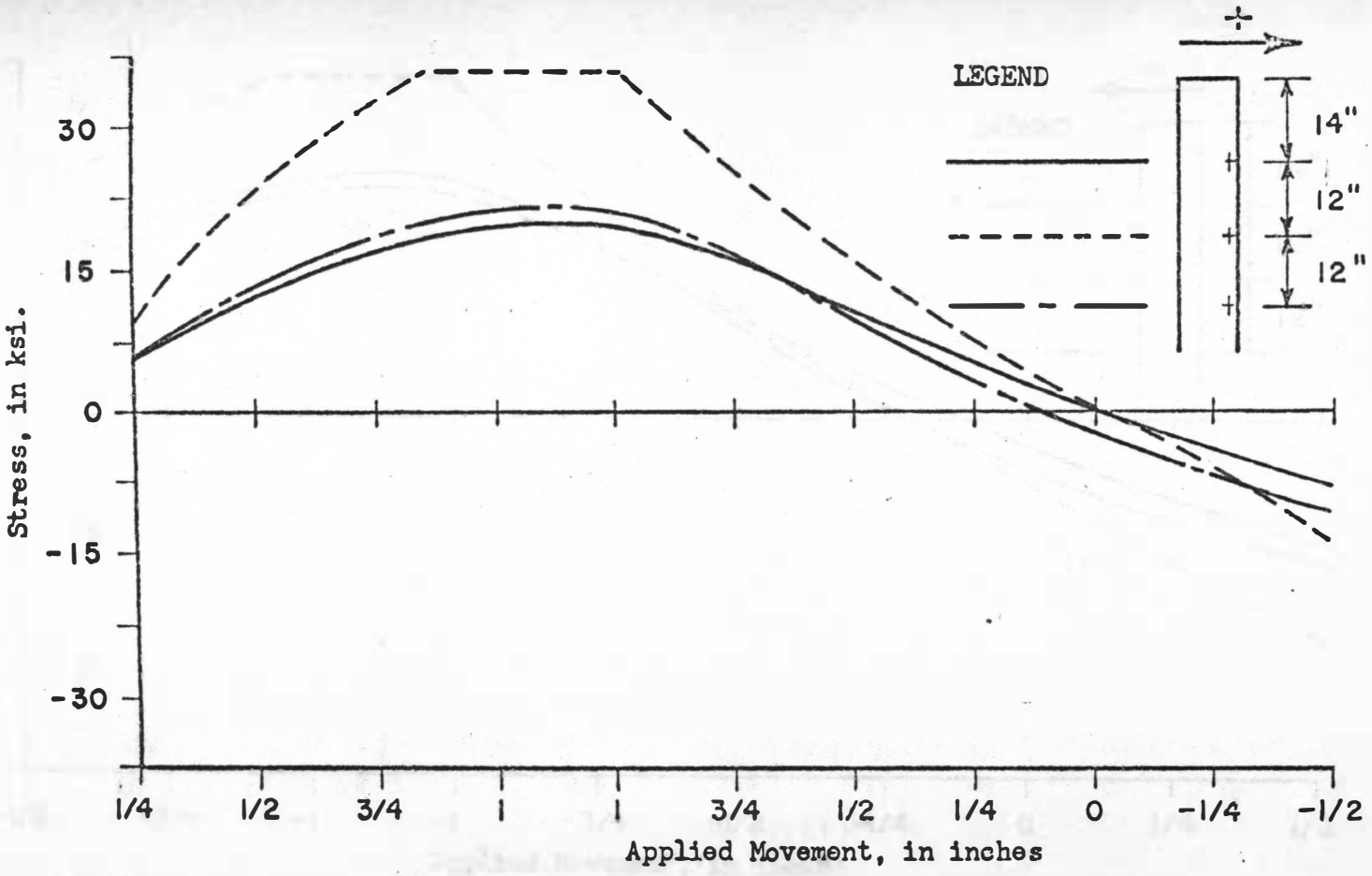

FIGURE 21. Piling Stresses vs Induced Movements. Stage II, Expansion Cycle.

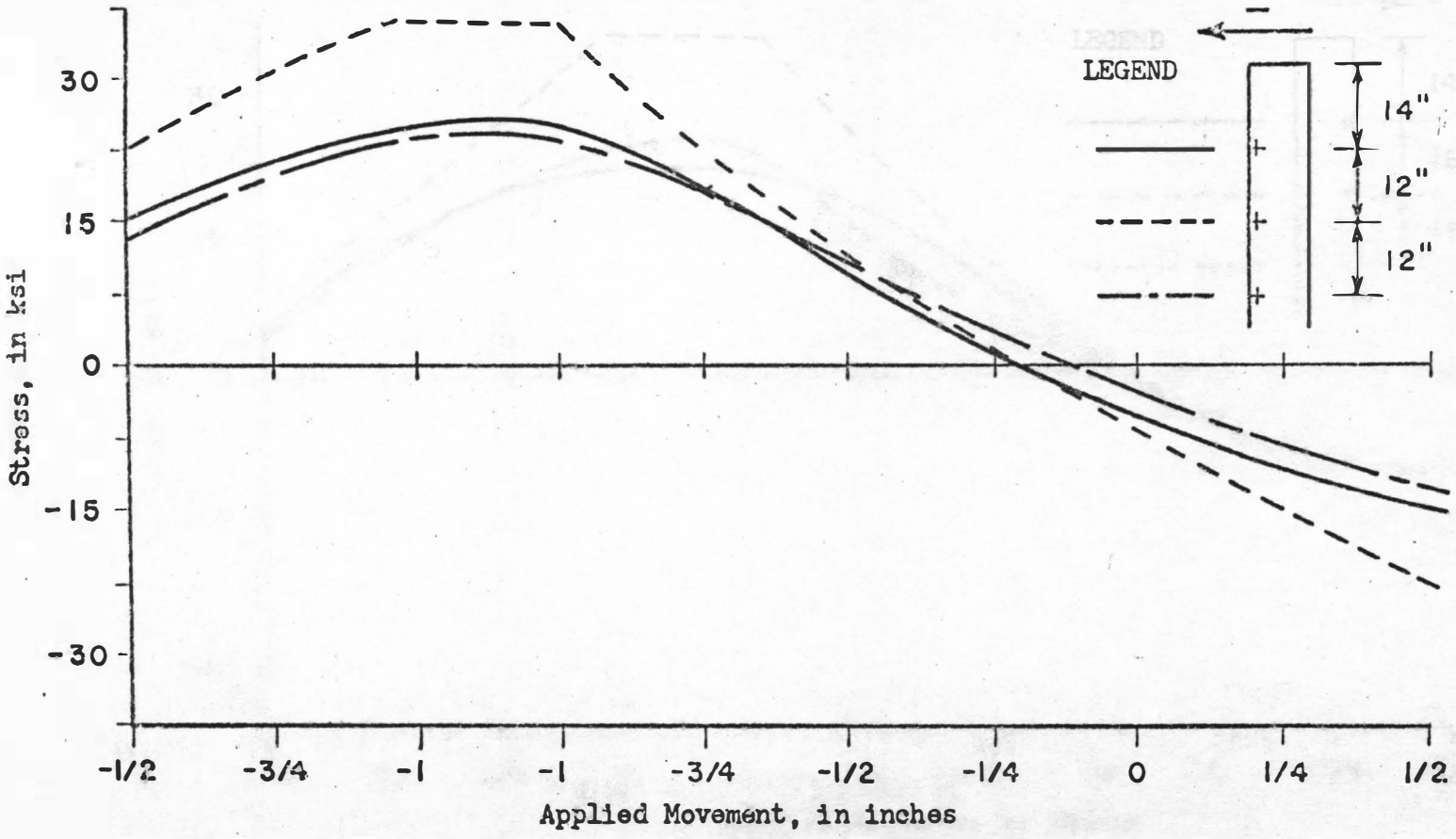

FIGURE 22. Piling Stresses vs Induced Movements. Stage III, Contraction Cycle.

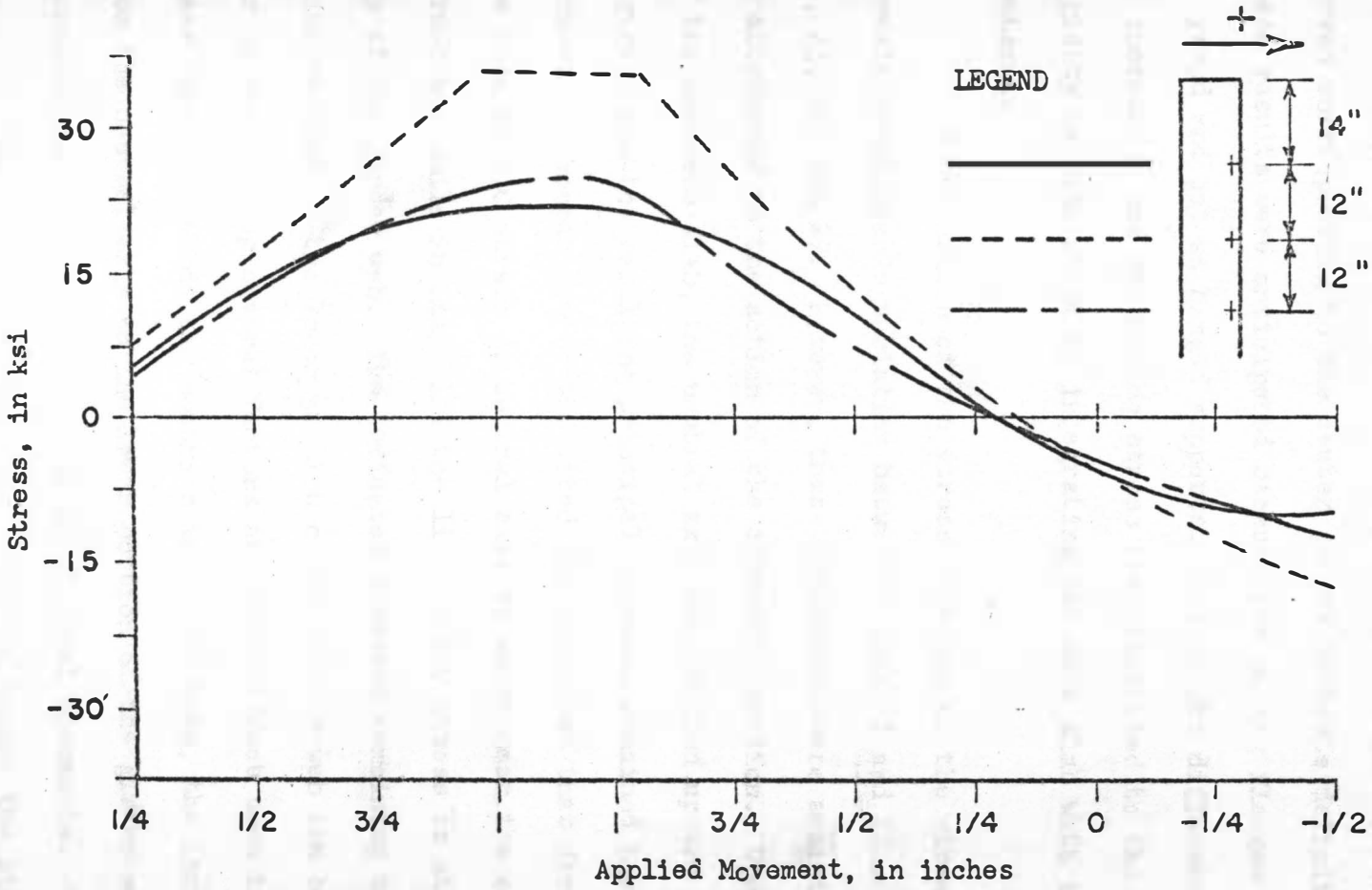

FIGURE 23. Piling Stresses vs Induced Movements. Stage III, Expansion Cycle.

and contraction of both Stages II and III. The flat portion of the curves corresponding to the center gauges indicate definite yielding. These results were anticipated because the piling flanges were designed to yield and act as hinged supports. The slight differences in rate of increasing and decreasing stress are attributed to the increased rigidity brought about by integrating the deck slab with the integral abutment.

A comparison of the stress contours on the girder web reveals considerable variation between Stages II and III. See Figures 24, 25, 26, and 27. However, these variations were anticipated and may be attributed to the action of the composite section. Upon the addition of the concrete slab, the neutral axis was shifted upward as shown in Figure 7 and the resulting principal stresses remained the same or were reduced. A comparison of the cited figures shows that for Stage II the line of 0.0 stress or neutral axis is at or near the center of the girder web while in Stage III the line of 0.0 stress is at or near the top of the girder web. The indicated stresses remaining the same or being reduced in the lower portion of the girder web can be accounted for by considering several factors and their effect upon the stress. These factors include the sections increased area, the increased distance from the neutral axis to the lower portion of the girder web, and the increased load needed to simulate the thermal movements.

The increase in the load needed to induce the simulated movements resulted from the greater rigidity of the structure. The change in load is shown by comparing Tables 1, 2, 3, and 4.

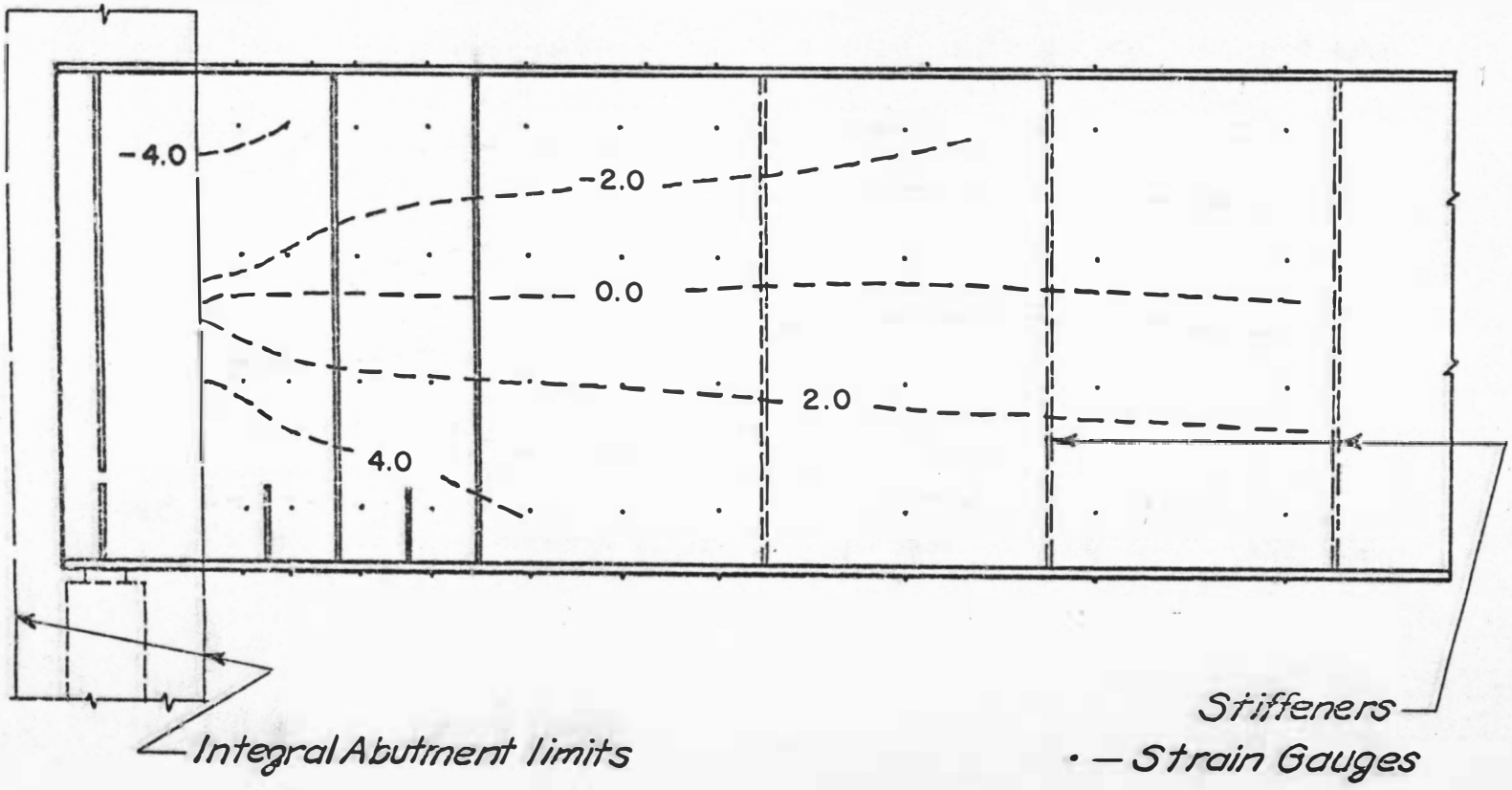

FIGURE 24. Principal Stress Contours, in ksi. Stage II, Contraction Cycle, -1".

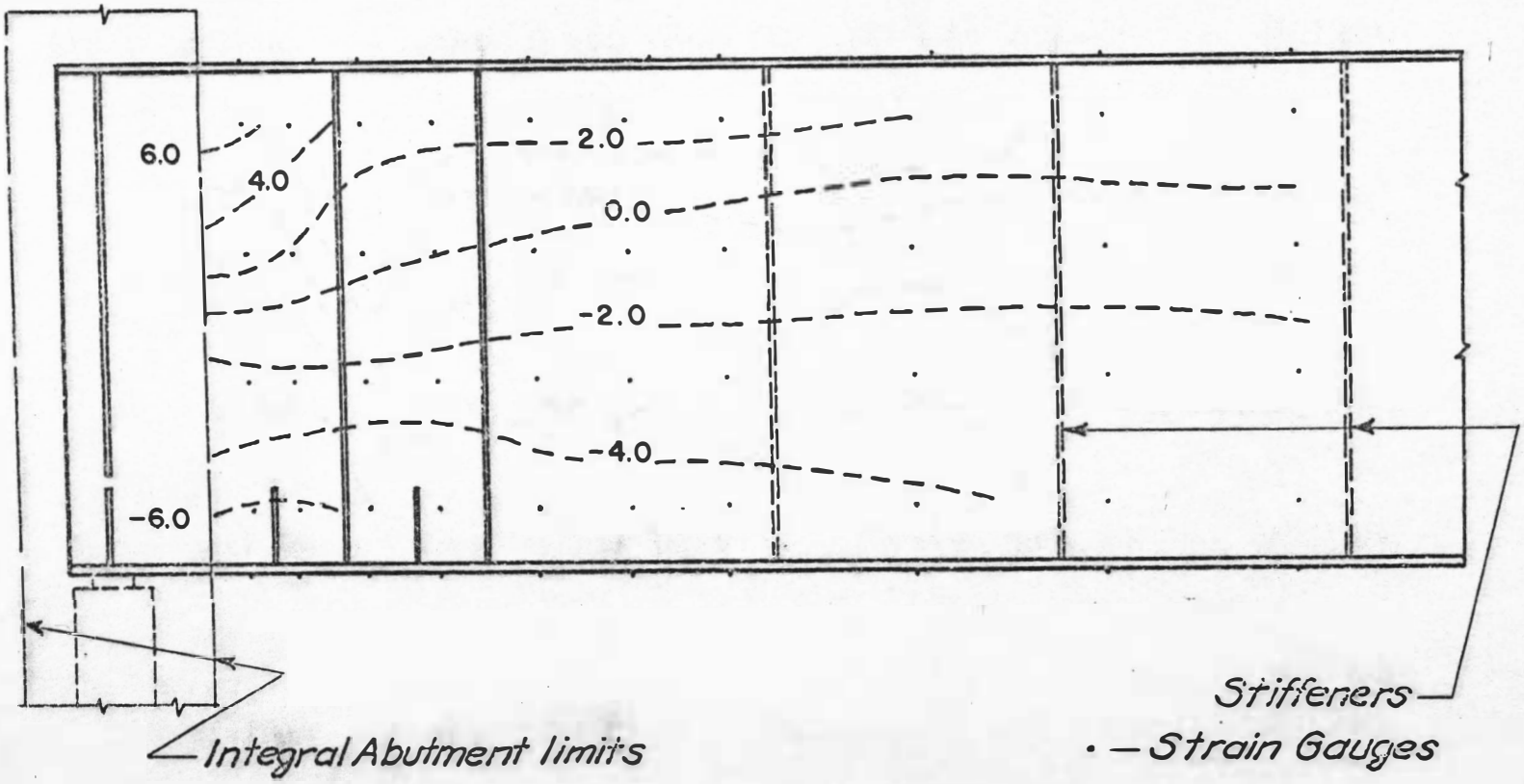

FIGURE 25. Principal Stress Contours, in ksi. Stage II, Expansion Cycle, +1".

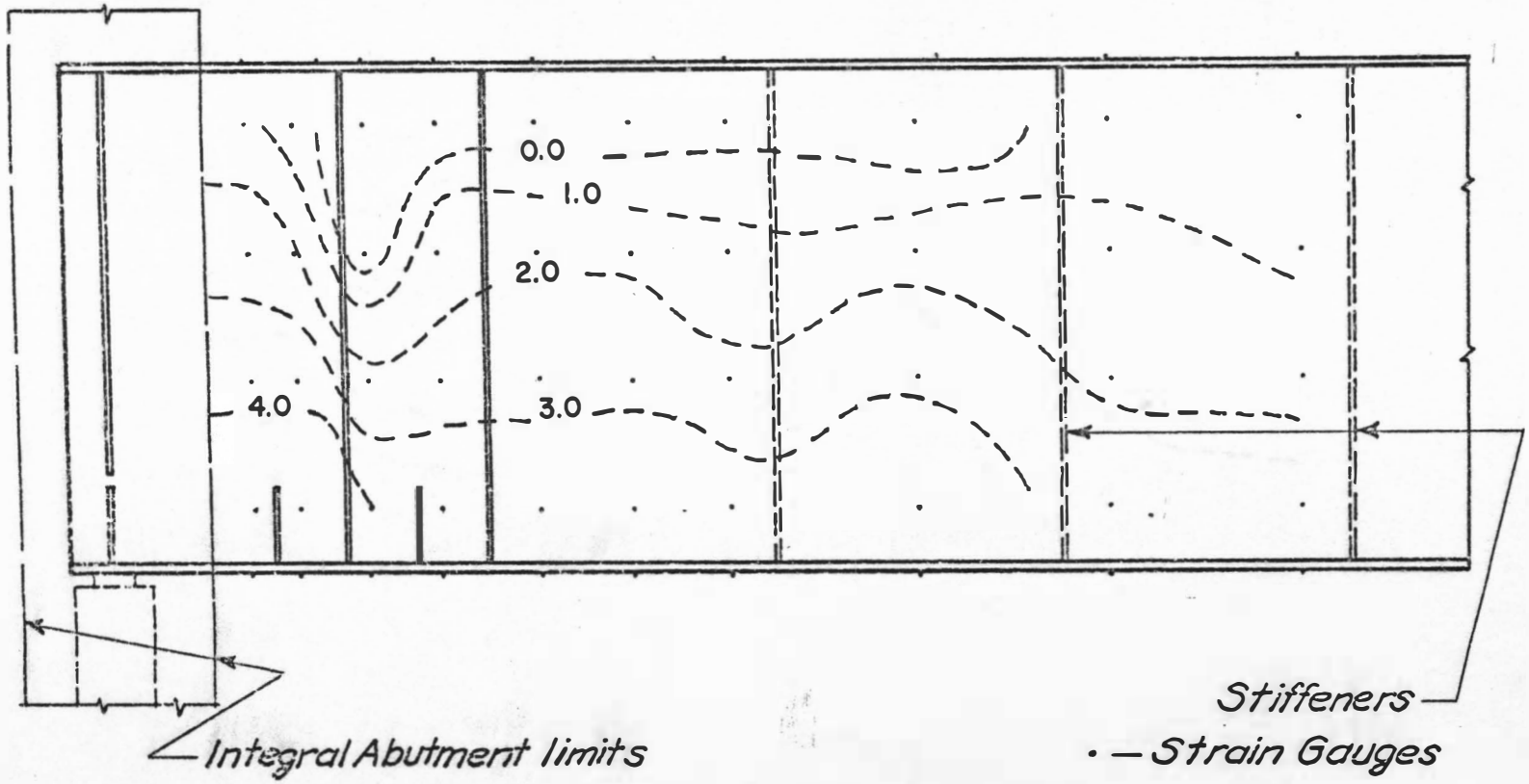

FIGURE 26. Principal Stress Contours, in ksi. Stage III, Contraction Cycle, -1".

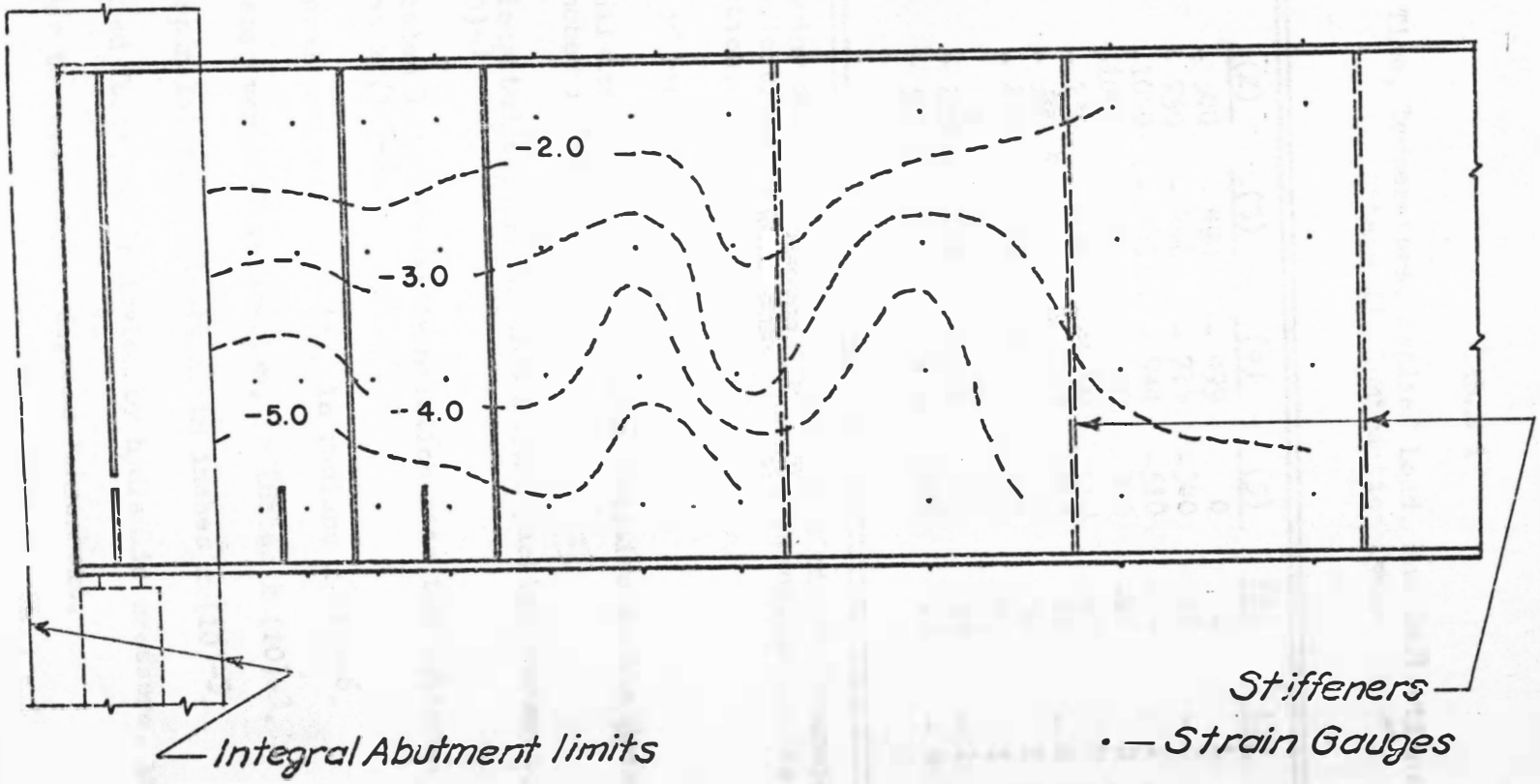

FIGURE 27. Principal Stress Contours, in ksi. Stage III, Expansion Cycle, +1".

TABLE 1

Time, Temperature, Applied Load, and Deflections.
Stage II, Contraction Cycle

(1)	(2)	(3)	(4)	(5)	(6)	(7)	(8)	(9)
7:45	- 500	- 490	- 499	0	2	1	-19.6	68.0
8:45	- 750	- 746	- 724	-340	-16	- 2	-27.4	69.0
9:45	-1000	- 983	- 944	-510	-24	1	-32.6	70.0
10:45	-1000	- 988	- 950	-340	-21	0	-	70.0
11:45	- 750	- 738	- 760	0	10	0	-	70.0
12:45	- 500	- 498	- 532	340	24	- 2		70.0
13:45	- 250	- 240	- 290	510	34	2	5.5	70.0
14:45	0	0	- 51	680	45	1	11.0	70.0
15:45	+ 250	+ 248	+ 238	680	59	- 1	19.2	70.0
16:45	+ 500	+ 501	+ 476	1190	73	- 4	26.2	70.0

The following directions are taken as "positive": Expansion movements, upward deflections, and forces causing compression in the girder cross-section.

(1) Time of recording.

(2) Nominal longitudinal translation relative to the jacking abutment, in inches x $(10)^{-3}$.

(3) Net longitudinal translation at the jacking abutment, in inches x $(10)^{-3}$.

(4) Indicated longitudinal translation near the integral abutment, in inches x $(10)^{-3}$.

(5) Integral abutment rotation, in radians x $(10)^{-6}$.

(6) Mid-span vertical deflection, in inches x $(10)^{-3}$.

(7) Mid-span lateral deflection, in inches x $(10)^{-3}$.

(8) Applied force, as indicated by hydraulic pressure, in Kips.

(9) Girder temperature, in degrees Fahrenheit.

TABLE 2

Time, Temperature, Applied Load, and Deflections.
Stage II, Expansion Cycle

(1)	(2)	(3)	(4)	(5)	(6)	(7)	(8)	(9)
7:30	+ 250	+ 260	+ 247	170	18	12	10.7	68.0
8:30	+ 500	+ 511	+ 482	850	39	8	22.0	68.0
9:30	+ 750	+ 763	+ 719	1020	55	4	30.2	69.0
10:30	+1000	+1002	+ 955	1360	67	- 2	35.7	69.5
11:30	+1000	+1003	+ 957	1360	65	- 3	-	69.5
12:30	+ 750	+ 760	+ 737	510	26	- 2	-	70.0
13:30	+ 500	+ 522	+ 504	340	11	0	-	70.5
14:30	+ 250	+ 269	+ 268	- 170	0	0	- 5.2	70.5
15:30	0	+ 31	+ 30	- 170	- 1	- 7	- 9.1	71.0
16:30	- 250	- 221	- 238	- 510	0	-18	-13.7	71.0
17:30	- 500	- 469	- 460	- 510	7	-27	-19.0	70.0

The following directions are taken as "positive": Expansion movements, upward deflections, and forces causing compression in the girder cross-section.

(1) Time of recording.

(2) Nominal longitudinal translation relative to the jacking abutment, in inches x $(10)^{-3}$.

(3) Net longitudinal translation at the jacking abutment, in inches x $(10)^{-3}$.

(4) Indicated longitudinal translation near the integral abutment, in inches x $(10)^{-3}$.

(5) Integral abutment rotation, in radians x $(10)^{-6}$.

(6) Mid-span vertical deflection, in inches x $(10)^{-3}$.

(7) Mid-span lateral deflection, in inches x $(10)^{-3}$.

(8) Applied force, as indicated by hydraulic pressure, in Kips.

(9) Girder temperature, in degrees Fahrenheit.

TABLE 3

Time, Temperature, Applied Load, and Deflections.
Stage III, Contraction Cycle

(1)	(2)	(3)	(4)	(5)	(6)	(7)	(8)	(9)
6:00	- 500	- 500	- 500	0	0	0	-	68.0
7:00	- 750	- 754	- 710	-340	- 8.0	- 1	35.8	68.0
8:00	-1000	-1004	- 930	-510	-15.0	- 2	41.8	68.0
9:00	-1000	-1008	- 934	-340	-14.0	- 2	-	68.5
10:00	- 750	- 747	- 762	0	+ 2.0	- 1	-	69.0
11:00	- 500	- 502	- 542	+170	+ 9.0	0	4.1	69.5
12:00	- 250	- 248	- 307	+340	+12.0	0	10.3	70.0
13:00	0	+ 1	- 74	1020	+25.0	+ 3	21.3	70.0
14:00	+ 250	+ 256	+ 235	1020	+30.0	+ 6	30.2	70.0
15:00	+ 500	+ 500	+ 472	1190	+37.0	+11	38.4	70.0

The following directions are taken as "positive": Expansion movements, upward deflections, and forces causing compression in the girder cross-section.

(1) Time of recording.

(2) Nominal longitudinal translation relative to the jacking abutment, in inches x $(10)^{-3}$.

(3) Net longitudinal translation at the jacking abutment, in inches x $(10)^{-3}$.

(4) Indicated longitudinal translation near the integral abutment, in inches x $(10)^{-3}$.

(5) Integral abutment rotation, in radians x $(10)^{-6}$.

(6) Mid-span vertical deflection, in inches x $(10)^{-3}$.

(7) Mid-span lateral deflection, in inches x $(10)^{-3}$.

(8) Applied force, as indicated by hydraulic pressure, in Kips.

(9) Girder temperature, in degrees Fahrenheit.

TABLE 4

Time, Temperature, Applied Load, and Deflections.
Stage III, Expansion Cycle

(1)	(2)	(3)	(4)	(5)	(6)	(7)	(8)	(9)
6:30	+ 250	+ 252	+ 224	+ 340	+10	+ 7	13.8	66.5
7:30	+ 500	+ 502	+ 456	+ 510	+20	+16	25.4	66.0
8:30	+ 750	+ 751	+ 682	+ 510	+31	+27	35.0	66.5
9:30	+1000	+1002	+ 910	+ 680	+42	+34	42.5	67.0
10:30	+1000	+1005	+ 914	+ 680	+41	+34	-	67.0
11:30	+ 750	+ 750	+ 720	+ 170	+11	+26	-	67.0
12:30	+ 500	+ 490	+ 489	0	+ 4	+28	-	67.0
13:30	+ 250	+ 249	+ 257	0	- 1	+30	9.1	67.5
14:30	0	- 4	- 7	- 170	- 6	+28	15.3	67.5
15:30	- 250	- 253	- 222	- 340	-10	+28	22.8	68.0
16:30	- 500	- 504	- 443	- 680	-15	+25	30.7	68.5

The following directions are taken as "positive": Expansion movements, upward deflections, and forces causing compression in the girder cross-section.

(1) Time of recording.

(2) Nominal longitudinal translation relative to the jacking abutment, in inches x $(10)^{-3}$.

(3) Net longitudinal translation at the jacking abutment, in inches x $(10)^{-3}$.

(4) Indicated longitudinal translation near the integral abutment, in inches x $(10)^{-3}$.

(5) Integral abutment rotation, in radians x $(10)^{-6}$.

(6) Mid-span vertical deflection, in inches x $(10)^{-3}$.

(7) Mid-span lateral deflection, in inches x $(10)^{-3}$.

(8) Applied force, as indicated by hydraulic pressure, in Kips.

(9) Girder temperature, in degrees Fahrenheit.

The largest difference between Stages II and III was the observed rotation occurring at the integral abutment. The amount of rotation is indicated in the previously cited tables. The rotation in the two contraction cycles agrees quite closely. This agreement is accounted for by considering that the increased dead weight of the slab was of sufficient magnitude to offset the increased rigidity of the structure. The rotation of the integral abutment during Stage II at 1.0 inch of simulated expansion was twice that of Stage III at 1.0 inch of expansion. This difference is also accounted for by the greater rigidity and dead load.

Because of the existing similarities between Stages II and III, detailed results of Stage III are not presented. However, the representative results already introduced for Stage III will be used for making comparisons with the results presented for Stage IV.

B. Stage IV

1. Winter Cycle

This cycle would correspond to a fall or winter condition where the temperature was depressed causing contraction of the completed structure. During the testing of this stage the backfill and soil surrounding the structure remained unfrozen. This condition is permissible for a fall condition, but is not entirely indicative of the partially frozen subgrade encountered during the extreme winter conditions. No attempt was made to simulate an extreme winter condition caused by the complications and variables which could not have been accounted for during testing.

The forces required for inducing the simulated movements in Stage IV are different from those of Stage III as seen when Tables 3 and 5 are compared. The differences required in loading were anticipated and were caused by the action of the compacted backfill. The active earth pressure of the backfill complimented the induced load in the early portion of the contraction cycle, thus reducing the required loading. In the release segment of the cycle, the passive earth pressure opposed the induced load; therefore, a larger load was required. It is also noted from Tables 3 and 5 that there were differences in the required magnitudes of induced loads for the initial and release segments. These differences are caused by the relatively low active earth pressure and corresponding higher passive earth pressure of granular soils. Table 6 shows the passive pressure developed in the release segment of the contraction cycle.

The observed rotation of the integral abutment, the net longitudinal translation near the integral abutment, and the midspan horizontal and vertical displacements for Stage IV are different when compared with those of Stage III. See Tables 3 and 5. The noted differences can be explained by the backfill pressure, either active or passive, and its subsequent magnitude.

The stress levels determined on the girder within the integral abutment are shown in Figure 28. Because of the variables involved, (1) no analysis of the stress is attempted except that the shear bars appear to be functioning. This conclusion is based

TABLE 5

Time, Temperature, Applied Load, and Deflections
Stage IV, Winter Cycle

(1)	(2)	(3)	(4)	(5)	(6)	(7)	(8)	(9)
6:00	- 500	- 501	- 481	- 240	0	0	-16.3	58.0
7:00	- 750	- 750	- 691	- 440	- 9	0	-26.2	58.0
8:00	-1000	-1002	- 912	- 540	-14	3	-30.8	58.0
9:00	-1000	-1007	- 917	- 510	-13	4	-	59.0
10:00	- 750	- 745	- 737	- 180	+ 4	5	-	59.0
11:00	- 500	- 500	- 533	+ 20	+14	14	+13.8	60.0
12:00	- 250	- 250	- 325	+ 220	+25	15	+31.8	61.0
13:00	0	+ 30	- 120	+ 400	+35	19	+48.6	61.0
14:00	+ 250	+ 200	+ 90	+ 630	+47	21	+69.0	61.0
15:00	+ 500	+ 463	+ 240	+ 800	+58	23	+81.0	62.0

The following directions are taken as "positive": Expansion movements, upward deflections, and forces causing compression in the girder cross-section.

(1) Time of recording.

(2) Nominal longitudinal translation relative to the jacking abutment, in inches x $(10)^{-3}$.

(3) Net longitudinal translation at the jacking abutment, in inches x $(10)^{-3}$.

(4) Indicated longitudinal translation near the integral abutment, in inches x $(10)^{-3}$.

(5) Integral abutment rotation, in radians x $(10)^{-6}$.

(6) Mid-span vertical deflection, in inches x $(10)^{-3}$.

(7) Mid-span lateral deflection, in inches x $(10)^{-3}$.

(8) Applied force, as indicated by hydraulic pressure, in Kips.

(9) Girder temperature, in degrees Fahrenheit.

TABLE 6

Earth Pressure and Vertical Reaction.
Stage IV, Winter Cycle

(1)	(2)	(3)	(4)	(5)	(6)
- 500	-	-	-	-	+4.85
- 750	-	-	-	-	+5.70
-1000	-	-	-	-	+5.30
-1000	-	-	-	-	+5.05
- 750	-	-	-	-	+2.92
- 500	-	-	-	-	+0.80
- 250	+ 7.5	+6.0	+11.0	+ 9.5	-
0	+11.5	+6.5	+16.2	+14.5	-
+ 250	+15.0	+8.0	+20.0	+19.5	-
+ 500	+18.0	+9.0	+22.0	+23.5	-

The following directions are taken as "positive": Expansion movements, upward deflections, and forces causing compression in the girder cross-section.

(1) Time of recording.

(2) Nominal longitudinal translation relative to the jacking abutment, in inches x $(10)^{-3}$.

(3) Net longitudinal translation at the jacking abutment, in inches x $(10)^{-3}$.

(4) Indicated longitudinal translation near the integral abutment, in inches x $(10)^{-3}$.

(5) Integral abutment rotation, in radians x $(10)^{-6}$.

(6) Mid-span vertical deflection, in inches x $(10)^{-3}$.

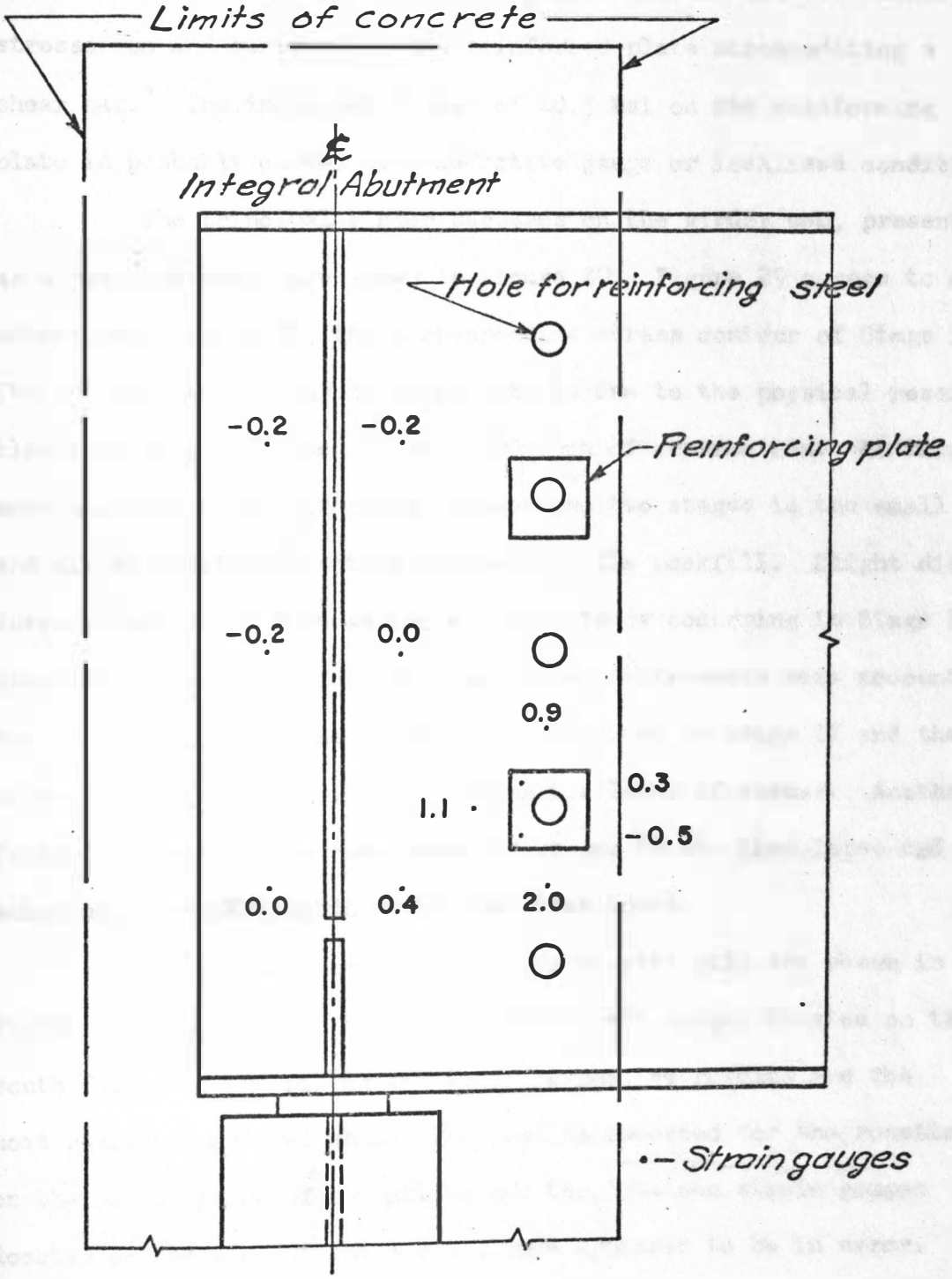

FIGURE 28. Normal Stresses on the Girder Web and Reinforcing Plate, Within the Integral Abutment, in ksi. Stage IV, Winter Cycle, -1".

upon the relation between the applied load and the observed tensile stresses on and surrounding the reinforced plate accommodating a shear bar.* The indicated stress of -0.5 ksi on the reinforcing plate is probably caused by a defective gauge or localized condition.

The principal girder stresses on the girder web, presented as stress contours, are shown in Figure 29. Figure 29 agrees to some extent with Figure 26, the corresponding stress contour of Stage III. The anticipated similarity in results is due to the physical resemblance of Stages III and IV at 1.000 inch of contraction. At this movement, the only difference between the two stages is the small and almost negligible active pressure of the backfill. Slight differences are found such as the maximum stress occurring in Stage IV being less than that of Stage III. These differences were accounted for by the effect of the reduced load required in Stage IV and the effect of the backfill in determining the level of stress. Another factor involved in the comparison of stages is the time lapse and subsequent uncontrollable variations that occur.

The stresses occurring on the bearing pile are shown in Figure 30. It is felt that the 1-inch strain gauges located on the south flange of the piling and their respective results are the most realistic and reliable. The results recorded for the rosettes on the north flange of the piling and the 1/4-inch strain gauges located on the edge of the south flange appeared to be in error.

---

* The stresses presented as minus are compressive in nature. All others presented are tensile stresses.

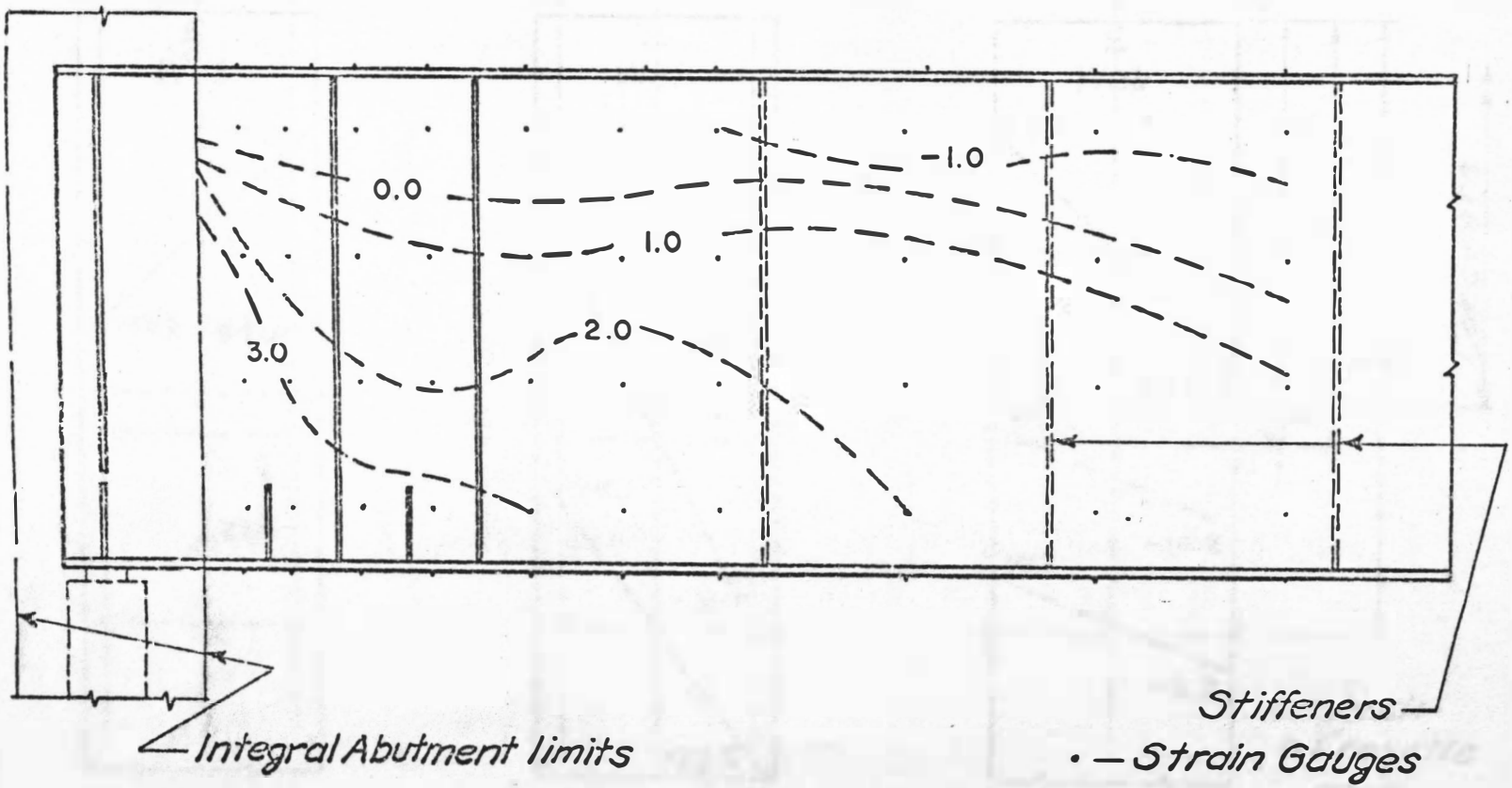

FIGURE 29. Principal Stress Contours, in ksi. Stage IV, Winter Cycle, -1".

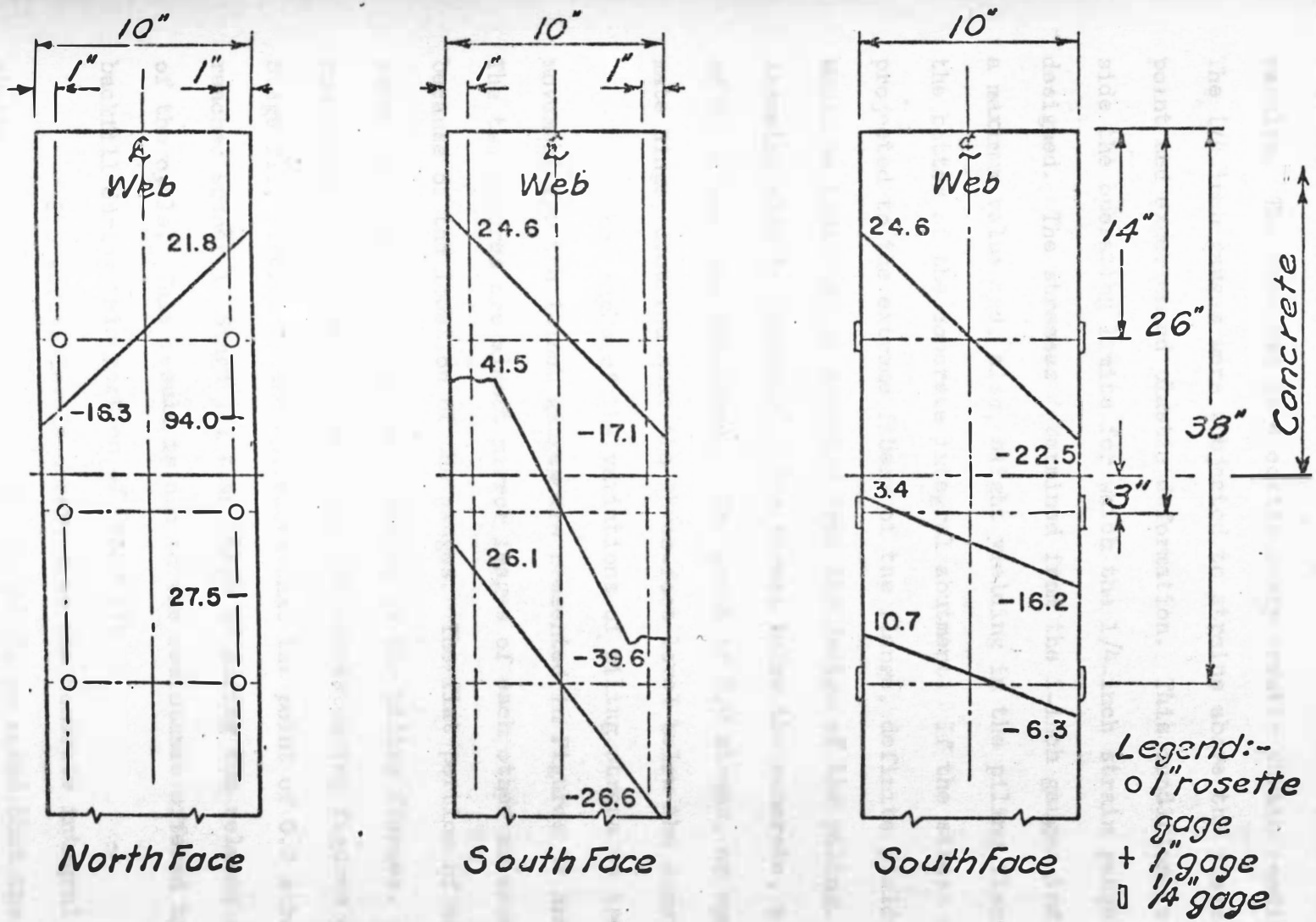

FIGURE 30. Stress Distribution on the Pile, in ksi. Stage IV, Winter Cycle, -1".

Nevertheless, they are presented to provide continuity of the results. The rosettes gave continuously erratic strain readings. The 1/4-inch gauges were subjected to strains above the yield point and experienced plastic deformation. This condition is outside the operating limits for which the 1/4-inch strain gauges were designed. The stresses determined from the 1-inch gauges indicate a maximum value and, also, slight yielding in the piling flange near the bottom of the concrete integral abutment. If the stress were projected to the extreme fibers of the flange, definite yielding would be indicated as expected from the design of the piling. Assuming elastic behavior of the stress below the concrete, a point of 0.0 stress was determined. The point of 0.0 stress, or approximate hinge, occurred near the three-foot level below the concrete.

The graphs of the variations of piling stress vs induced movement for the 1-inch gauges are presented in Figures 31 and 32. The two figures are almost mirror images of each other as expected because of the location of the gauges. The flat portion of each curve indicates the expected yielding of the piling flanges. A comparison of Figures 31 and 32 to the corresponding figures of Stage III, Figures 22 and 23, shows that the point of 0.0 stress is reached sooner in Stage III than Stage IV during the release segment of the cycle. This result is due to the resistance offered by the backfill during this portion of Stage IV.

The stress levels observed on the concrete integral abutment are shown in Figure 33. It should be noted that the stress

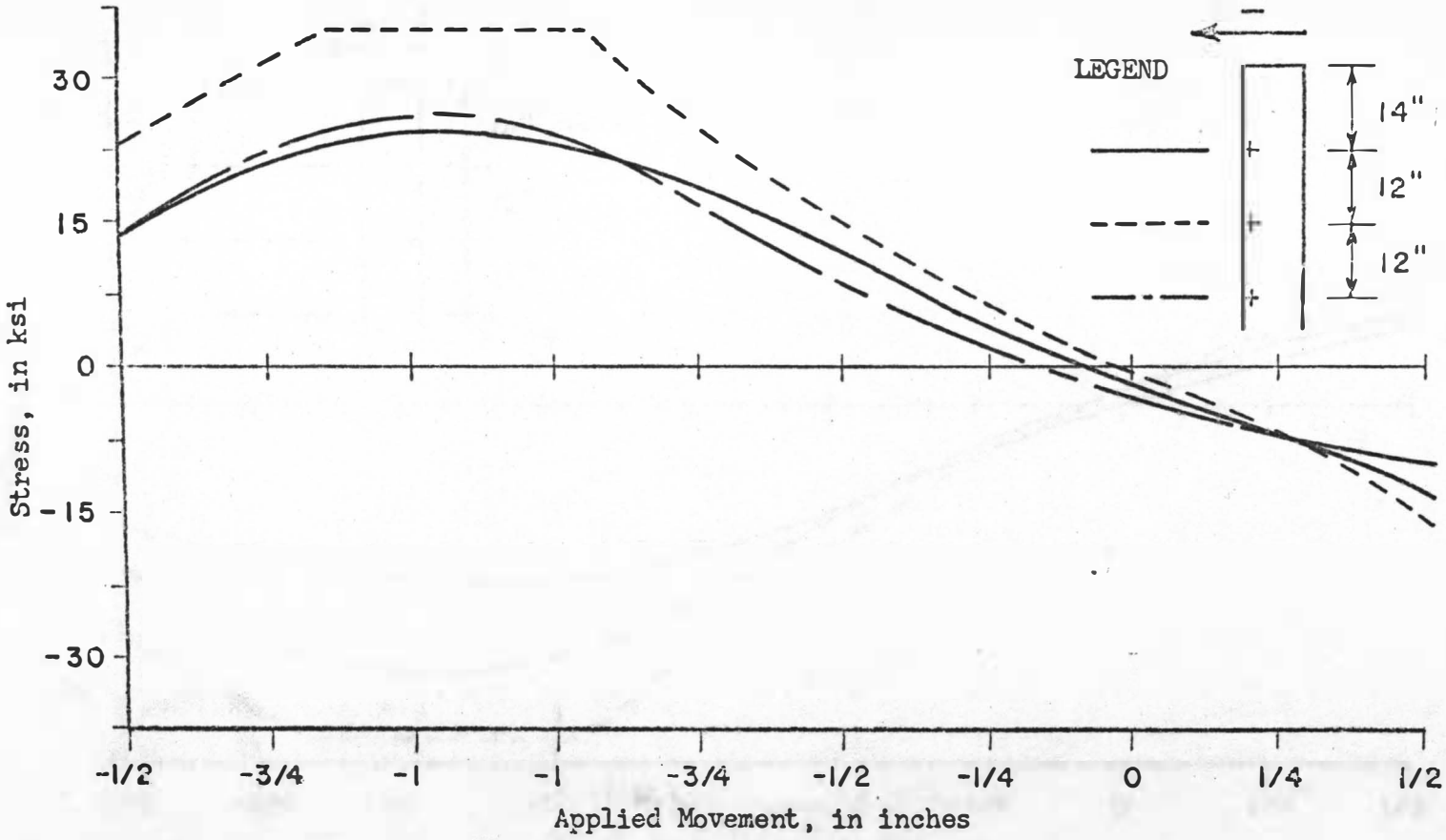

FIGURE 31. Piling Stress vs Induced Movements. Stage IV, Winter Cycle.

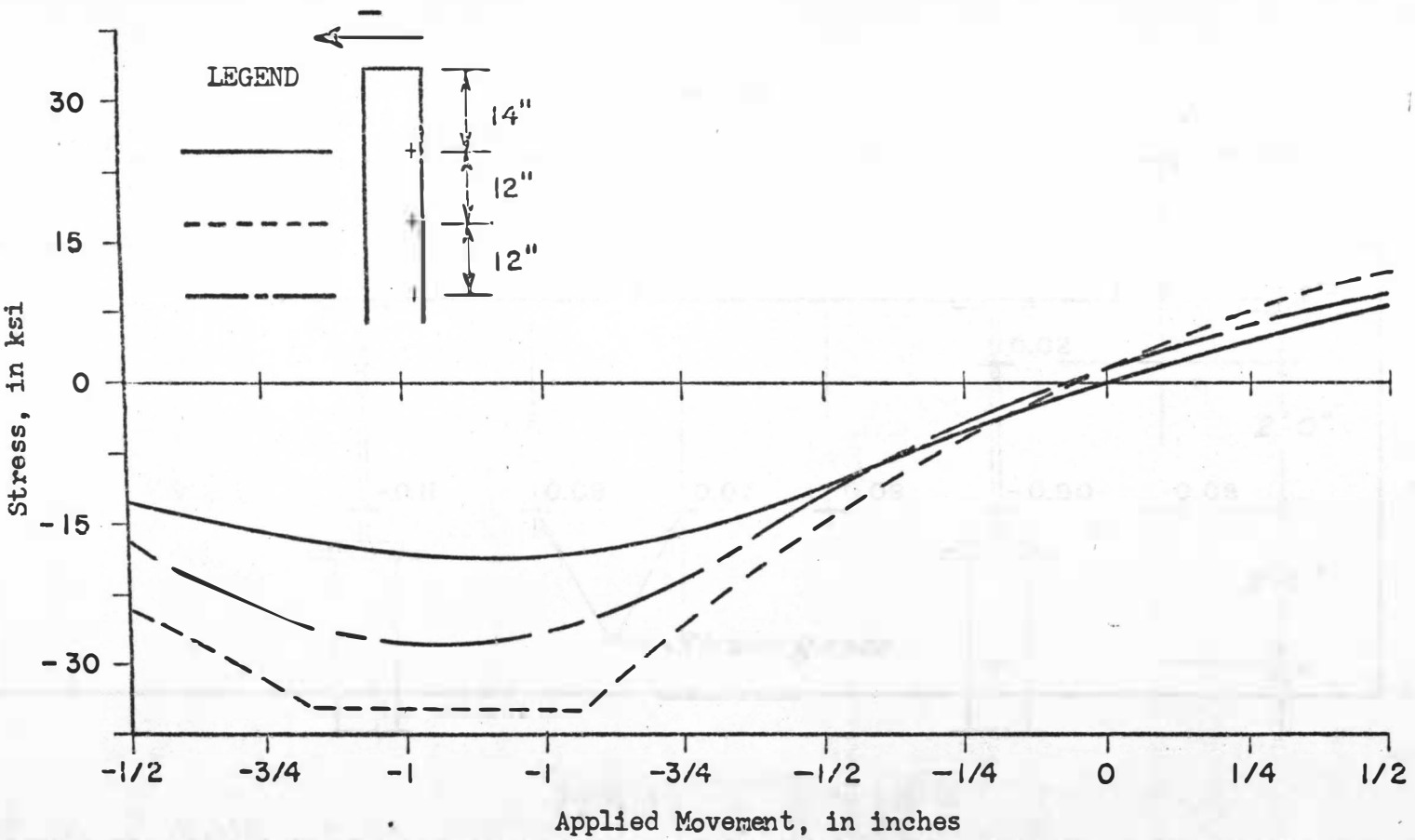

FIGURE 32. Piling Stress vs Induced Movements. Stage IV, Winter Cycle.

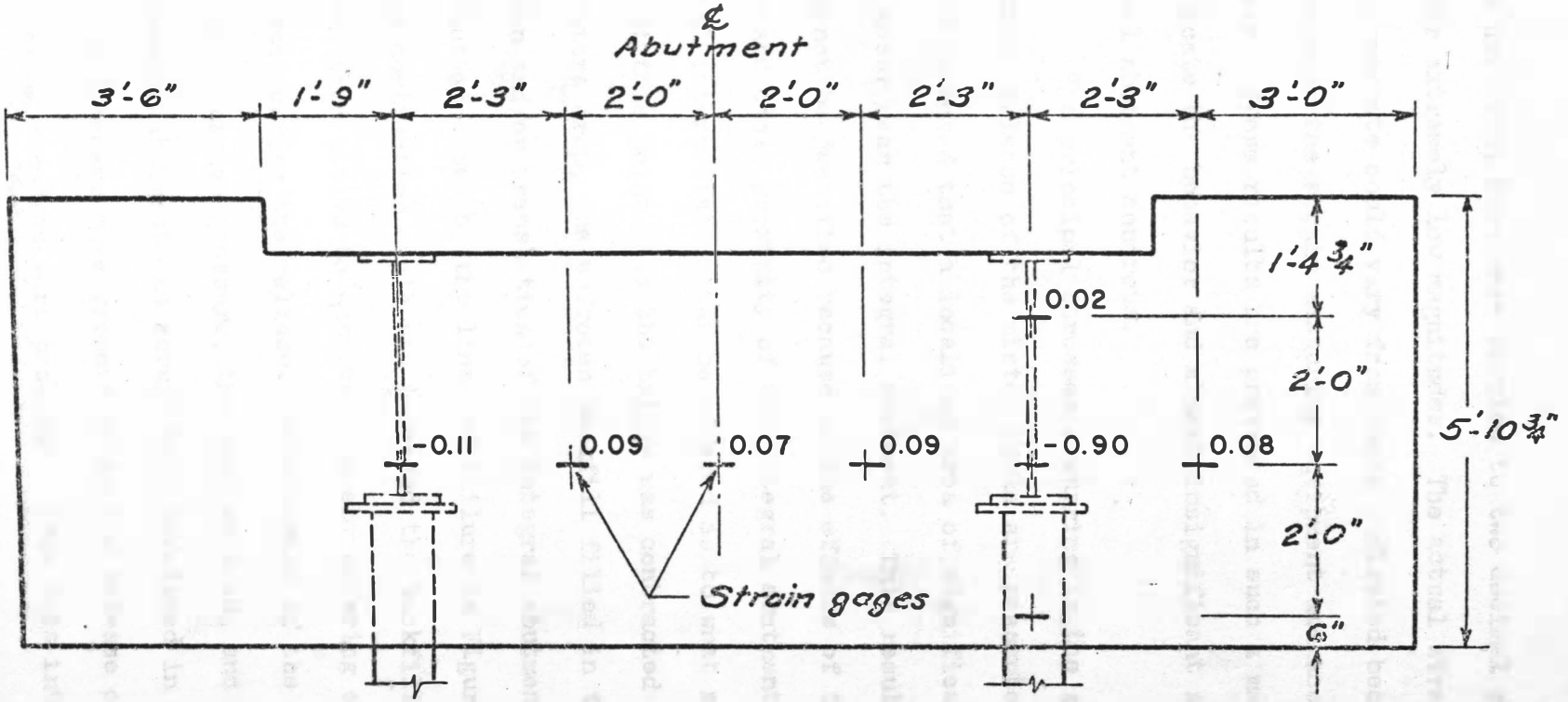

FIGURE 33. Stress Levels on Exterior Face of Integral Abutment, in ksi. Stage IV, Winter Cycle, -1".

levels occurring here were carried to two decimal places because of their extremely low magnitudes. The actual stresses occurring on the concrete could vary from those indicated because of the precision of the strain measuring equipment and accuracy of the operator. These results are presented in such a manner in order to indicate the behavior and almost insignificant stresses in the integral abutment concrete.

The principal stresses occurring in the girder web at + 1/2-inch release of the winter cycle are presented in Figure 34. It will be noted that a localized area of significant stress contours occur near the integral abutment. This result was unexpected and cannot be justified because of the effects of the nearby stiffeners and close proximity of the integral abutment. However, a physical interpretation can be offered as to what might have transpired at this point. As the bridge was contracted simulating a temperature drop, the unfrozen backfill filled in the void left by rotation and/or translation of the integral abutment. This filling-in effect is shown by the lines of failure in Figure 6. As the induced contraction cycle was released the backfill pressure switched from active to passive, thereby offering considerable resistance during the release. As a result of the action of the backfill's passive pressure, the applied load, and the rotation of the integral abutment, an abrupt bend developed in the indicated area. This became more pronounced as the release continued until the existing stresses were produced. From this interpretation the

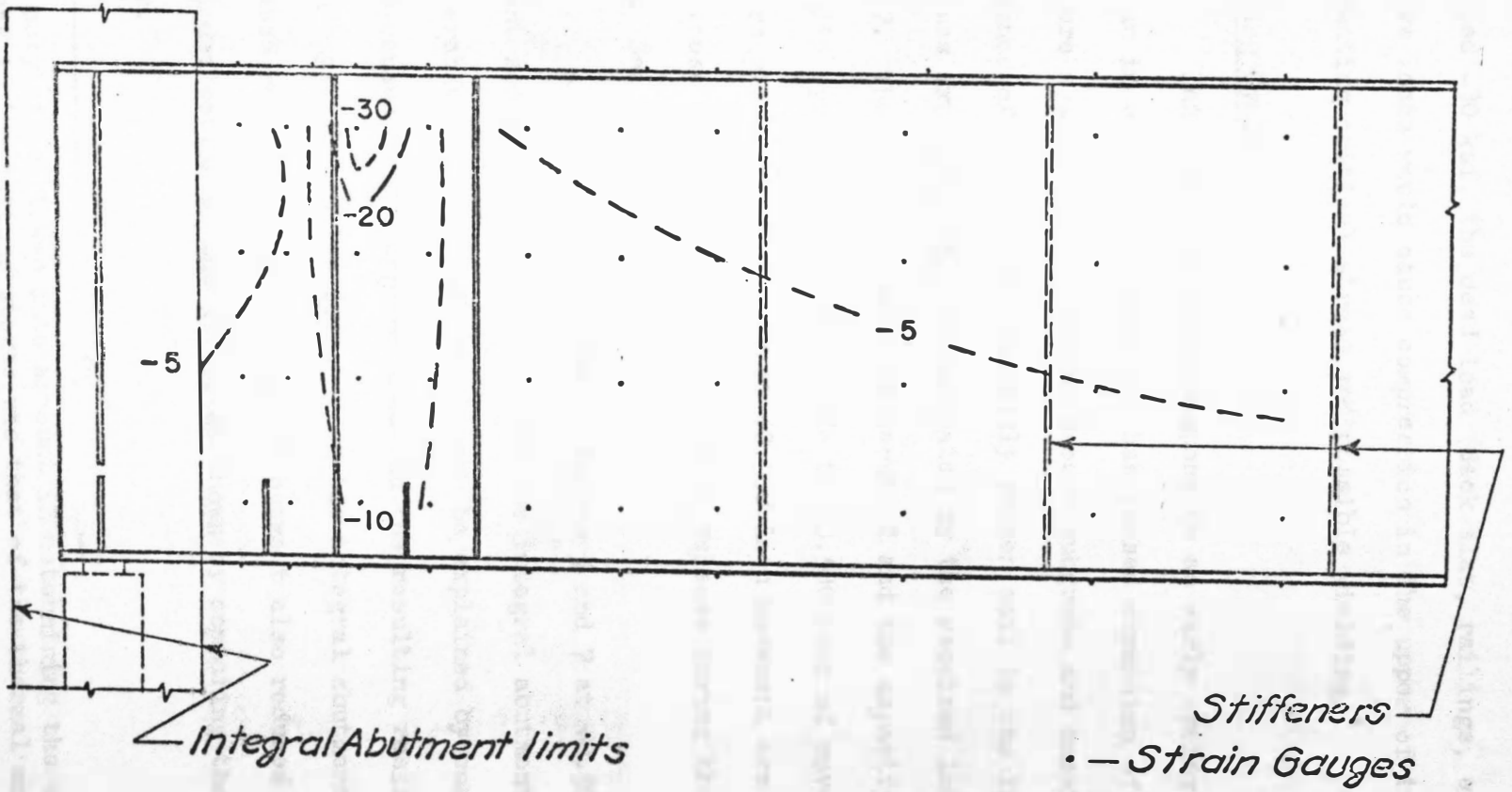

FIGURE 34. Principal Stress Contours, in ksi. Stage IV, Winter Cycle, + 1/2" Release.

observed stresses become very significant. In addition to the indicated -30 ksi, the dead load (deck slab, railings, etc.), and any live loads would cause compression in the upper of the girder web creating critical stress and possible yielding.*

2. Spring Cycle

This cycle would correspond to an early spring condition where an increase in temperature has caused expansion of the completed structure against the partially frozen subgrade and backfill. The resistance offered by the partially frozen soil to the induced movements was extremely high as indicated by the required loads shown in Table 7. The magnitude of load required and the capacity of the hydraulic system limited the cycle to +0.500 inch of movement. The loads required in this cycle at +0.500-inch movement are almost twice those observed at +0.500 inch of release during the winter cycle. See Tables 5 and 7.

A further comparison of Tables 5 and 7 at +0.500 inch of movement shows that the rotation of the integral abutment is also considerably larger. This result can be explained by considering the couple caused by the applied load and the resulting resistance of the frozen backfill and its effect upon the integral abutment. The increased rotation of the integral abutment also reduces the horizontal deflection of the girder as shown by comparing the cited tables.

---

* The only effect taken into account in determining the state of stress in the various stages was that of the thermal movements.

TABLE 7

Time, Temperature, Applied Load, and Deflections.
Stage IV, Spring Cycle

(1)	(2)	(3)	(4)	(5)	(6)	(7)	(8)	(9)
9:30	+250	+241	+145	+1110	20	61	126	59.0
10:30	+500	+499	+377	+1730	10	26	142	58.0

The following directions are taken as "positive": Expansion movements, upward deflections, and forces causing compression in the girder cross-section.

(1) Time of recording.

(2) Nominal longitudinal translation relative to the jacking abutment, in inches x $(10)^{-3}$.

(3) Net longitudinal translation at the jacking abutment, in inches x $(10)^{-3}$.

(4) Indicated longitudinal translation near the integral abutment, in inches x $(10)^{-3}$.

(5) Integral abutment rotation, in radians x $(10)^{-6}$.

(6) Mid-span vertical deflection, in inches x $(10)^{-3}$.

(7) Mid-span lateral deflection, in inches x $(10)^{-3}$.

(8) Applied force, as indicated by hydraulic pressure in Kips.

(9) Girder temperature, in degrees Fahrenheit.

The soil pressure acting on the integral abutment, shown in Table 8, provides information concerning the action of the backfill. It is noted that the recorded pressures are relatively uniform regardless of depth. This result indicates that the backfill is acting with uniform pressure and not with the familiar triangular pressure distribution usually associated with granular soils.

The stress levels within the integral abutment are shown in Figure 35 for this cycle. The stresses observed indicate proper functioning of the shear bars. It is also noted that the stress in the reinforcing plates was less than the stress on the surrounding girder web. This result was expected because of the increased area associated with the reinforcing plates.

The principal stresses occurring in the girder web are shown in Figure 36. The stresses shown indicate that the neutral axis or line of 0.0 stress is relatively close to the flange. This behavior was expected, as pointed out in the previous discussion. The magnitude of the observed stress is relatively high compared to the previous stresses presented in a similar manner. This result is brought about by the large magnitudes of loading required to simulate expansion.

The stresses occurring on the bearing pile are shown in Figure 37. The relatively low stress magnitudes shown on the section does not indicate yielding, even though the girder stresses are relatively high. This observation, combined with the substantial

TABLE 8

Earth Pressure and Vertical Reaction.
Stage IV, Spring Cycle

(1)	(2)	(3)	(4)	(5)	(6)
+250	+ 3.5	+ 4.5	+ 2.5	+ 6.5	-1.63
+500	+14.0	+14.5	+11.0	+14.0	-.185

The following directions are taken as "positive": Expansion movements, upward deflections, and forces causing compression in the girder cross-section.

(1) Time of recording

(2) Nominal longitudinal translation relative to the jacking abutment, in inches x $(10)^{-3}$.

(3) Net longitudinal translation at the jacking abutment, in inches x $(10)^{-3}$.

(4) Indicated longitudinal translation near the integral abutment, in inches x $(10)^{-3}$.

(5) Integral abutment rotation, in radians x $(10)^{-6}$.

(6) Mid-span vertical deflection, in inches x $(10)^{-3}$.

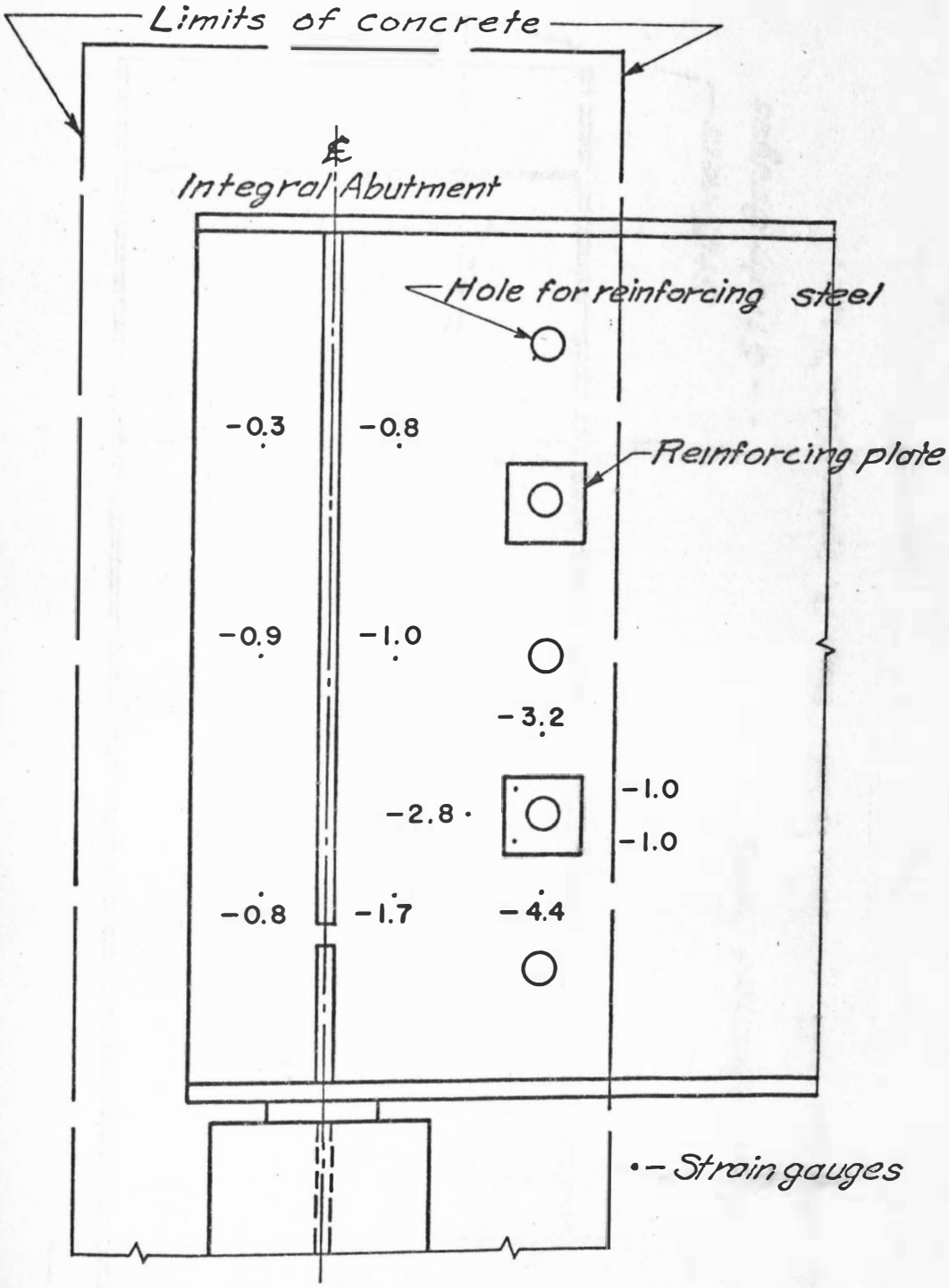

FIGURE 35. Normal Stresses on the Girder Web and Reinforcing Plate, Within the Integral Abutment, in ksi. Stage IV, Spring Cycle, + 1/2".

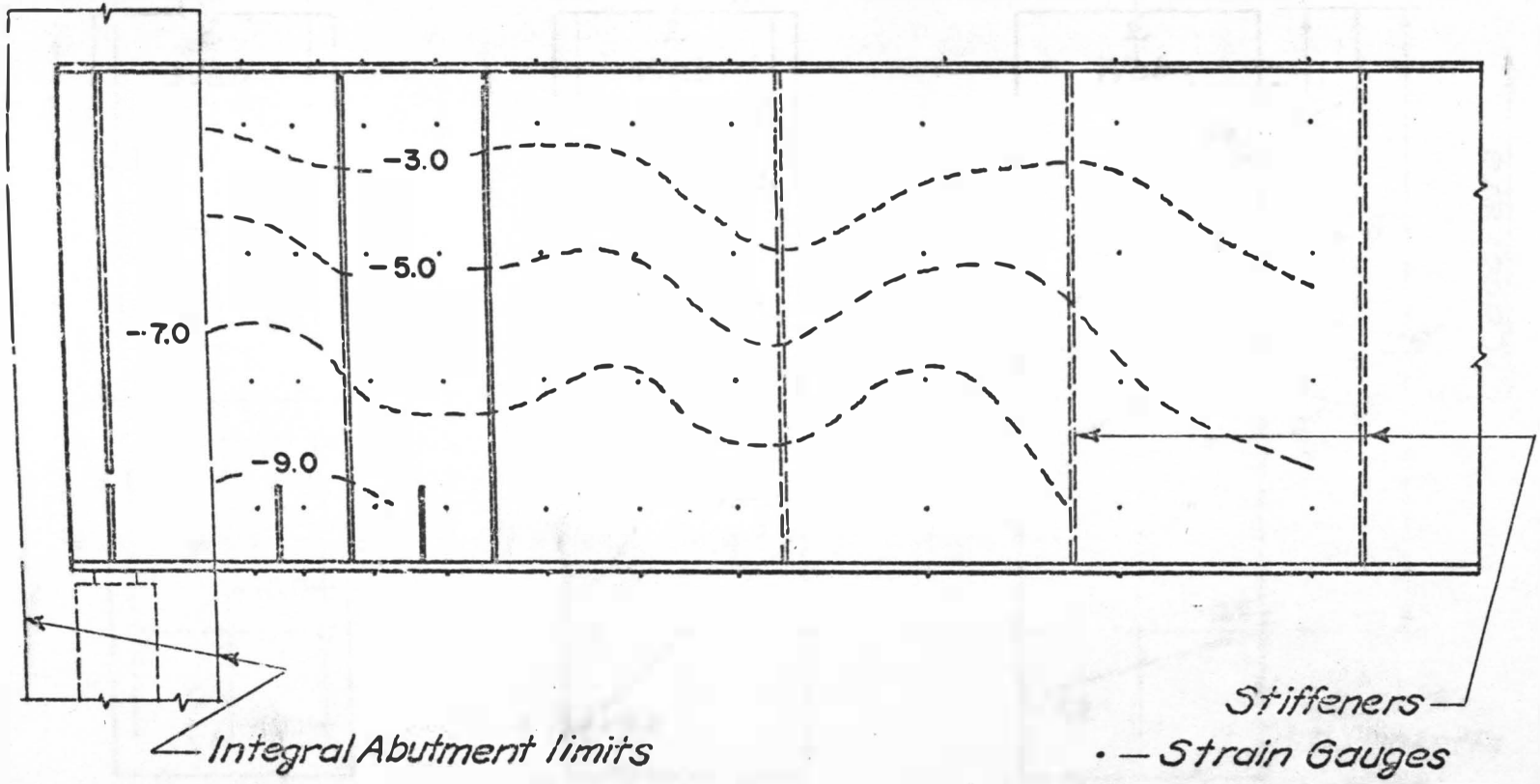

FIGURE 36. Principal Stress Contours, in ksi. Stage IV, Spring Cycle, + 1/2".

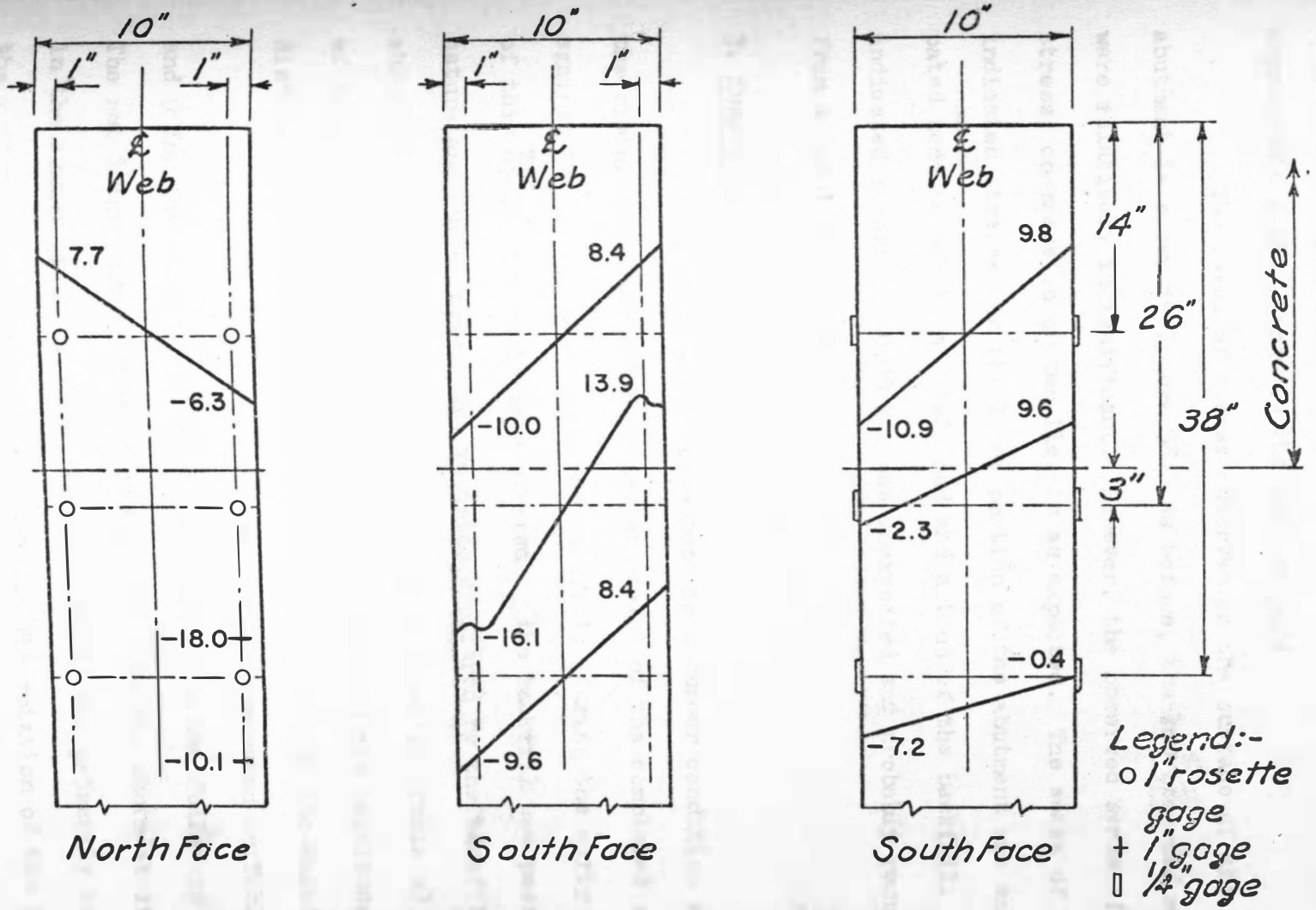

FIGURE 37. Stress Distribution on the Pile, in ksi. Stage IV, Spring Cycle, + 1/2".

rotation previously noted, indicates that the stress patterns approximate a true hinge in the bearing pile.

The level of stress observed on the surface of the integral abutment is shown in Figure 38. As before, the low recorded magnitudes were relatively insignificant. However, the observed sense of the stress, compressive or tensile, is as expected. The sense of the six indicated stresses on the lower portion of the abutment was anticipated because of the applied load and action of the backfill. The indicated stress of -0.03 ksi was unexpected and probably resulted from a localized condition.

3. Summer Cycle

This cycle would correspond to a summer condition where the rising temperature has caused expansion of the completed structure against the unfrozen subgrade and backfill. During the early portions of this cycle, the resistance offered by the backfill was passive in nature and quite large. The resistance offered by the backfill is shown by comparing the required loading of Stage IV (Table 9) to that of Stage III (Table 4). Table 10 also indicates the magnitude and distribution of the resistance (pressure) offered by the backfill.

Further comparison of the results presented in Tables 4 and 9 for the early portions of each cycle give the following results. The net longitudinal translation near the integral abutment is less in the summer cycle of Stage IV. This result was primarily caused by the resistance offered by the backfill. The rotation of the integral

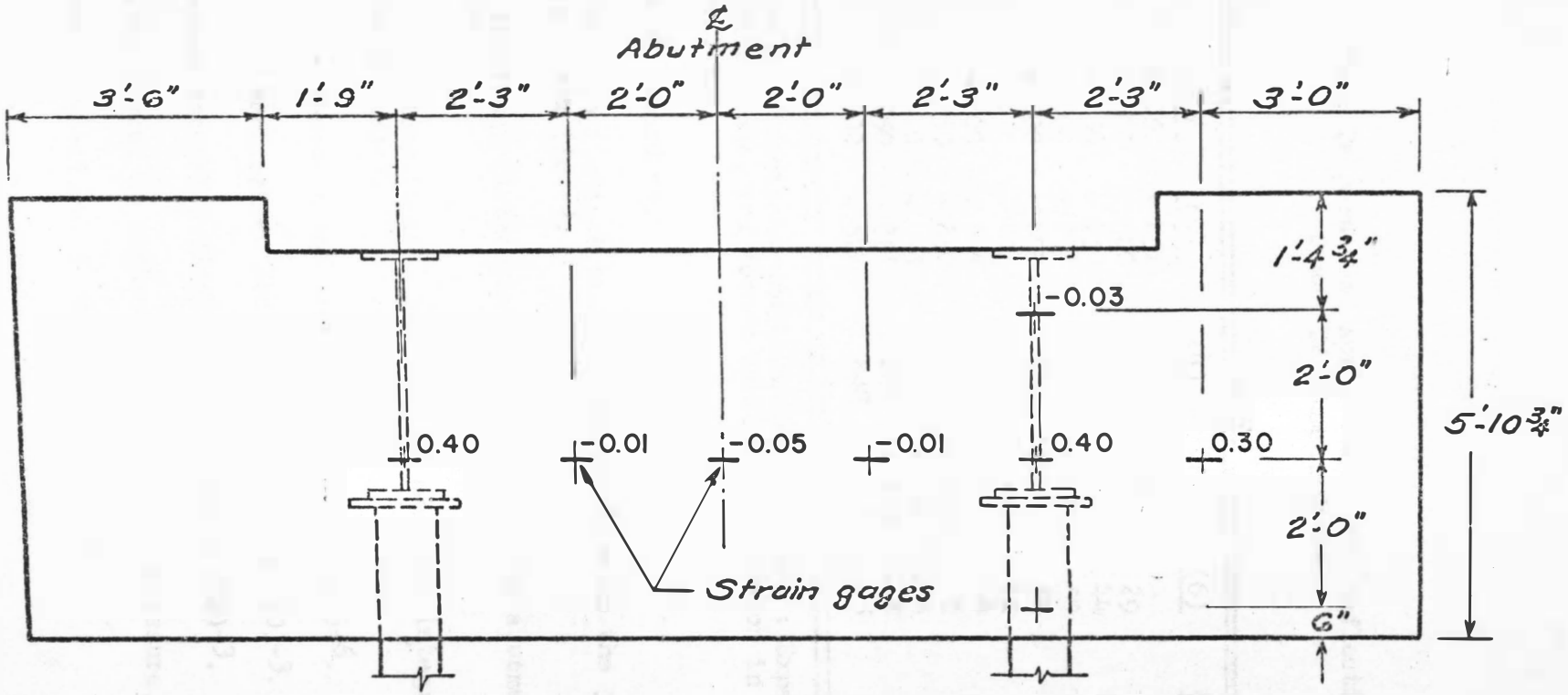

FIGURE 38. Stress Levels on Exterior Face of Integral Abutment, in ksi. Stage IV, Spring Cycle, + 1/2".

TABLE 9

Time, Temperature, Applied Load and Deflections.
Stage IV, Summer Cycle

(1)	(2)	(3)	(4)	(5)	(6)	(7)	(8)	(9)
9:00	+ 250	+ 251	-	-	-	-	-	55.0
10:00	+ 500	+ 500	+ 327	+ 400	29	8	+54.2	59.0
11:00	+ 750	+ 750	+ 532	+ 750	44	11	+73.7	59.0
12:00	+1000	+1003	+ 756	+1020	57	13	+97.4	60.0
13:00	+1000	+1008	+ 768	+1020	52	12	-	61.0
14:00	+ 750	+ 752	+ 560	+ 420	12	4	-	60.5
15:00	+ 500	+ 504	+ 344	+ 280	4	4	-	60.0
16:00	+ 250	+ 250	+ 116	+ 100	1	1	-	60.0
17:00	0	- 3	- 20	+ 40	- 4	2	-	60.0
18:00	- 250	- 251	- 224	- 120	- 9	4	-	60.0
19:00	- 500	- 502	- 448	- 270	-15	5	-	60.0

The following directions are taken as "positive": Expansion movements, upward deflections, and forces causing compression in the girder cross-section.

(1) Time of recording.

(2) Nominal longitudinal translation relative to the jacking abutment, in inches x $(10)^{-3}$.

(3) Net longitudinal translation at the jacking abutment, in inches x $(10)^{-3}$.

(4) Indicated longitudinal translation near the integral abutment, in inches x $(10)^{-3}$.

(5) Integral abutment rotation, in radians x $(10)^{-6}$.

(6) Mid-span vertical deflection, in inches x $(10)^{-3}$.

(7) Mid-span lateral deflection, in inches x $(10)^{-3}$.

(8) Applied force, as indicated by hydraulic pressure, in Kips.

(9) Girder temperature, in degrees Fahrenheit.

TABLE 10

Earth Pressure and Vertical Reaction.
Stage IV, Summer Cycle

(1)	(2)	(3)	(4)	(5)	(6)
+ 250	-	-	-	-	-
+ 500	+ 7.5	+4.0	+10.0	+ 9.0	-0.34
+ 750	+12.0	+4.5	+15.8	+14.0	-0.45
+1000	+16.0	+6.5	+20.5	+19.0	-0.56
+1000	+14.0	+5.5	+14.5	+17.0	-0.44
+ 750	-	-	-	-	-
+ 500	-	-	-	-	-
+ 250	-	-	-	-	-
0	-	-	-	-	+0.13
- 250	-	-	-	-	+1.78
- 500	-	-	-	-	+4.15

The following are taken as "positive": Expansion movements, upward reactions, and passive earth pressure.

(1) Nominal longitudinal translation relative to the jacking abutment, in inches x $(10)^{-3}$.

(2) Net earth pressure on cell #1 on integral abutment, in psi.

(3) Net earth pressure on cell #2 on integral abutment, in psi.

(4) Net earth pressure on cell #3 on integral abutment, in psi.

(5) Net earth pressure on cell #4 on integral abutment, in psi.

(6) Vertical reaction at jacking abutment, in Kips.

abutment was greater in the summer cycle of Stage IV because of the couple caused by the applied loads acting on the integral abutment. As a result of the increased rotation of the integral abutment, the vertical deflection near the midspan of the girder was greater during the summer cycle of Stage IV.

Comparison of the results obtained for the release portion of each testing cycle (Tables 4 and 9) indicates many similarities. The similarities observed result from the physical resemblance of the cycles in question. If the active pressure were eliminated, the two cycles would be identical. It is felt that the rate of release reduced the effects of the active pressure to a point where the cycles were practically the same.

The stress levels within the integral abutment are presented in Figure 39. They indicate proper functioning of the shear bar as was observed in previous cycles of testing. The stress indicated on the reinforcing plate (-1.3 ksi) is less than that observed on the surrounding girder web. This state of stress is associated with the increased area of the reinforcing plate. The stress of 1.8 ksi that is also indicated on the reinforcing plate is probably the result of a faulty gauge or switch in obtaining the strain reading.

The principal stresses observed on the girder web are presented in Figure 40. The stress contours were as expected in regard to those obtained in Stage III expansion, Figure 27. The level of stress was higher in Stage IV than Stage III as a result

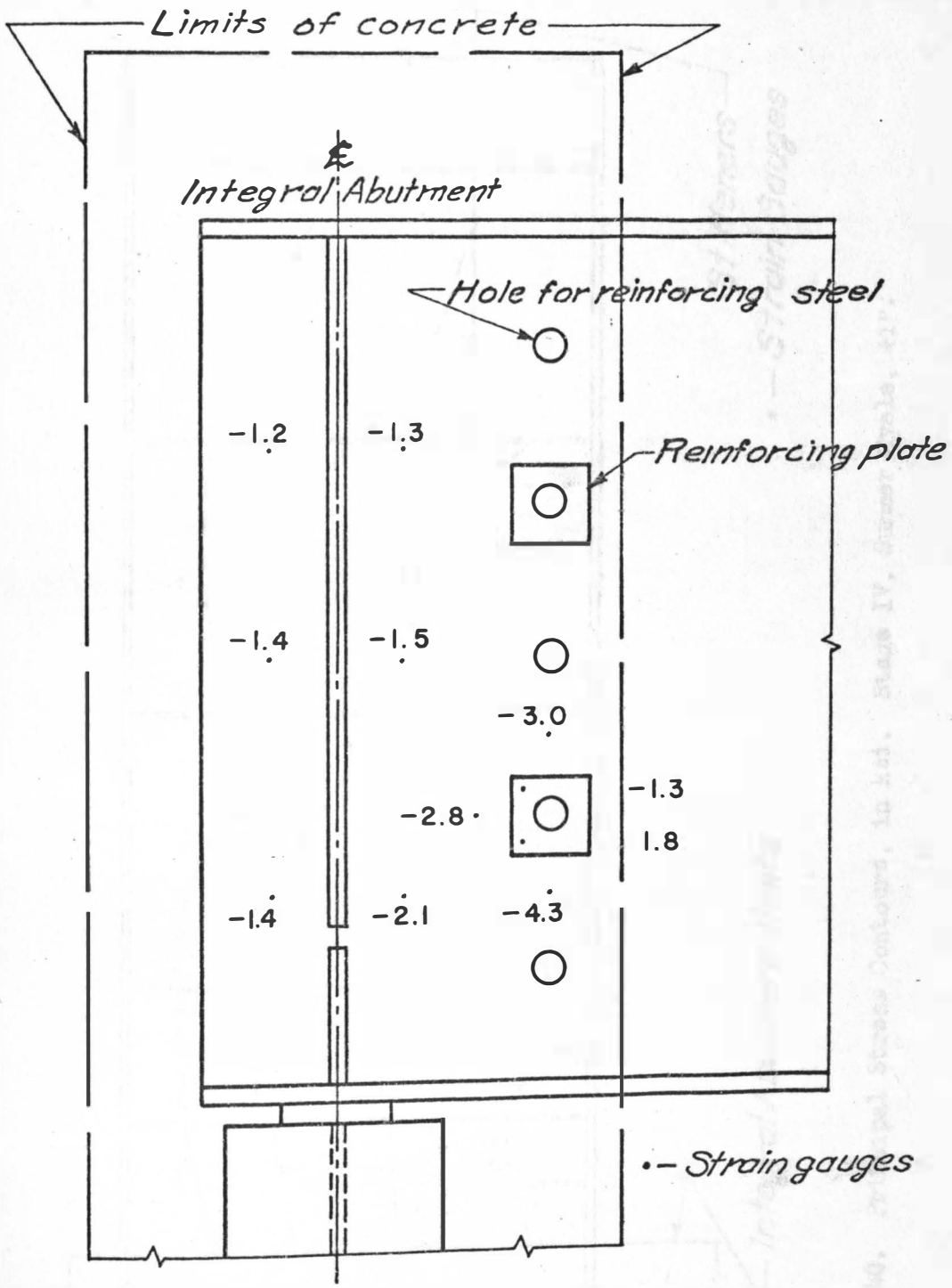

FIGURE 39. Normal Stresses on the Girder Web and Reinforcing Plate, Within the Integral Abutment, in ksi. Stage IV, Summer Cycle, +1".

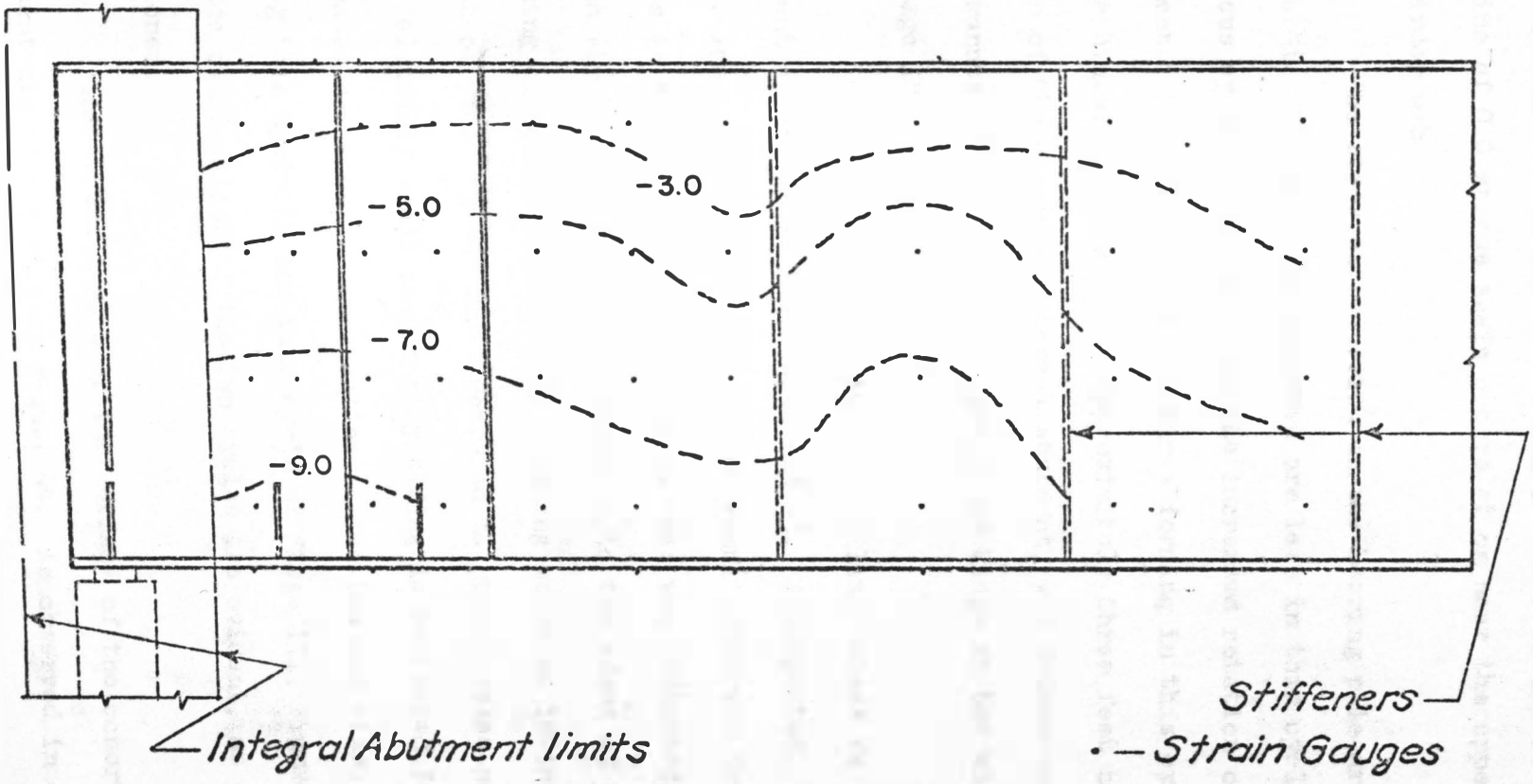

FIGURE 40. Principal Stress Contours, in ksi. Stage IV, Summer Cycle, +1".

of the increase in required loading and the bending of the section. The line of 0.0 stress again occurs at or near the upper portion of the girder web.

The stresses occurring on the bearing pile are shown in Figure 41. The stresses observed are less in this cycle than the previous cycles as a result of the increased rotation of the integral abutment. It is felt that the hinge forming in this cycle approaches a true hinge. Its location, approximately three feet below the bottom of the concrete integral abutment, was determined in the same manner as locating the approximate hinge in the winter cycle of Stage IV.

The graphs of variations in piling stress vs induced movement are shown in Figures 42 and 43. As expected, these are mirror images. The most significant result observed from these graphs is that no yielding of the flanges was indicated. However, if the stresses observed are projected to the edges of the piling, assuming elastic behavior, some yielding would be indicated. This amount of yielding was small compared to other cycles of testing. This relatively small amount of yielding is accounted for by the increased rotation or hinge action of the bearing pile. By comparing this cycle to the same cycle of Stage III, Figures 23 and 43, the similarities of the two cycles are evident, as previously mentioned.

The stress levels on the surface of the concrete integral abutment are illustrated in Figure 44. As observed in other cycles

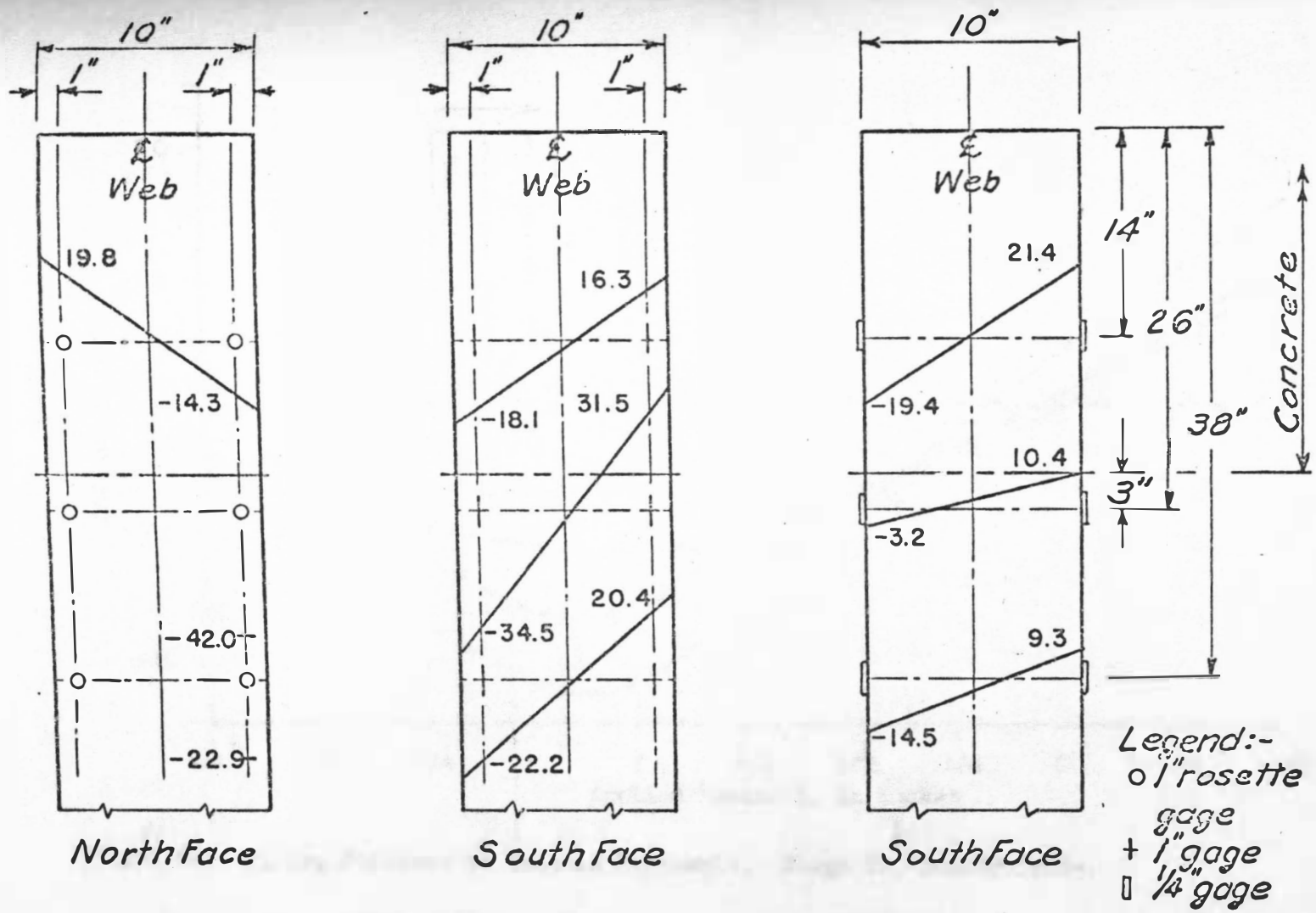

FIGURE 41. Stress Distribution on the Pile, in ksi. Stage IV, Summer Cycle, +1".

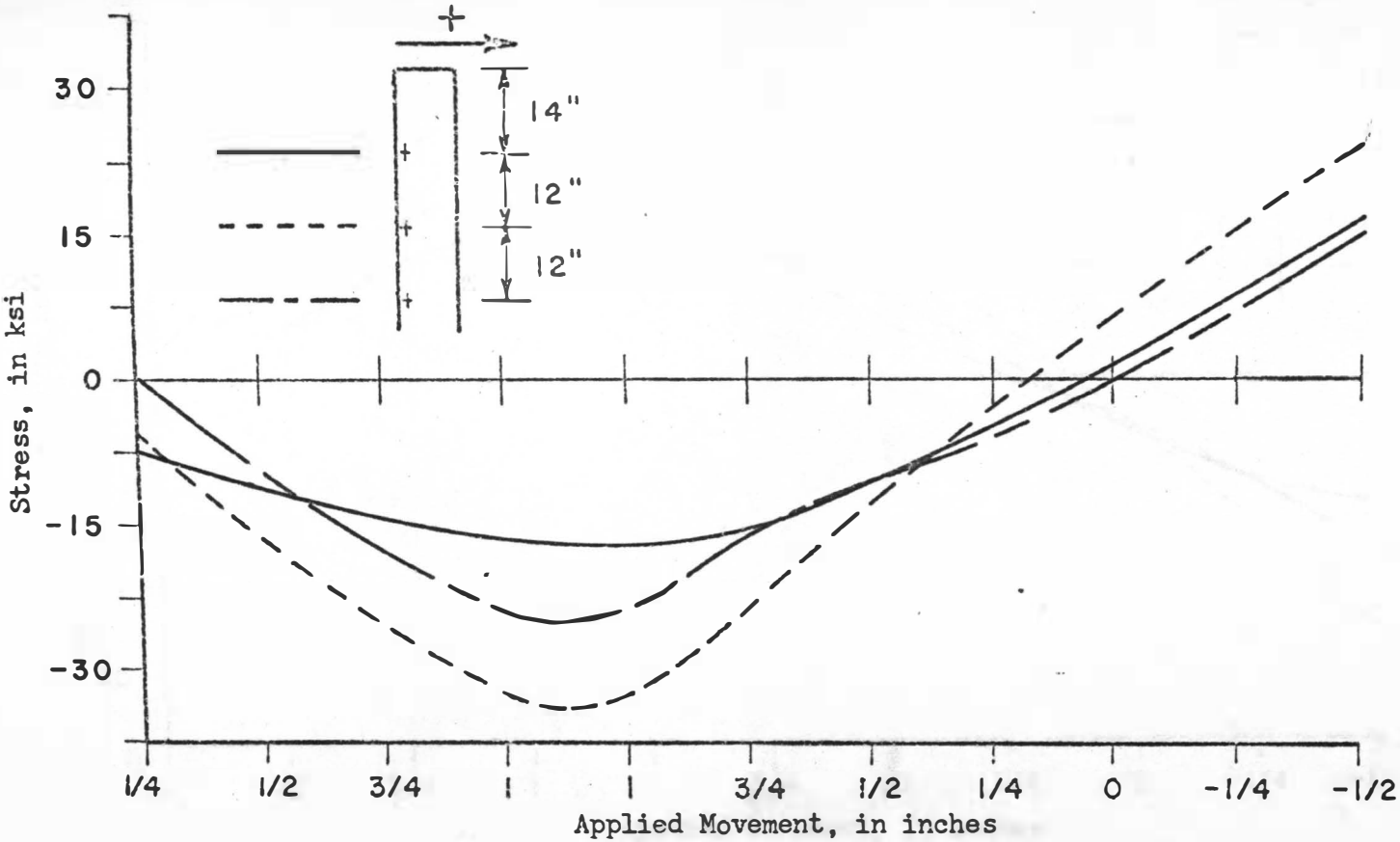

FIGURE 42. Piling Stresses vs Induced Movements. Stage IV, Summer Cycle.

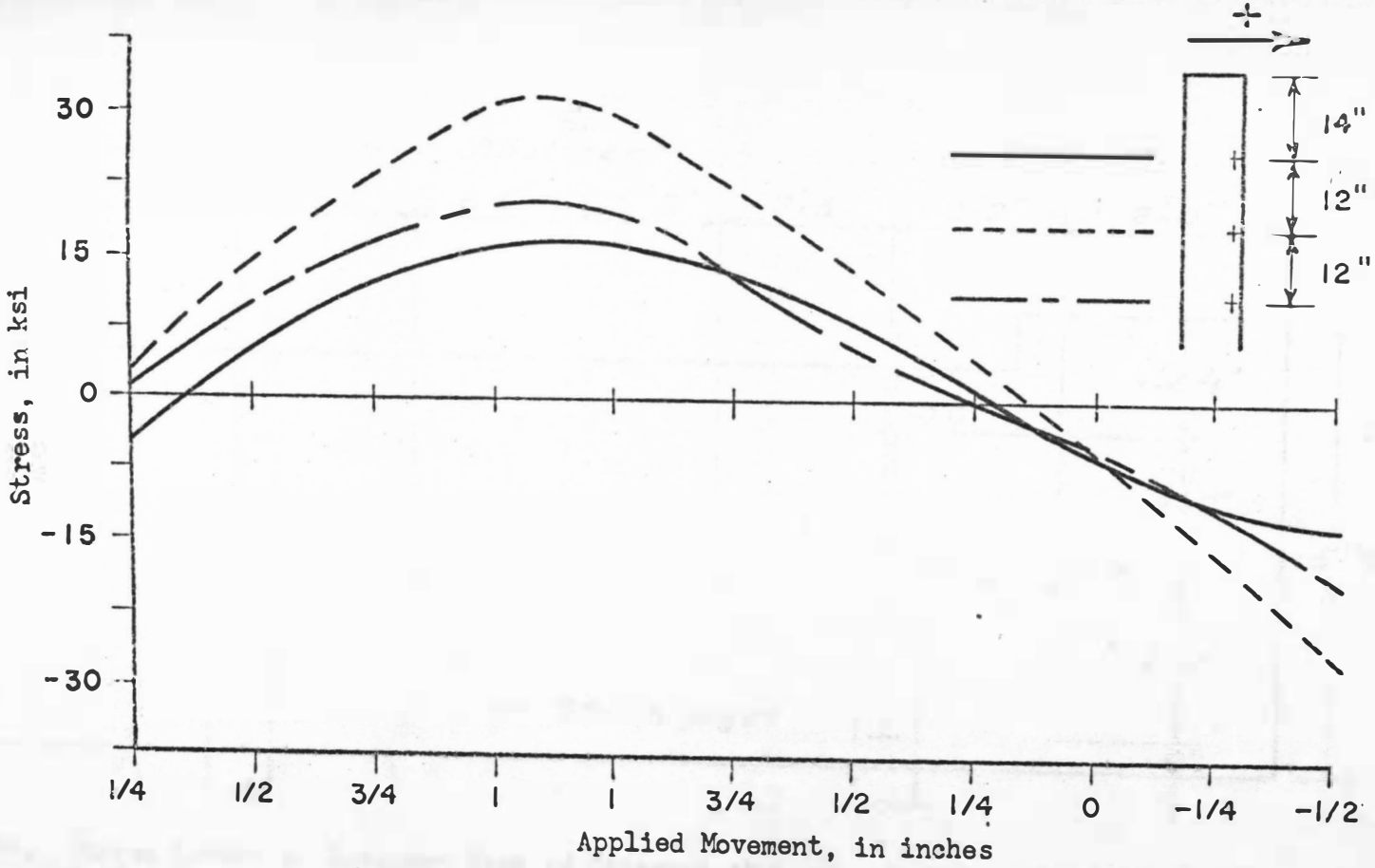

FIGURE 43. Piling Stresses vs Induced Movements. Stage IV, Summer Cycle.

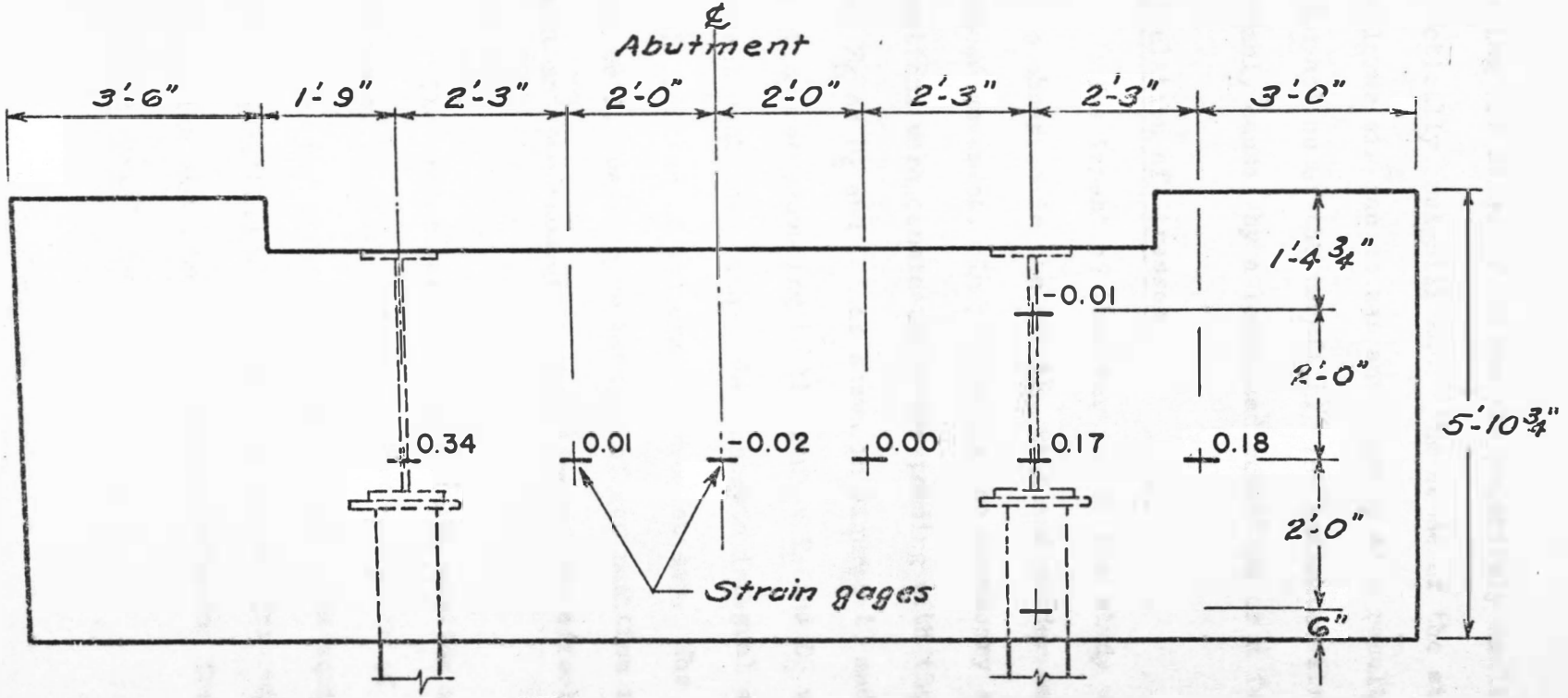

FIGURE 44. Stress Levels on Exterior Face of Integral Abutment, in ksi. Stage IV, Summer Cycle, +1".

of testing for Stage IV, these are relatively small in magnitude and practically insignificant. The sense of the stresses indicated by the lower six gauges was anticipated as a result of the applied load and action of the backfill. The indicated stress of -0.01 ksi is probably caused by a localized condition or a faulty gauge.

4. Calculation of Stresses

The intent of this portion of the study was to verify the stresses observed in the bearing pile and girder web at ±1.000 inch of induced movement. In performing the necessary stress calculations, two sections were considered corresponding with the location of strain gauges, E_6 or D_6 and L-I as shown in Figures 13 and 15, respectively. The section corresponding to the gauges E_6 and D_6 was chosen because it was not contained within the concrete integral abutment and was below the section of maximum observed stress. The location corresponding to L-I was chosen because of its position near the integral abutment and the subsequent reduction of the effects of lateral deflection.

The properties of the composite section were calculated by methods of statics. (10) One-half the width of the slab was considered as the effective flange width. The equivalent area of steel was calculated using eight as the modular ratio. The properties of the steel bearing pile were obtained from the Steel Construction Manual. (2)

In calculating the stresses occurring at the indicated locations, several assumptions were used. These dealt with: (a) the action of the structure, (b) the lateral resistance of the subgrade when subjected to a horizontal load, and (c) the frictional forces. The structure was supported by a roller at the jacking abutment and an assumed hinge in the bearing pile, as previously discussed. These supports allowed the structure to be analyzed as a simply supported frame. The lateral resistance of the subgrade was calculated by using the equation developed by Broms: (11)

$$P = 9\,c\,D(L - 1.5\,D) \qquad \text{Eq. 9}$$

where

P = lateral resistance, in pounds

c = cohesion of soil, in psi

L = distance from bottom of integral abutment to the location of the assumed hinge, in inches

D = width of bearing pile, in inches

The use of this equation required several assumptions, including (a) the subgrade was a cohesive soil and (b) the bearing pile acted as a short pile. Any frictional forces that may have existed were assumed negligible and were not considered. Only the forces created by the induced load and resulting translation and/or rotation of the integral abutment were considered in calculating the desired stress. This approach is valid because the initial strain readings included the strain of all loads except those resulting from the application of the required loading.

For the -1.000 movement of the winter cycle, the observed and calculated loads were applied to the simply supported frame. The loads applied included the induced load of 30.8 Kips as presented in Table 5, the uplift reaction presented in Table 6, and the lateral earth pressure calculated from Equation 9 using 0.677 ksi for C. The value of C was determined in the laboratory by finding the unconfined compressive strength of the subgrade by standard methods. The active pressure of the backfill was taken to be zero, as previously discussed for the winter cycle. Moments were then summed about the assumed hinge to check the forces acting on the frame. If the moments did not sum up to zero (summation of moments about a hinge equals zero), the uplift reaction was corrected to create zero moment. It was felt that the uplift reaction at the jacking abutment was the most likely force to be in error.

After a determination of the magnitudes of the various forces, they were applied to the frame. The stresses were then calculated taking free body diagrams at the appropriate section on the bearing pile and girder. For the bearing pile, a section was taken corresponding to E_6 and D_6 and the flexural stress calculated from equation 4. It was assumed that any change in the reaction at the integral abutment was initially taken by the bearing capacity of the soil. This assumption would make the stress caused by the axial load or reaction in the bearing pile equal to zero. The average experimental stress of $\pm$ 26.4 ksi shown in Figure 31 deviated eight percent from the calculated stress of $\pm$ 28.6. The close

agreement indicates that the strain gauges were functioning properly and more significantly that the bearing pile was acting as designed.

In calculating the principal stress of L-I in the girder web, the following equation was used: (8)

$$\sigma_{pi} = \frac{\sigma_x + \sigma_y}{2} \pm \sqrt{\left(\frac{\sigma_x - \sigma_y}{2}\right)^2 + \tau_{xy}^2} \qquad \text{Eq. 10}$$

where

σ_{pi} = principal stress, in psi

σ_x, σ_y = stress in the x and y direction, in psi

τ_{xy} = shearing stress, in psi

σ_x was determined by methods of mechanics of materials. (8) σ_y was taken as zero. τ_{xy} was obtained by dividing the shearing force, calculated by methods of mechanics of materials, by the area of the girder web. The experimental stress of 0.7 ksi deviated 60 percent from the calculated stress of 1.6 ksi. The calculated deviation of 50 percent is within reasonable limits. This conclusion is a result of the many variables and assumptions made in calculating the stress. It is possible for the printed strain readings to be ten micro-inches per inch in error; therefore, the deviation could be reduced to 35 percent.

The stress occurring at the selected locations for the +1.000-inch movement during the summer cycle were calculated in the same manner as the stresses for the -1.000-inch movement during the winter cycle. The only difference was the additional force acting on the structure as a result of the backfill passive pressure. The

passive pressure was determined experimentally and analytically. The experimental values are shown in Table 10 as pressure acting on the integral abutment. The calculated passive pressure was determined by the following equation: (12)

$$P_p = \gamma K p h$$

where

P_p = passive pressure, in psf

γ = density of backfill in pounds per cubic foot (pcf)

$K_p = \tan^2(45 + \phi/2)$

h = depth of backfill, in feet

The density was determined by field density tests to be 119 pcf. The angle of internal friction (ϕ) was determined in the laboratory to be 41.2 degrees. The average experimental pressure of 18.8 psi at 15 inches above the base of the integral abutment deviated 2 percent from the calculated pressure of 19.2 psi. The calculated passive pressure multiplied by the area of the integral abutment yielded the force acting on the structure because of passive resistance of the backfill. The calculation of the stresses was then continued as previously discussed. The average experimental piling stress of $\pm$ 21.3 ksi deviated 0.5 percent from the calculated stress of 21.4 ksi. Again, the close agreement indicates that the steel bearing pile was functioning as designed.

The experimental principal stress on the girder web of 3.7 ksi deviated 3 percent from the calculated value of 3.6 ksi.

This close agreement was not anticipated and probably resulted from the variables involved and their effects on each other.

It should be noted that although the stress contours on the girder web are relatively parallel, their distance from the neutral axis varies. This variation in distance is due to the extremely large number of variables involved such as the twisting of the entire structure, frictional resistance, voids in the concrete, residual stresses of welding, and increased or decreased moment about the y axis resulting from lateral deflections.

CHAPTER IV

SUMMARY AND RESULTS

A. Summary of Results

The following results have been formulated from the observed and calculated results of this study:

1. The shear bars within the integral abutment were functioning properly in all stages of testing.
2. The recorded girder stresses of Stage III and the Spring and Summer Cycles of Stage IV are within allowable working stresses.
   (3) The stresses occurring in the girder web are very difficult to calculate because of the large numbers involved.
3. The girder stresses recorded during the release of the winter cycle for Stage IV indicate an area of high concentrated stress and possible yielding near the integral abutment.
4. Although yielding of the extreme fibers of the bearing pile was noted in Stages III and IV, the recorded strain does not indicate any structural failure. Based upon the results of this study, the stresses occurring on the bearing pile can be calculated within ten percent of the experimental stresses.
5. The stresses occurring on the concrete integral abutment are insignificant and are within the allowable working stresses. (3)
6. The results of the expansion cycles were generally more severe than those of the contraction cycles.

B. Conclusions

For the final stages of construction, the only forces affecting the structure are those resulting from simulated lateral thermal movements. The effects of all vertical forces are excluded. The following conclusions, based on the results of this study, have been formulated:

1. After the deck slab and backfill are placed, but prior to any further construction, the integral abutment design for short steel bridges used by the South Dakota Department of Highways is satisfactory provided the following conditions are met:
   a. The lateral deflection due to a temperature change does not exceed one inch.
   b. The soil strata is similar to the one at the test site. (1)
   c. The girder web near the integral abutment is reinforced.
   d. Ideal conditions leading to the lateral and longitudinal symmetrical behavior of the structure are assured.
   e. Fatigue effects are assumed to be trivial and, therefore, have little effect on the structure.
2. If all conditions are not met, the design would still be satisfactory provided that the lateral deflection was limited to less than or equal to three-fifths of an inch.

C. Recommended Areas of Future Study

In order to arrive at valid and useful conclusions which would aid bridge designers, the following areas of future study are recommended:

1. A piling study to determine its behavior and distribution of stress over its entire length as a result of lateral loads.
2. A fatigue study on the piling.
3. A study to determine the most suitable type of reinforcement for the girder web near the integral abutment.
4. A study of the structure subjected to unsymmetrical lateral thermal movements or twisting.
5. A study of the structure subjected to a combination of loads, namely live loads and loads resulting from thermal movements.
6. A study to determine the most suitable type of approach slab to be used in conjunction with this type of bridge.

BIBLIOGRAPHY

(1) Sarsam, Mumtaz B., "Temperature Effects on Integral Abutment Bridges During Early Construction Stages," M. S. Thesis, Unpublished, South Dakota State University, (1972).

(2) Manual of Steel Construction, 7th Ed., American Institute of Steel Construction, New York, N. Y., (1970).

(3) Standard Specifications for Highway Bridges, American Association of State Highway Officials, Washington, D. C., (1969).

(4) Standard Specifications for Roads and Bridges, South Dakota Department of Highways, Pierre, S. D., (1969).

(5) Strain Gage Handbook, BLH Electronics, Inc., Waltham, Mass., (1967).

(6) Dally, James W., and Riley, William F., Experimental Stress Analysis, McGraw-Hill, New York, N. Y., (1965).

(7) Soil and Foundation Instrumentation, Lauks Laboratories, Inc., Redmond, Washington.

(8) Higdon, Archie; Ohlsen, Edward H.; Stiles, William B., and Weese, John A., Mechanics of Materials, 2nd Ed., John Wiley & Sons, Inc., New York, N. Y., (1967).

(9) Van Vlack, L. H., Elements of Material Science, 2nd Ed., Addison-Wesley Publishing Company, Reading, Mass., (1964).

(10) Beer, Ferdinand P., and Johnston, Russell E., Jr., Vector Mechanics for Engineers: Statics, McGraw-Hill, New York, N. Y., (1962).

(11) Broms, Bengt B., "Lateral Resistance of Piles in Cohesive Soils," ASCE Journal, Soil Mechanics and Foundation Division, Vol. 90, No. SM 2, (March, 1964).

(12) Scott, Ronald F. and Schoustra, Jack J., Soil Mechanics and Engineering, McGraw-Hill, New York, N. Y., (1968).

APPENDIX A

PILING AND GIRDER STRESSES

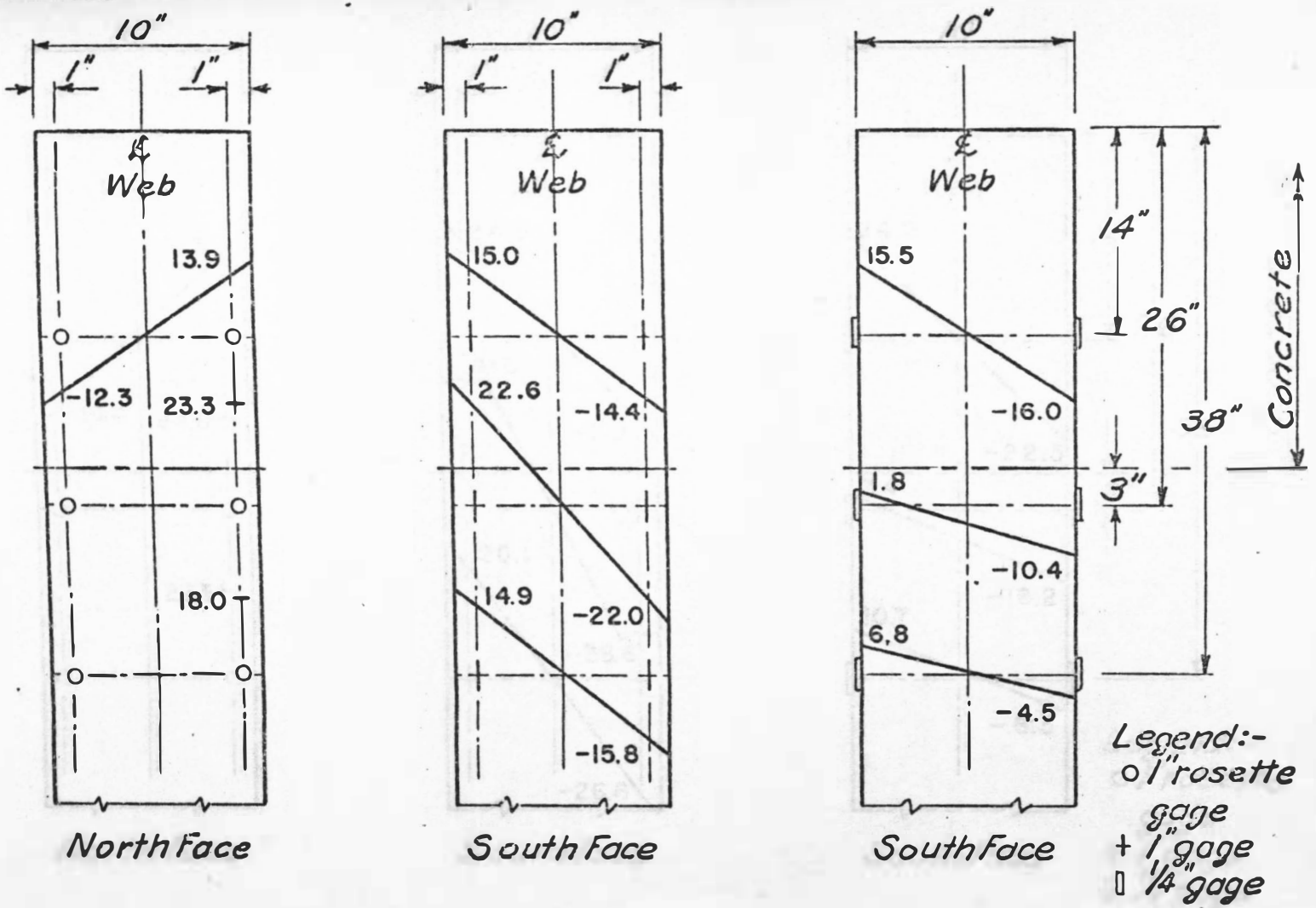

FIGURE 1a. Stress Distribution on the Pile, in ksi. Stage IV, Winter Cycle, -1/2".

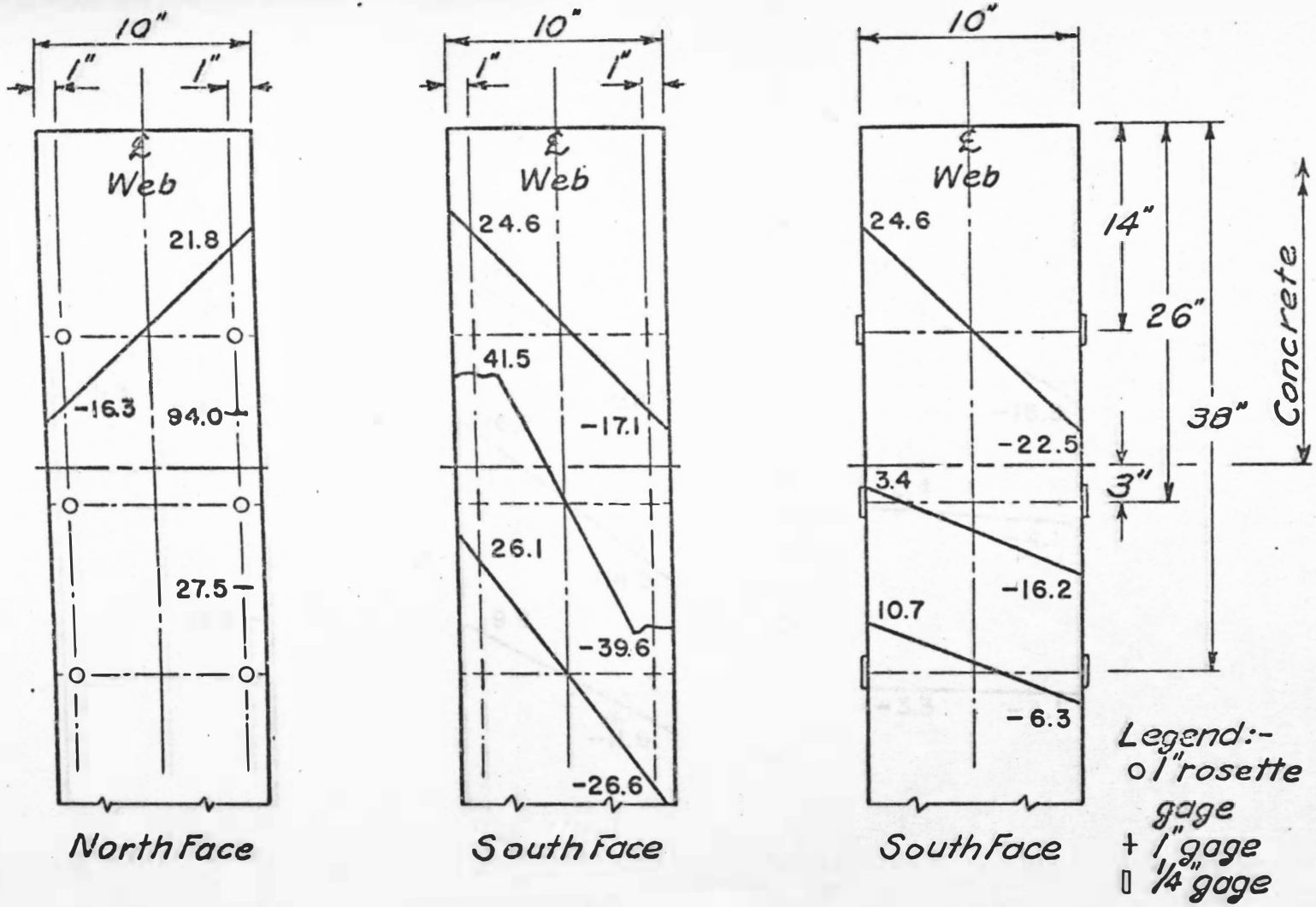

FIGURE 1b. Stress Distribution on the Pile, in ksi. Stage IV, Winter Cycle, -1".

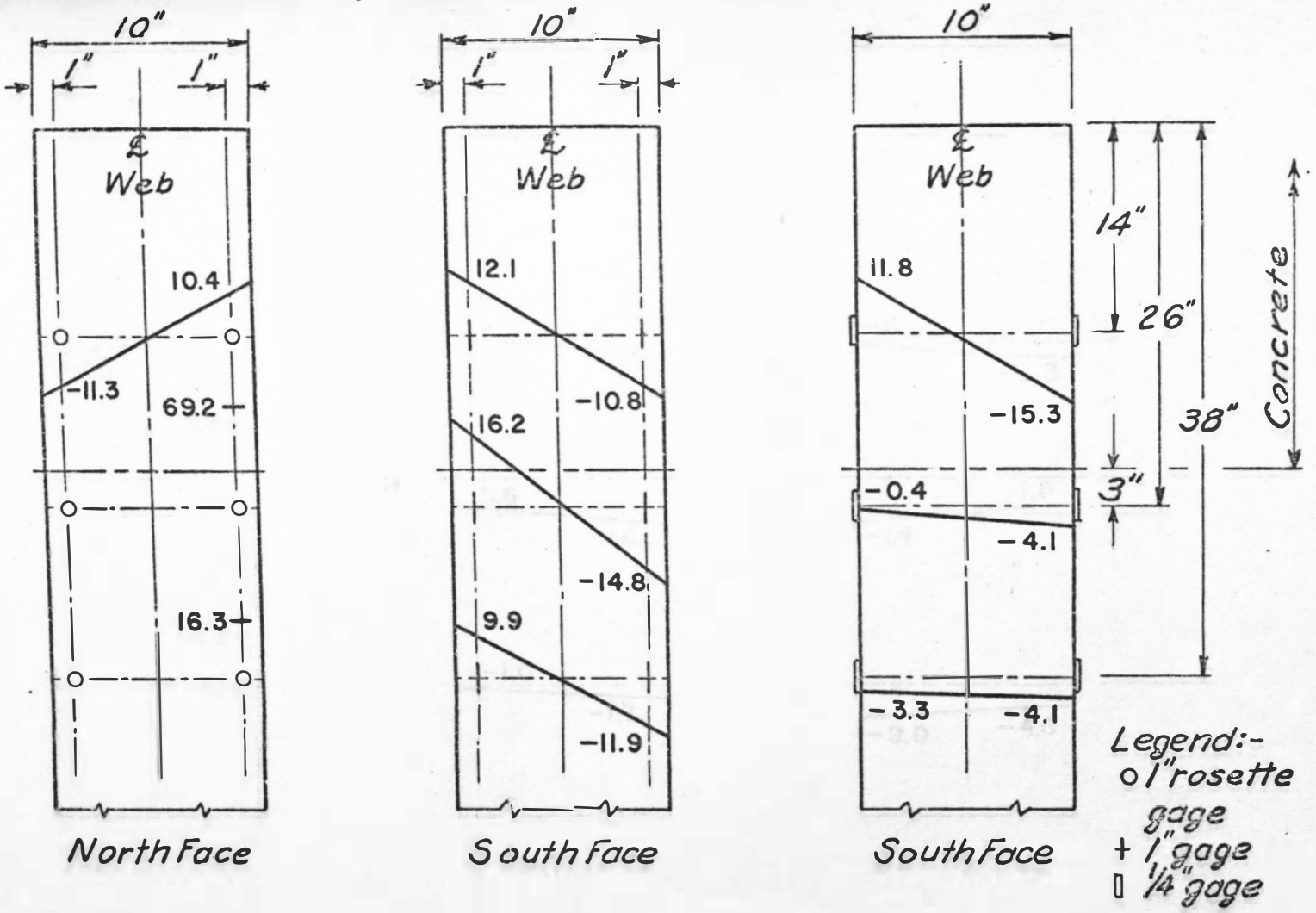

FIGURE 1c. Stress Distribution on the Pile, in ksi. Stage IV, Winter Cycle, -1/2" Release.

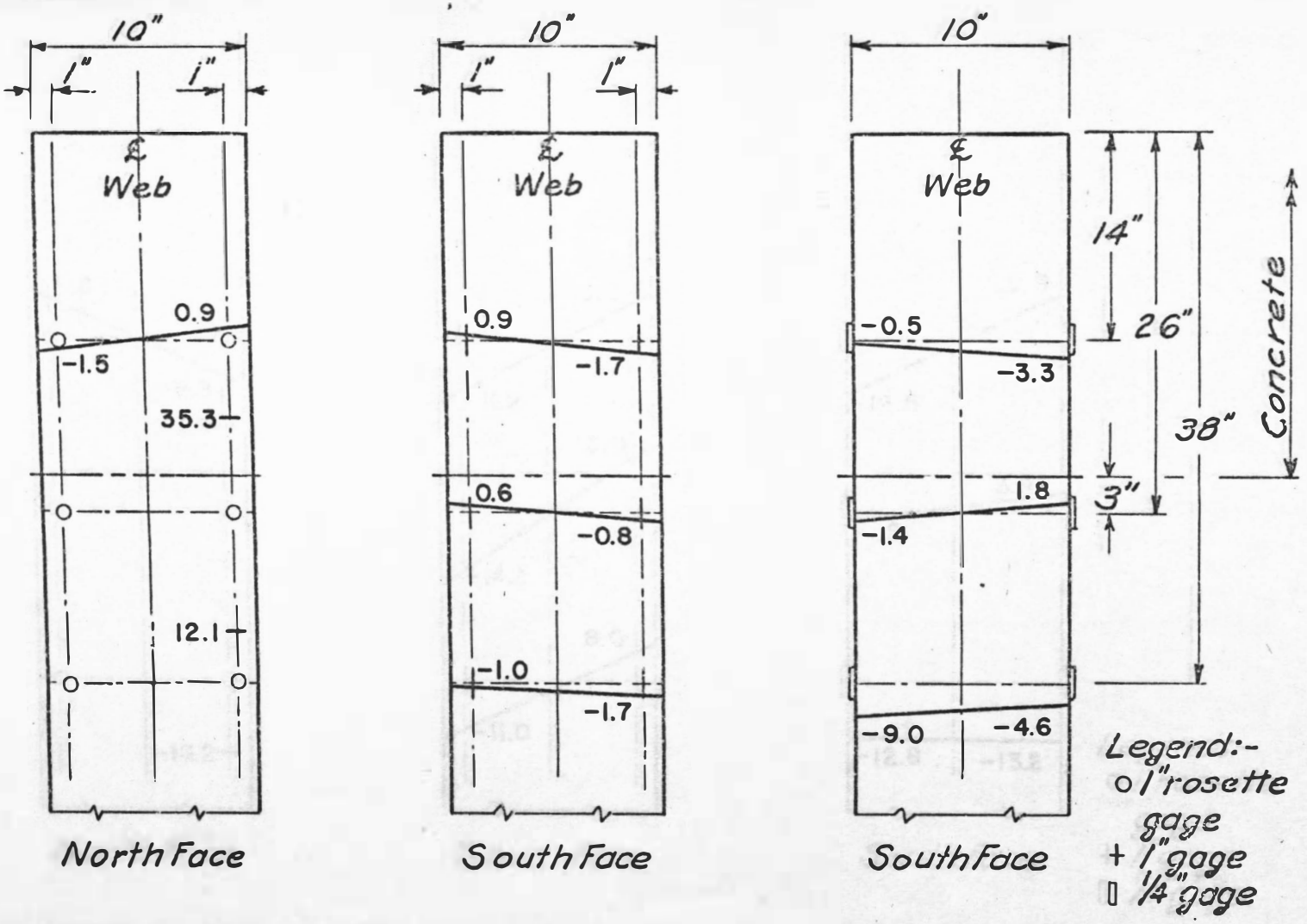

FIGURE 1d. Stress Distribution on the Pile, in ksi. Stage IV, Winter Cycle, 0".

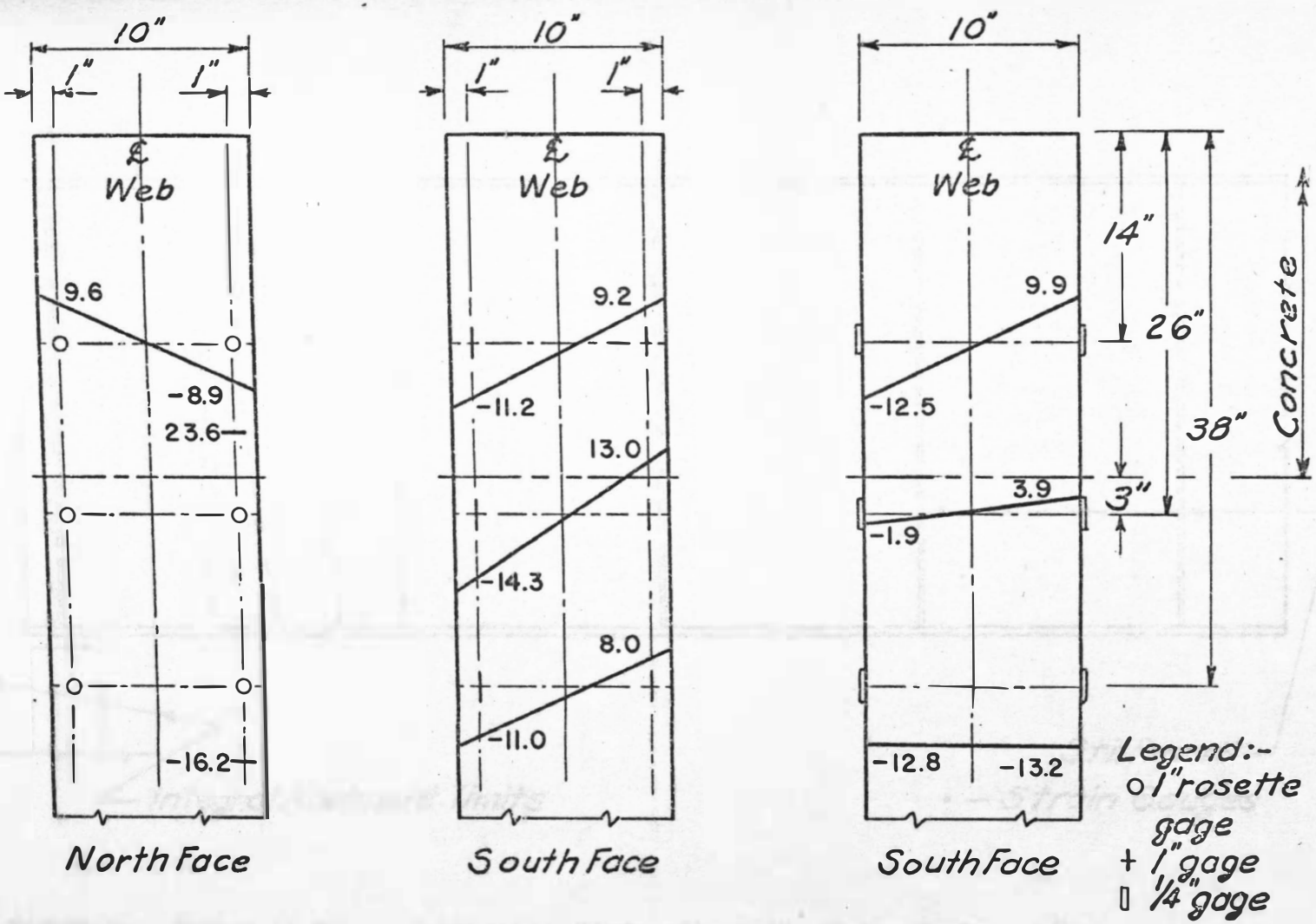

FIGURE 1e. Stress Distribution on the Pile, in ksi. Stage IV, Winter Cycle, +1/2".

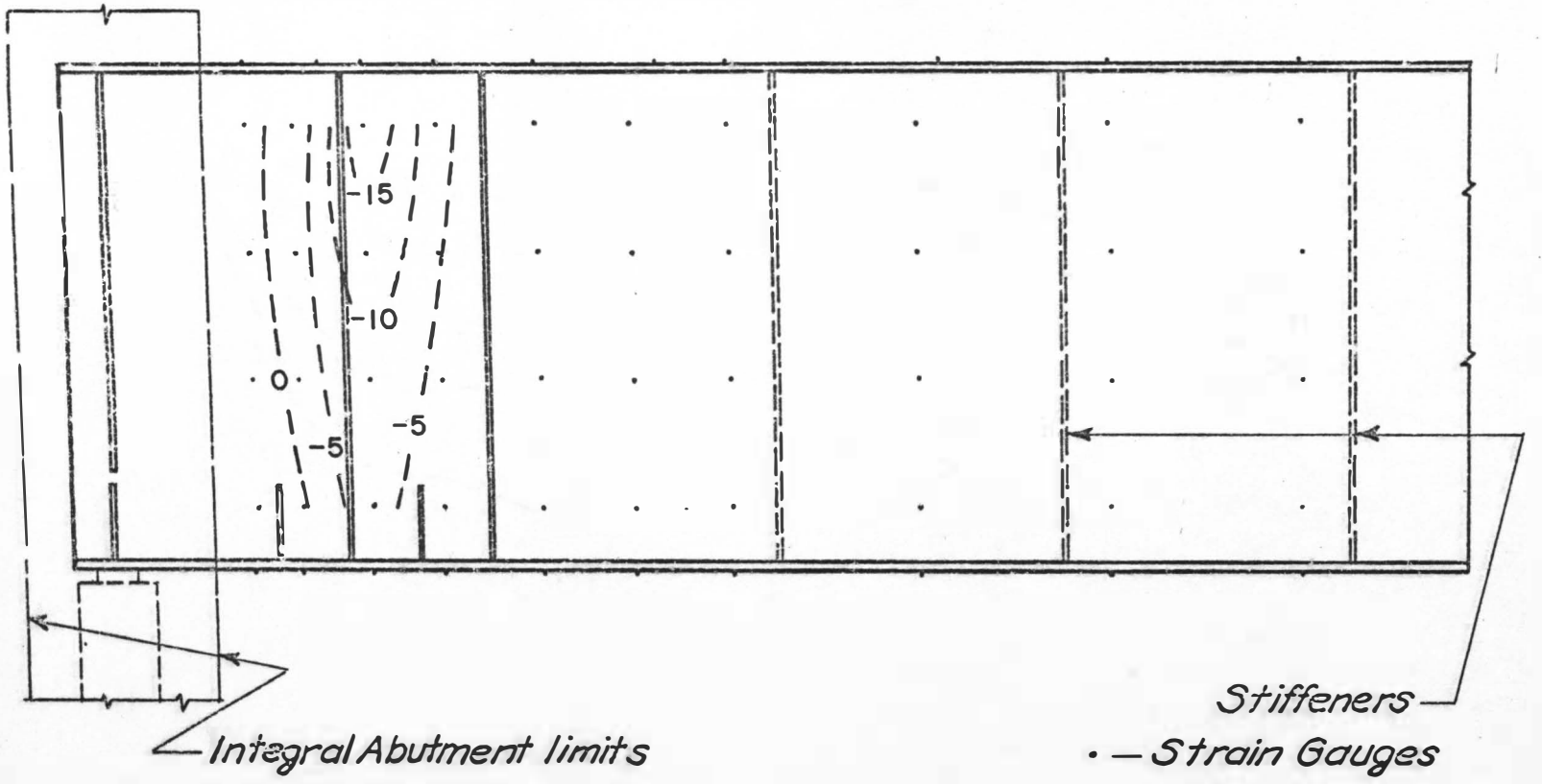

FIGURE 2a. Principal Stress Contours, in ksi. Stage IV, Winter Cycle, -1/2".

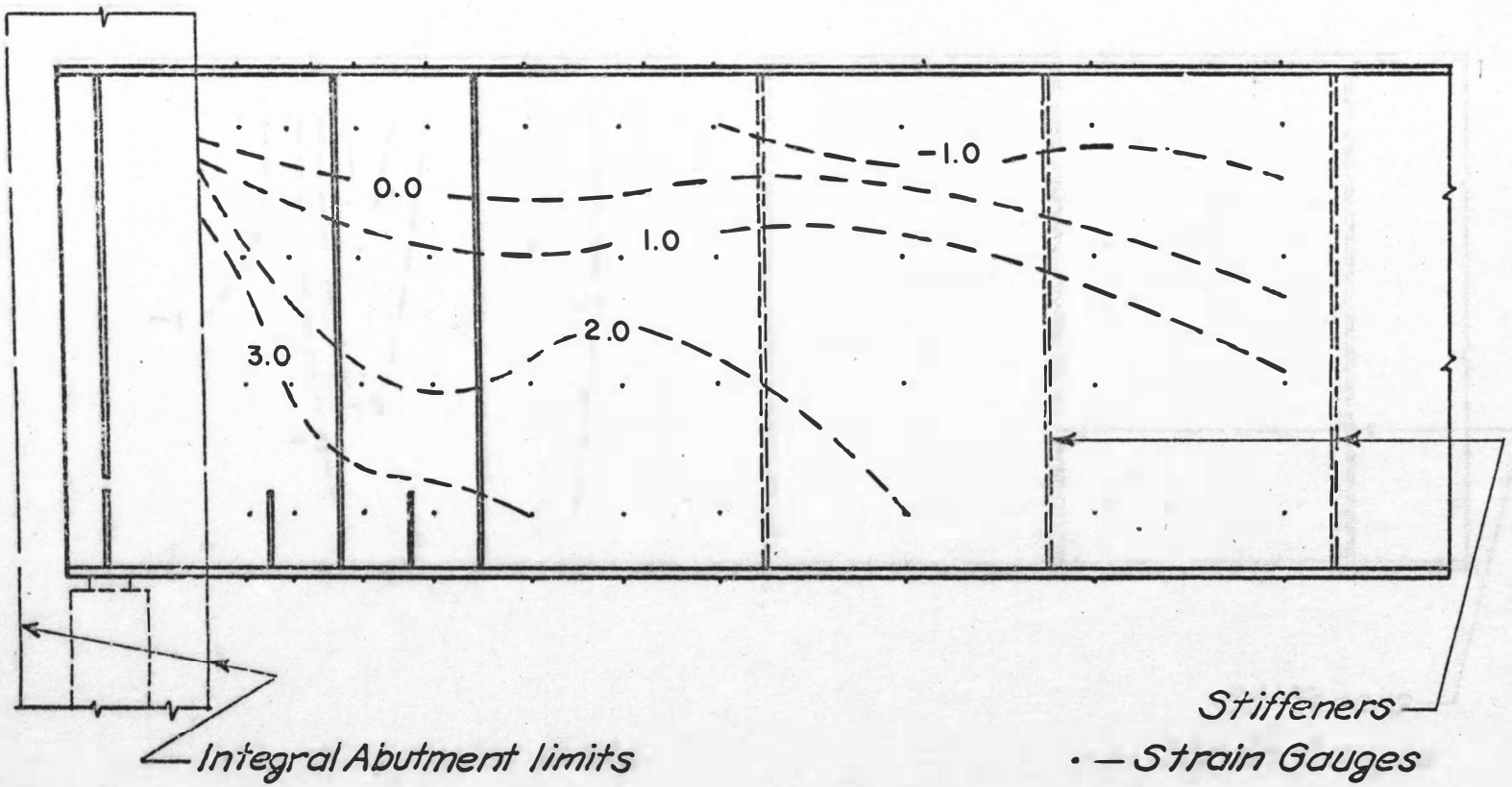

FIGURE 2b. Principal Stress Contours, in ksi. Stage IV, Winter Cycle, -1".

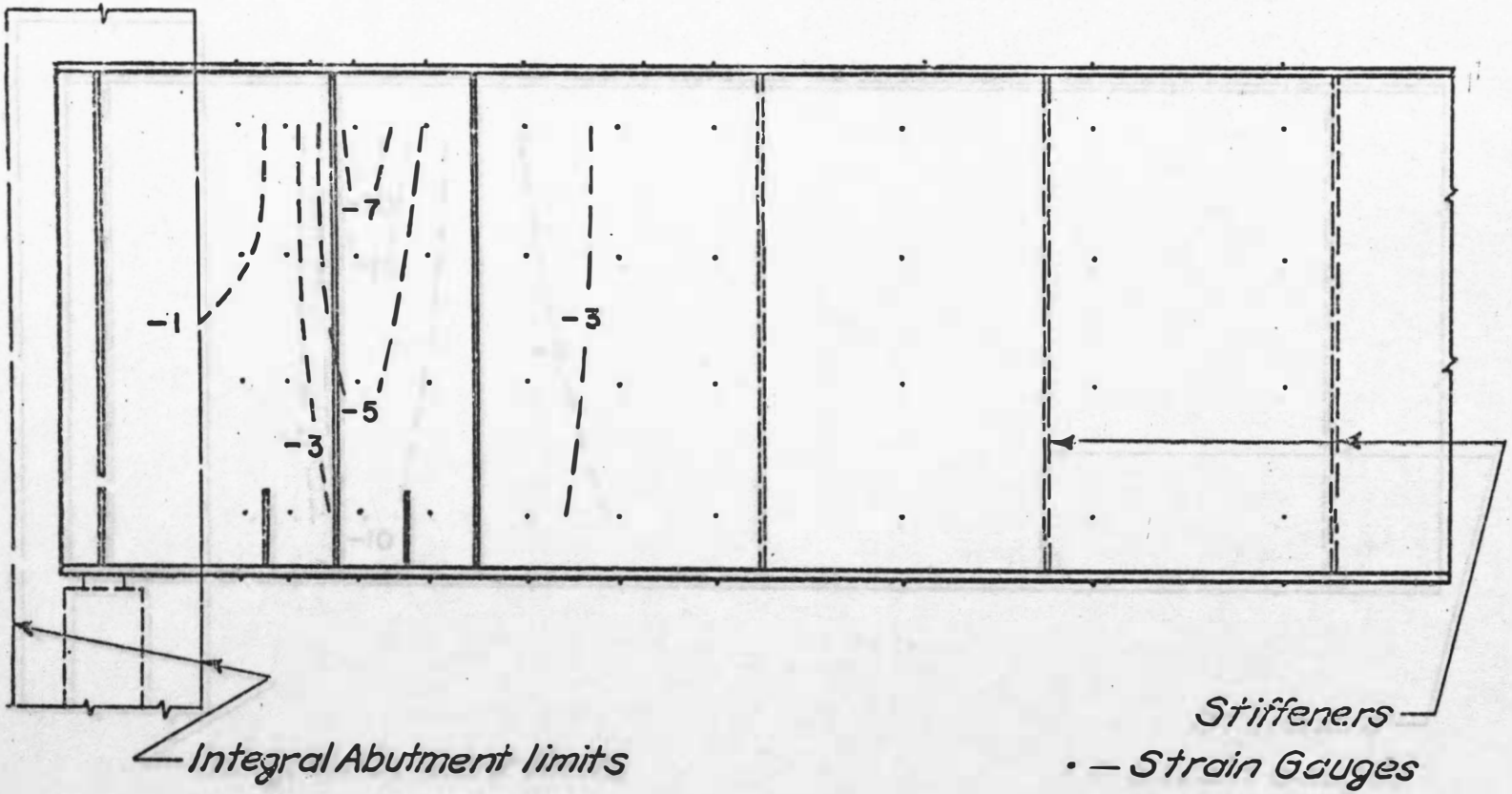

FIGURE 2c. Principal Stress Contours, in ksi. Stage IV, Winter Cycle, -1/2" Release.

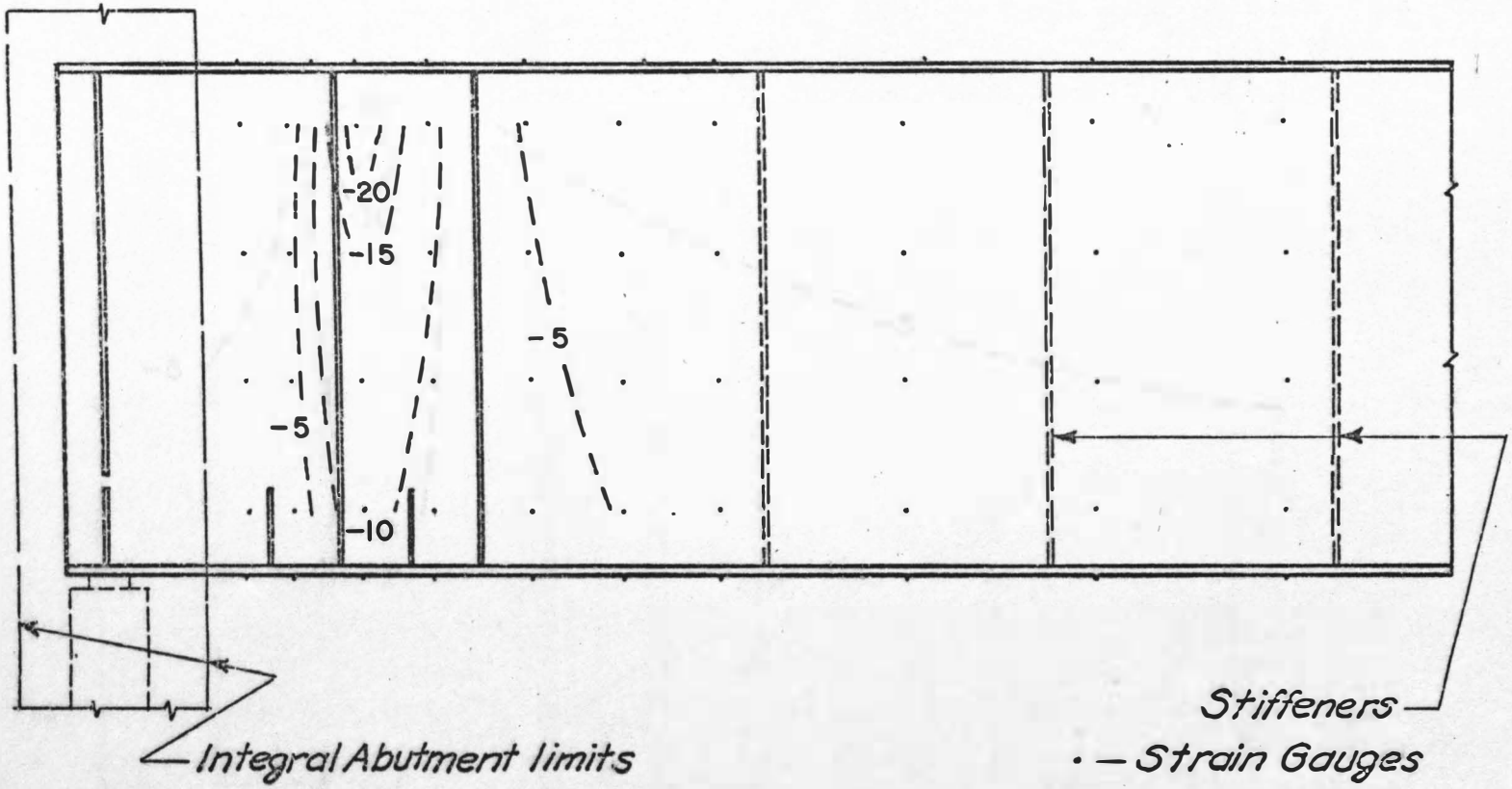

FIGURE 2d. Principal Stress Contours, in ksi. Stage IV, Winter Cycle, 0".

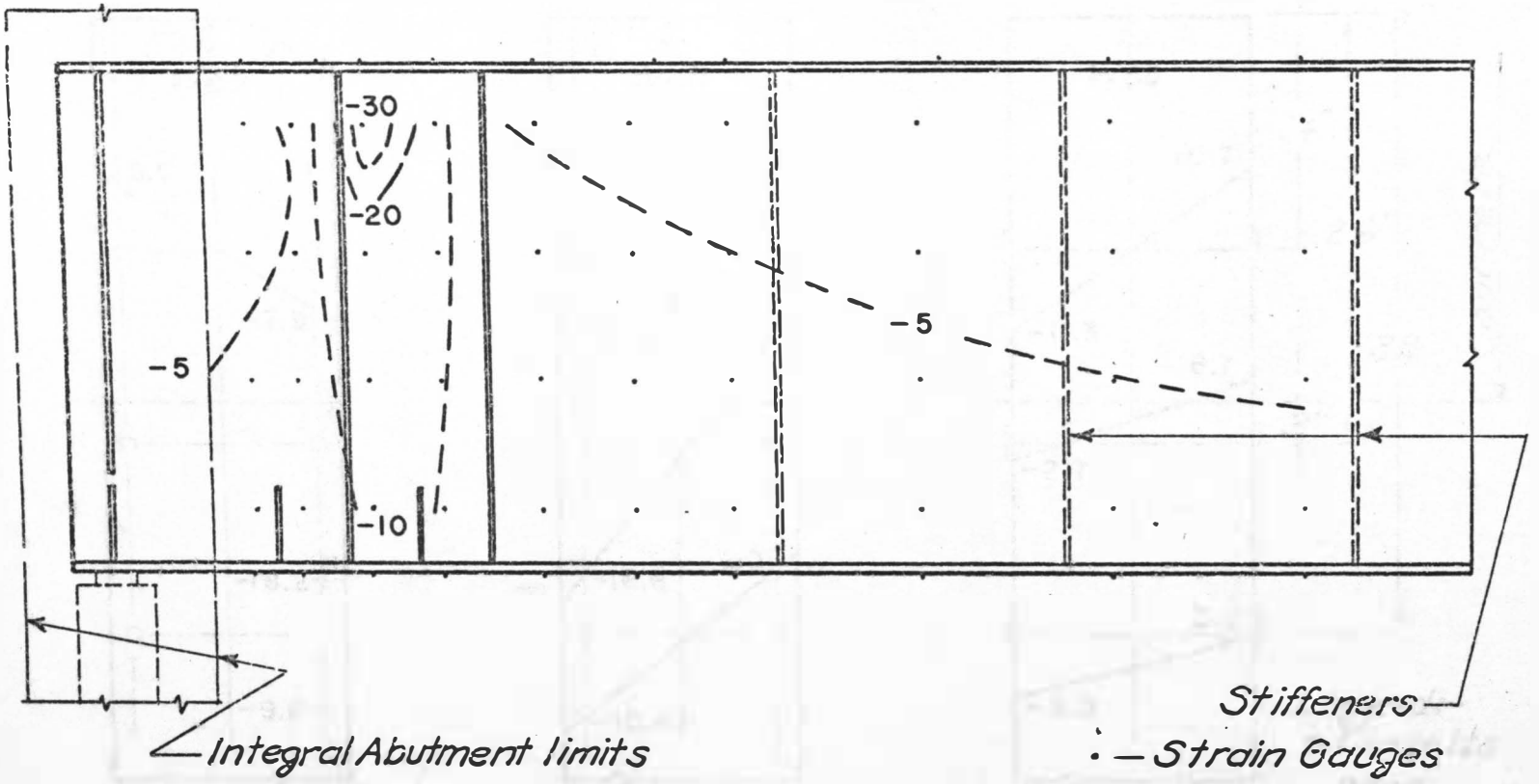

FIGURE 2e. Principal Stress Contours, in ksi. Stage IV, Winter Cycle, +1/2".

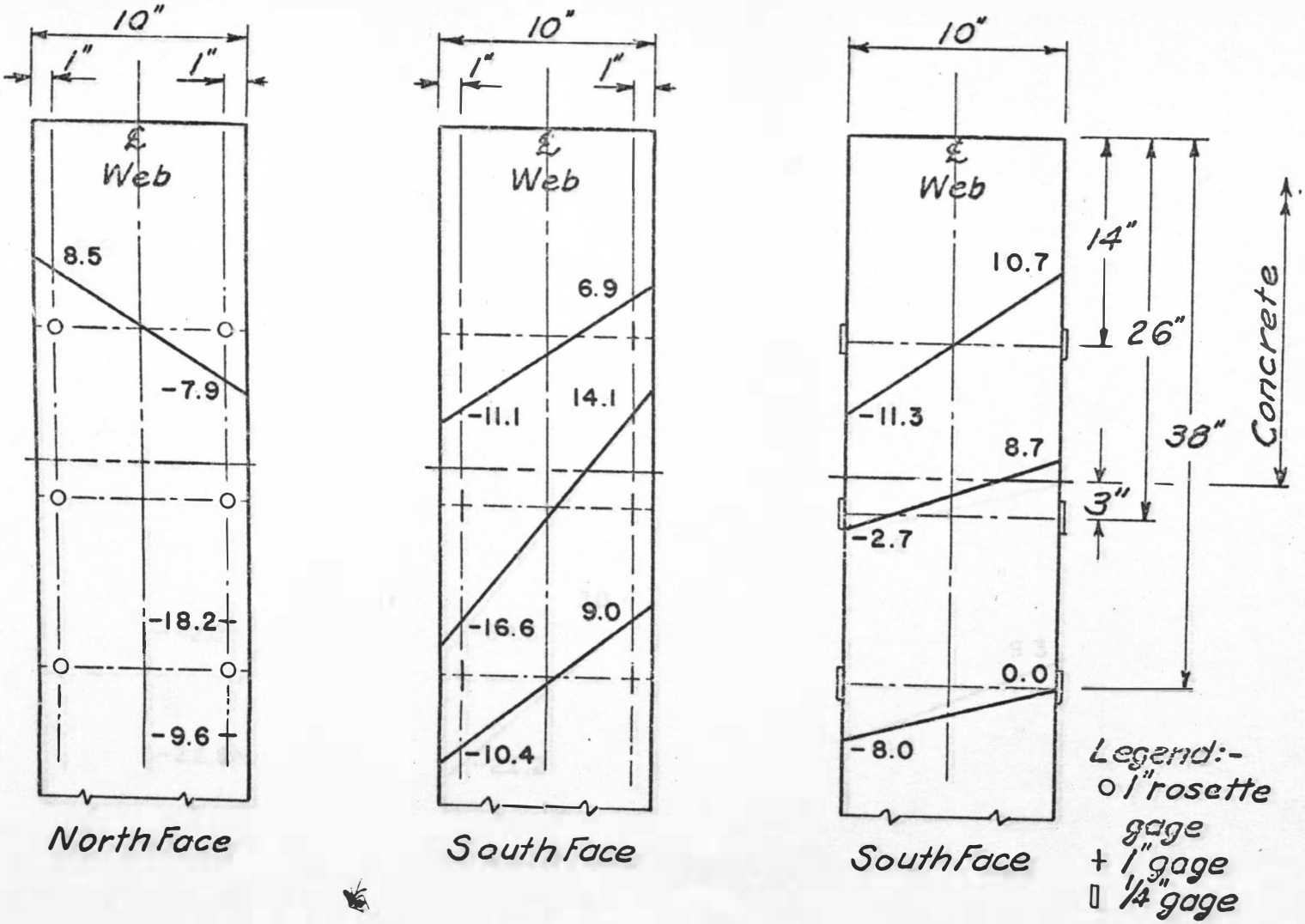

FIGURE 3a. Stress Distribution on the Pile, in ksi. Stage IV, Summer Cycle, +1/2".

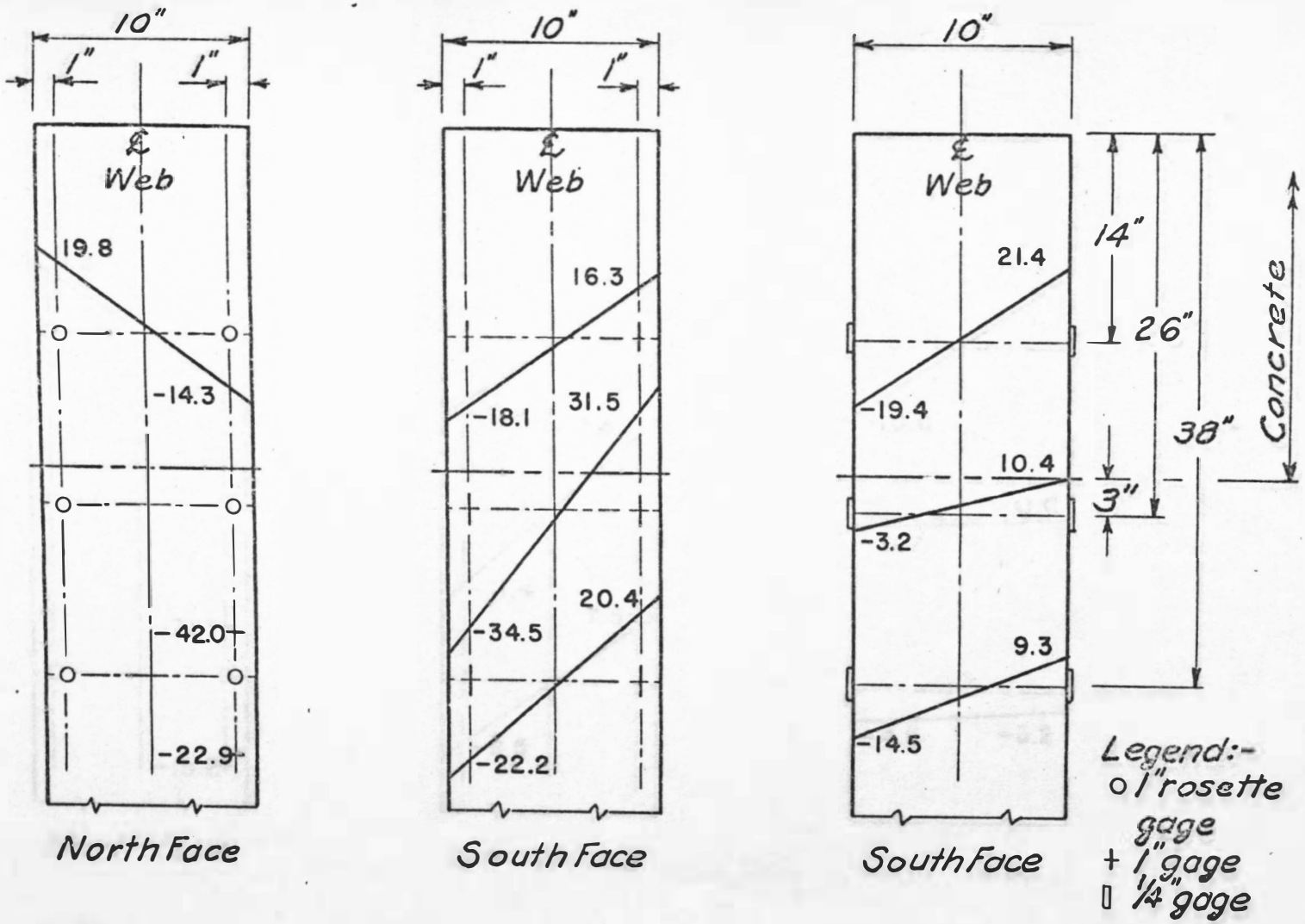

FIGURE 3b. Stress Distribution on the Pile, in ksi. Stage IV, Summer Cycle, +1".

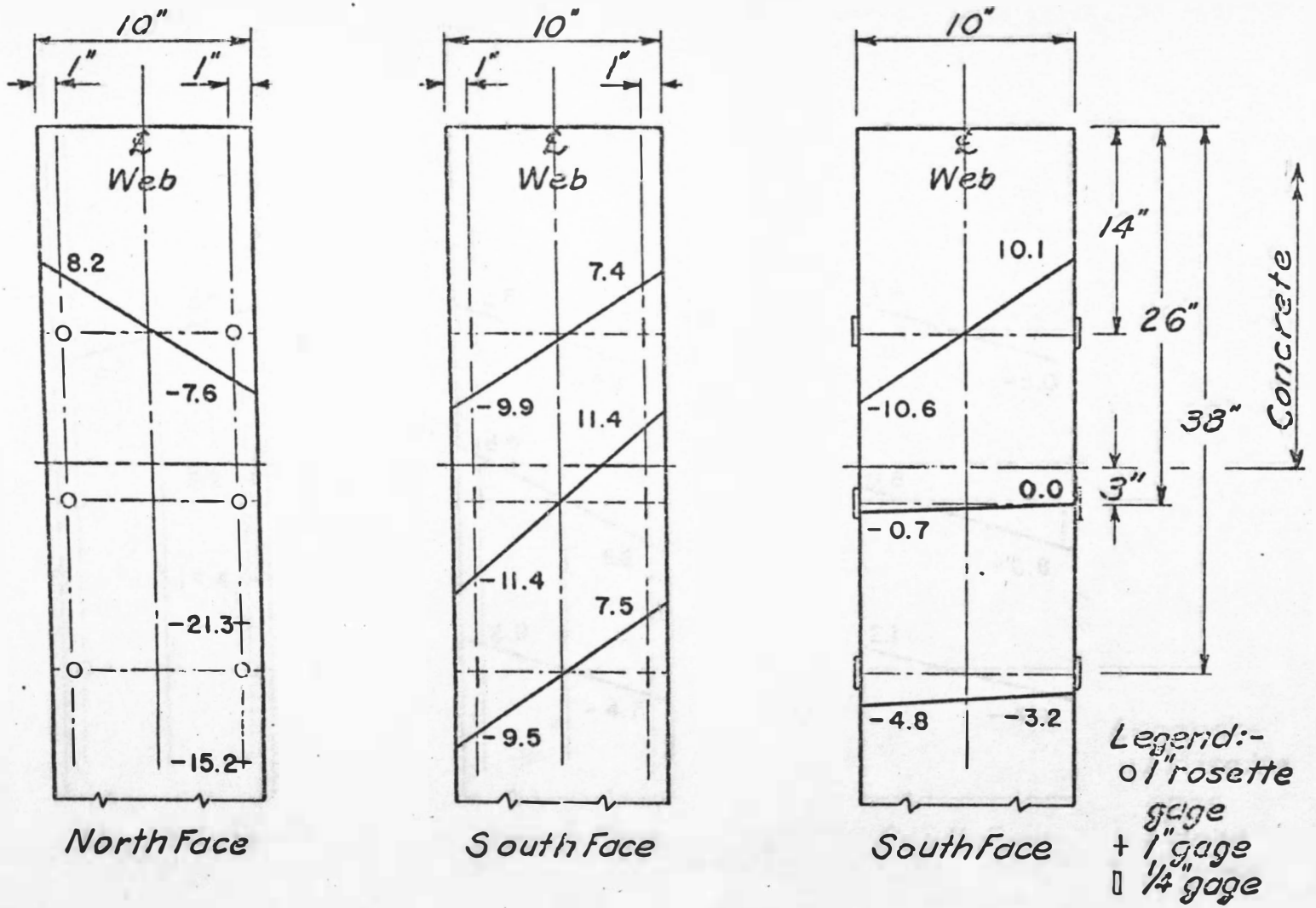

FIGURE 3c. Stress Distribution on the Pile, in ksi. Stage IV, Summer Cycle, +1/2" Release

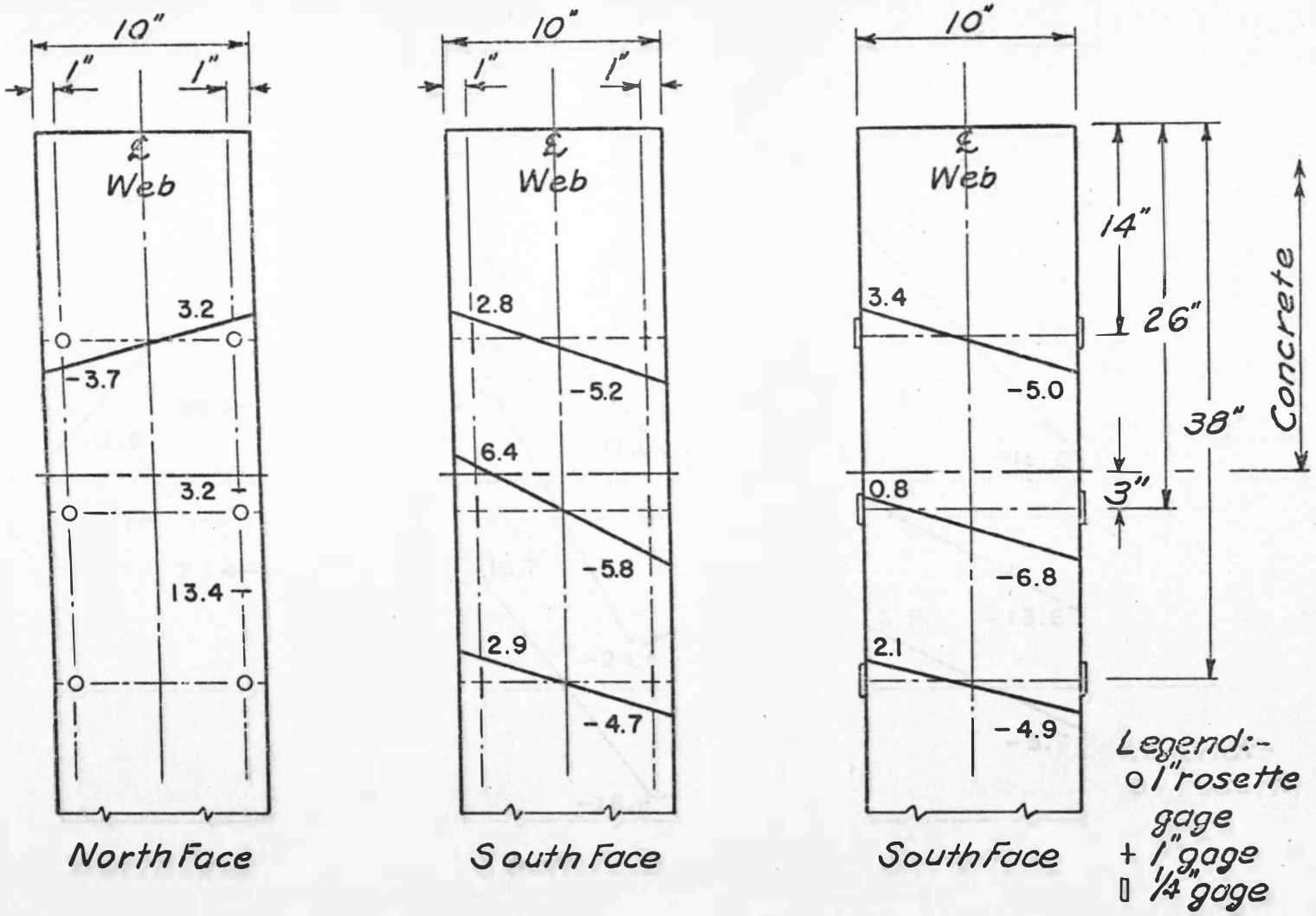

FIGURE 3d. Stress Distribution on the Pile, in ksi. Stage IV, Summer Cycle, 0".

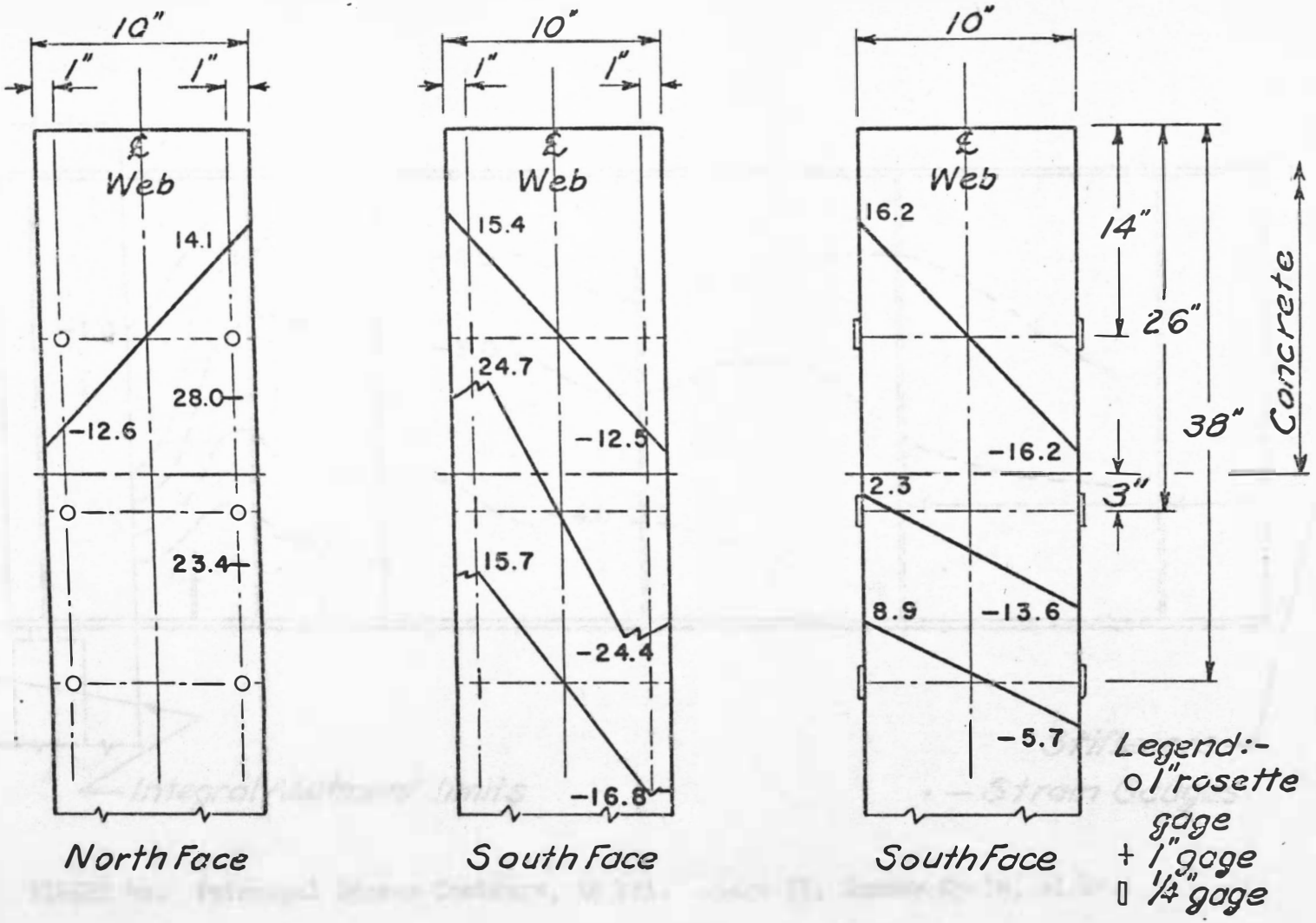

FIGURE 3e. Stress Distribution on the Pile, in ksi. Stage IV, Summer Cycle, -1/2".

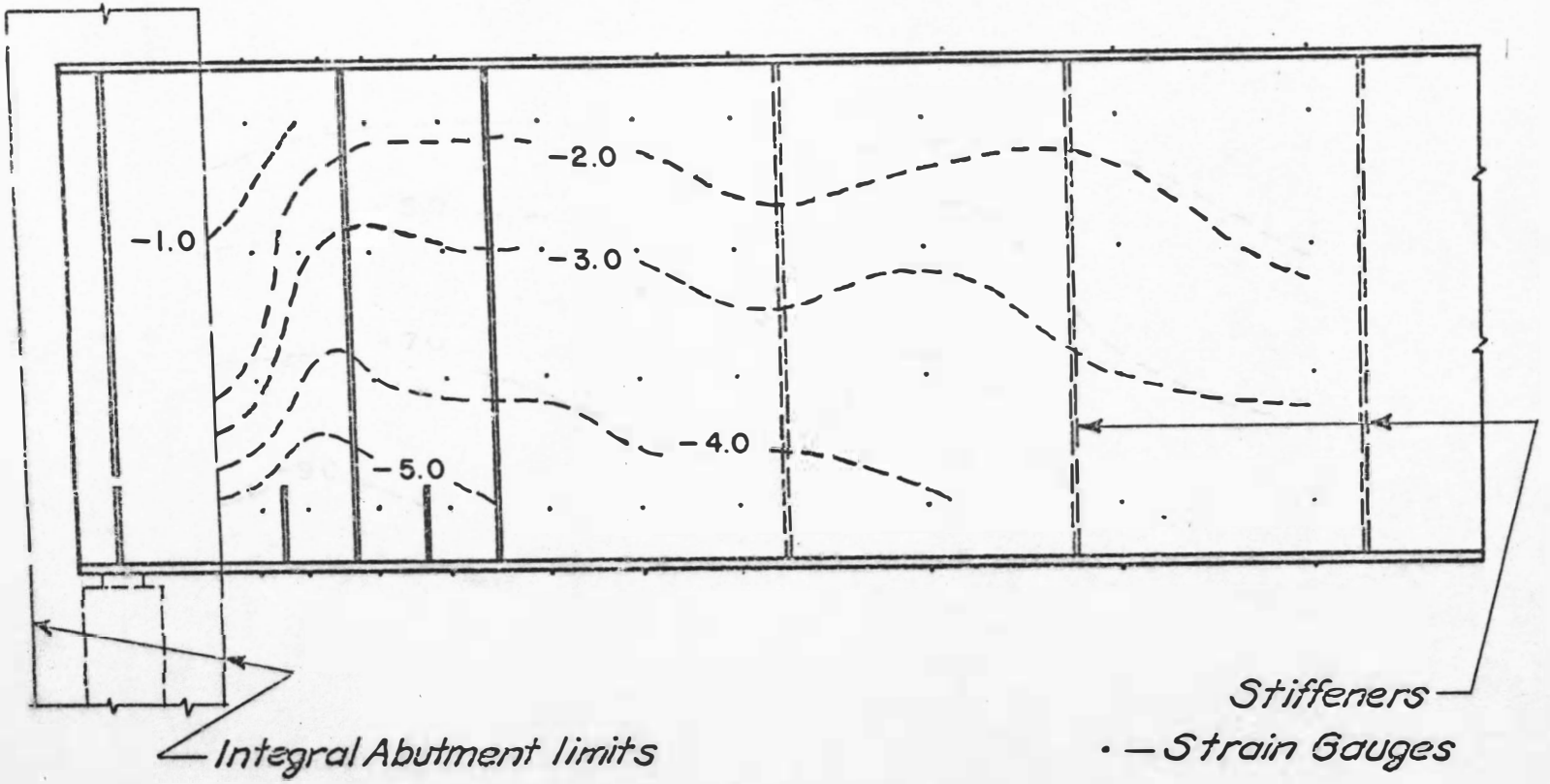

FIGURE 4a. Principal Stress Contours, in ksi. Stage IV, Summer Cycle, +1/2".

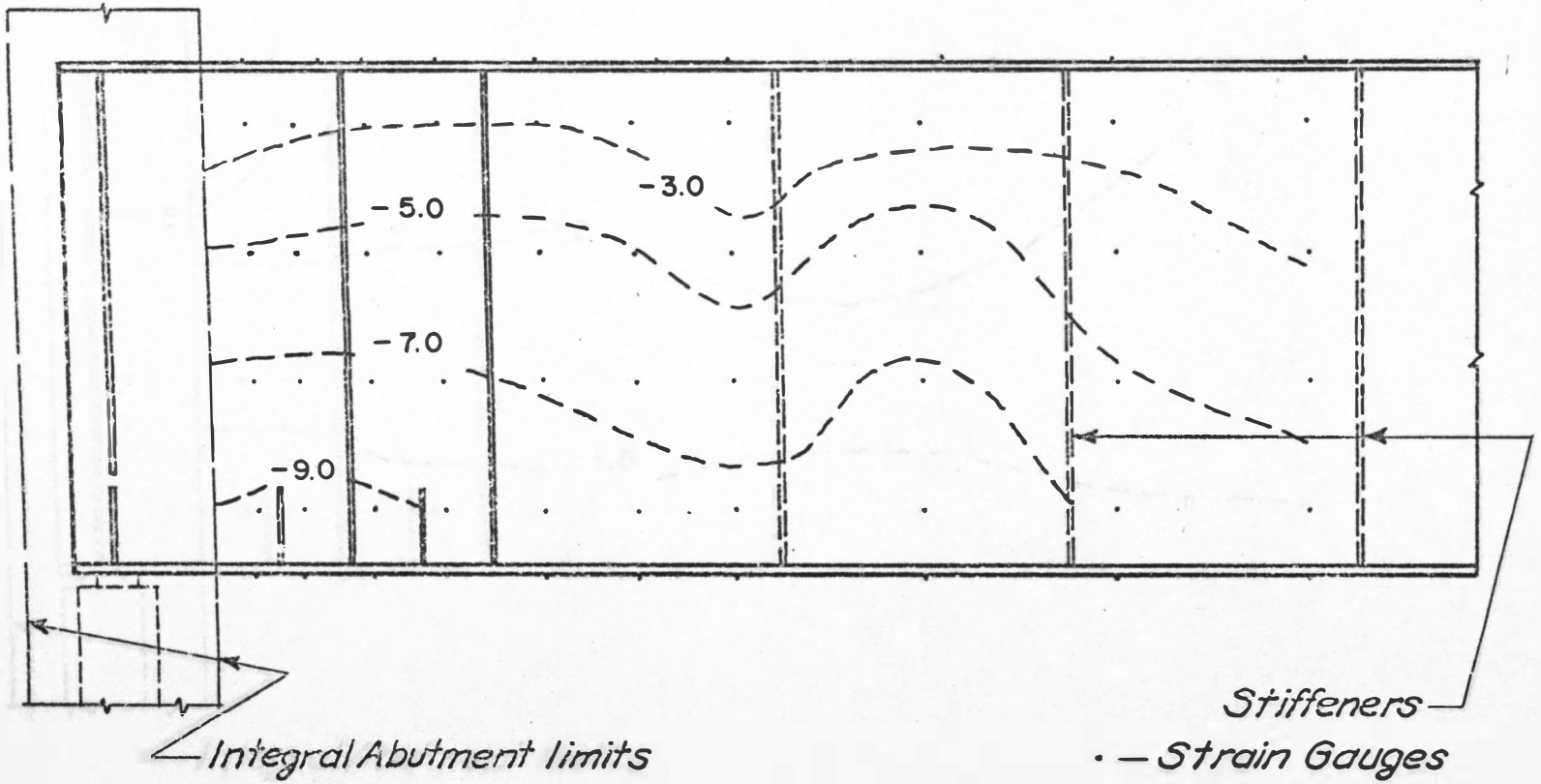

FIGURE 4b. Principal Stress Contours, in ksi. Stage IV, Summer Cycle, +1".

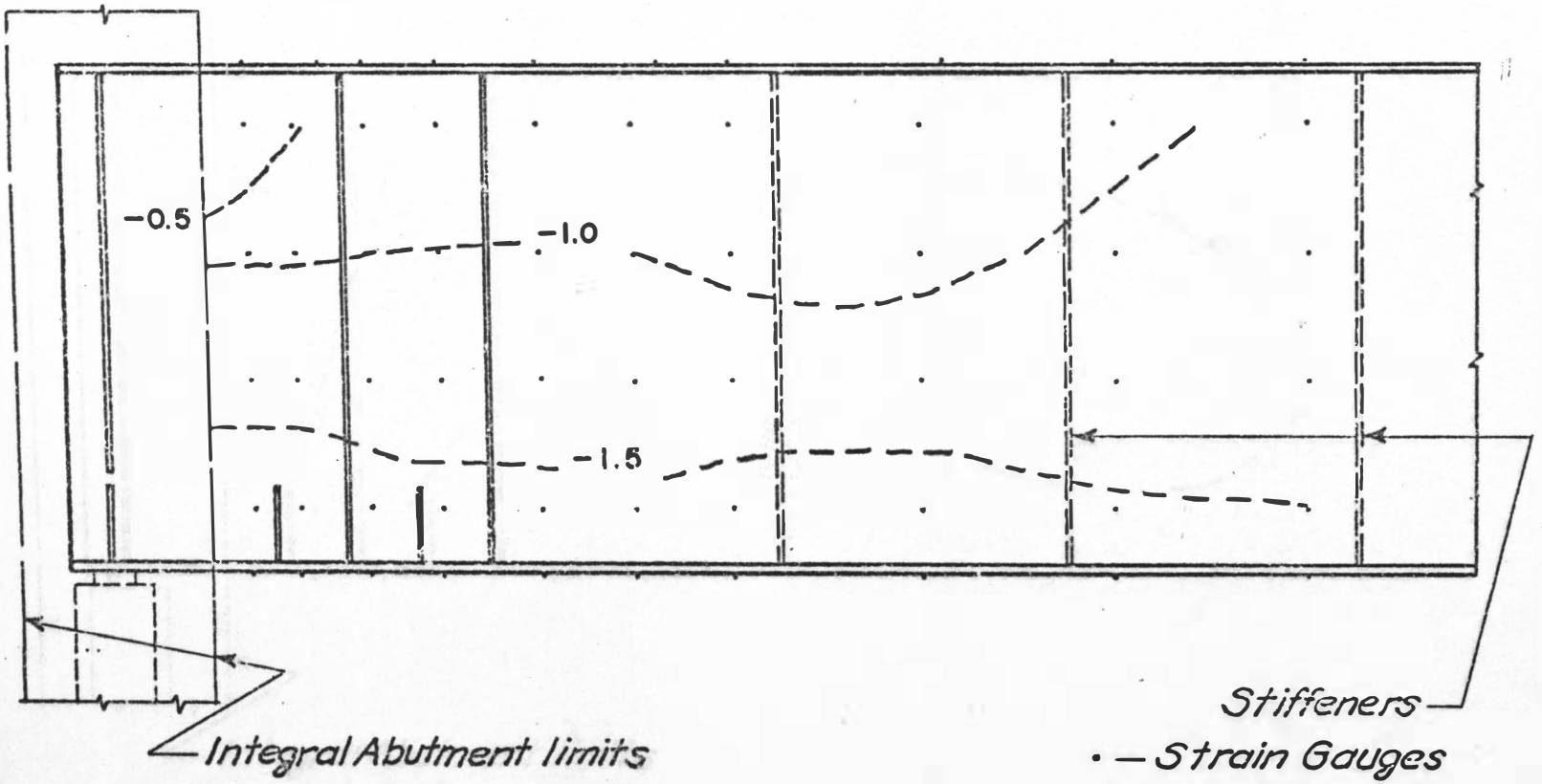

FIGURE 4c. Principal Stress Contours, in ksi. Stage IV, Summer Cycle, +1/2" Release.

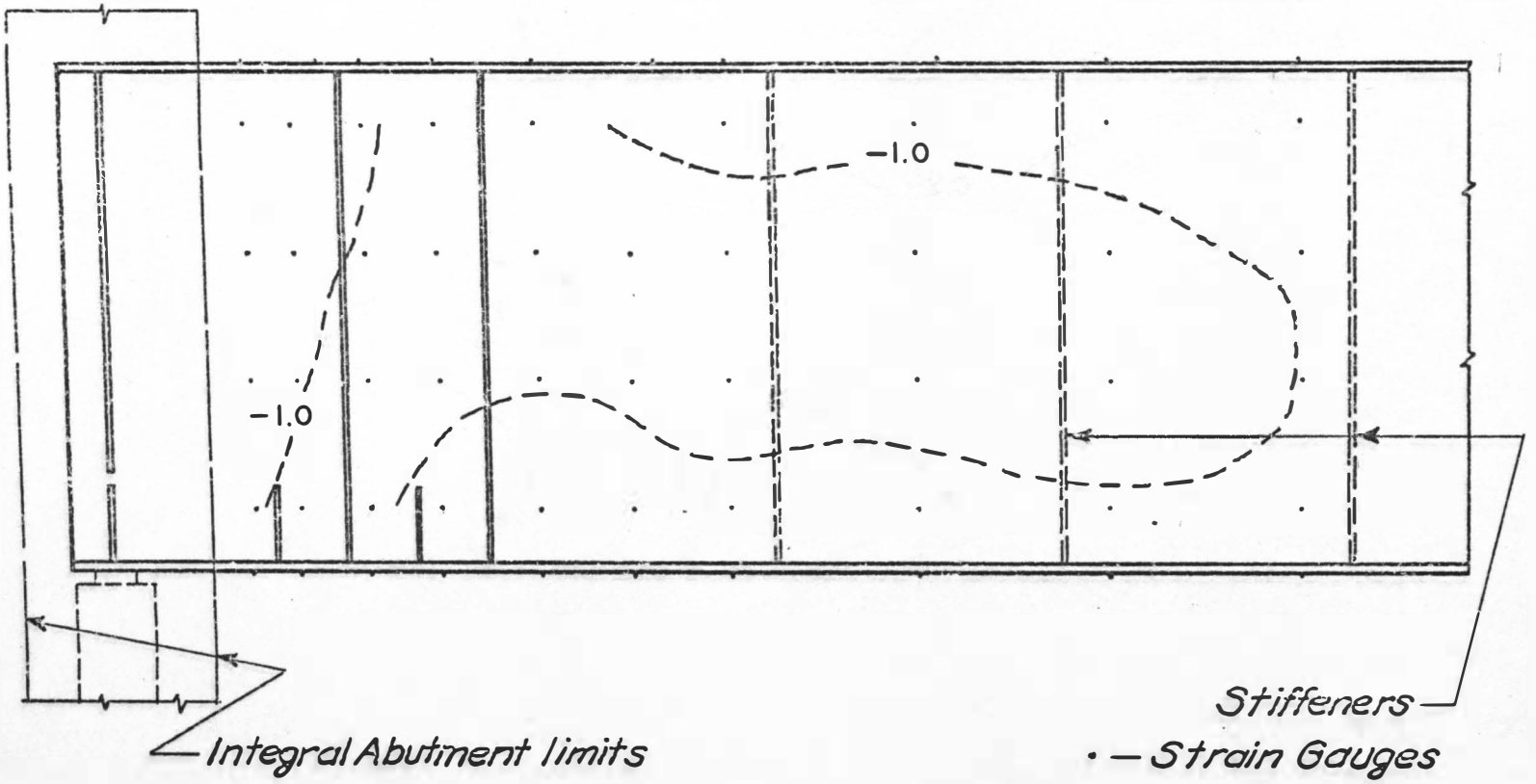

FIGURE 4d. Principal Stress Contours, in ksi. Stage IV, Summer Cycle, 0".

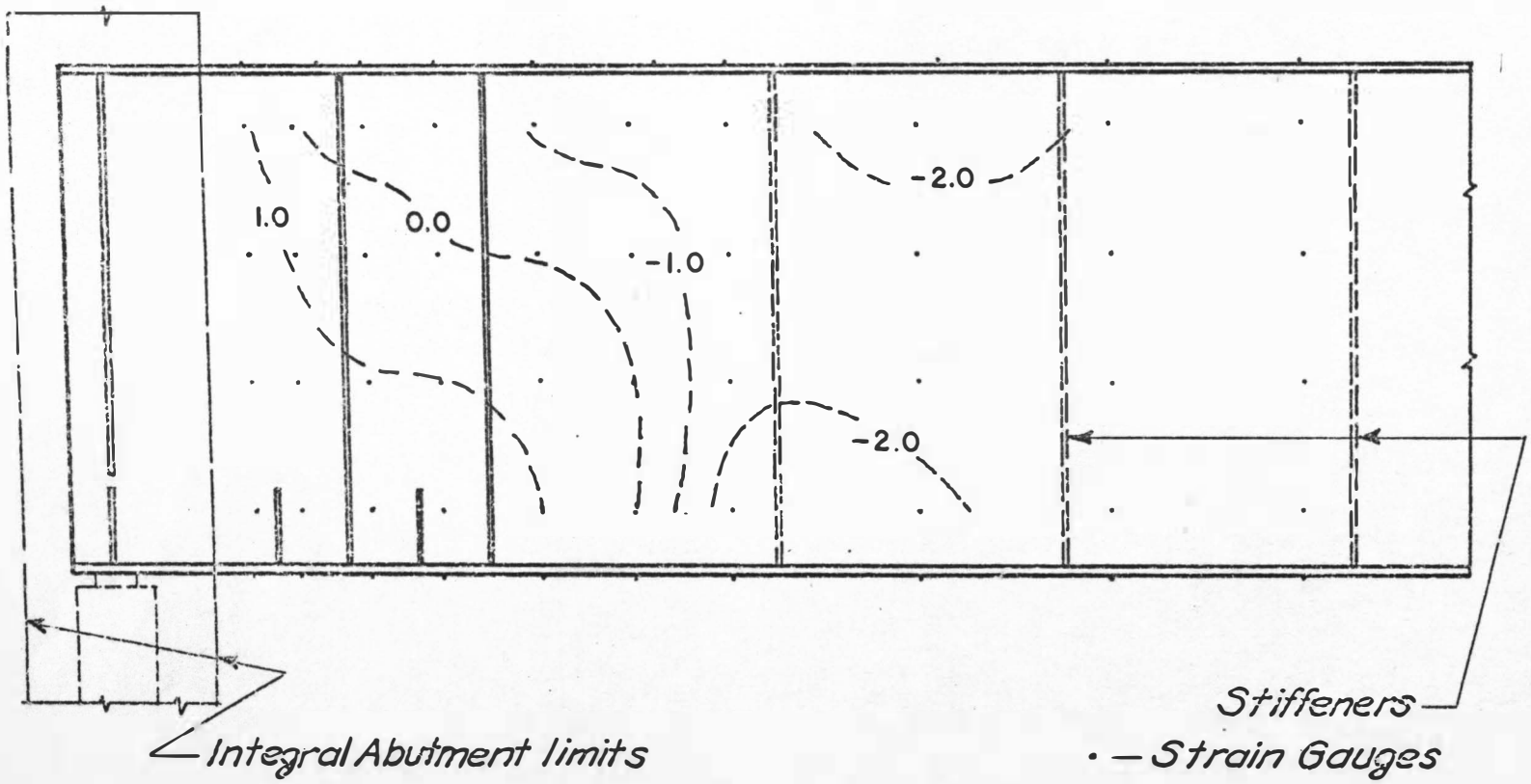

FIGURE 4e. Principal Stress Contours, in ksi. Stage IV, Summer Cycle, -1/2".